Hydrogen, nitrogen and syngas enriched diesel combustion

Fanos Christodoulou

A dissertation submitted for the degree of
Doctor of Philosophy

School of Engineering and Design
Brunel University
United Kingdom

London, July 2014

Abstract

On-board hydrogen and syngas production is considered as a transition solution from fossil fuel to hydrogen powered vehicles until problems associated with hydrogen infrastructure, distribution and storage are resolved. A hydrogen- or syngas-rich stream, which substitutes part of the main hydrocarbon fuel, can be produced by supplying diesel fuel in a fuel-reforming reactor, integrated within the exhaust pipe of a diesel engine.

The primary aim of this project was to investigate the effects of intake air enrichment with product gas on the performance, combustion and emissions of a diesel engine. The novelty of this study was the utilisation of the dilution effect of the reformate, combined with replacement of part of the hydrocarbon fuel in the engine cylinder by either hydrogen or syngas.

The experiments were performed using a fully instrumented, prototype 2.0 litre Ford HSDI diesel engine. The engine was tested in four different operating conditions, representative for light- and medium-duty diesel engines. The product gas was simulated by bottled gases, the composition of which resembled that of typical diesel reformer product gas. In each operating condition, the percentage of the bottled gases and the start of diesel injection were varied in order to find the optimum operating points.

The results showed that when the intake air was enriched with hydrogen, smoke and CO emissions decreased at the expense of NO_x. Supply of nitrogen-rich combustion air into the engine resulted in a reduction in NO_x emissions; nevertheless, this technique had a detrimental effect on smoke and CO emissions. Under low-speed low-load operation, enrichment of the intake air with a mixture of hydrogen and nitrogen led to simultaneous reductions in NO_x, smoke and CO emissions. Introduction of a mixture of syngas and nitrogen into the engine resulted in simultaneous reductions in NO_x and smoke emissions over a wide range of the engine operating window. Admission of bottled gases into the engine had a negative impact on brake thermal efficiency.

Although there are many papers in the literature dealing with the effects of intake air enrichment with separate hydrogen, syngas and nitrogen, no studies were found examining how a mixture composed of hydrogen and nitrogen or syngas and nitrogen would affect a diesel engine. Apart from making a significant contribution to existing knowledge, it is

believed that this research work will benefit the development of an engine-reformer system since the product gas is mainly composed of either a mixture of hydrogen and nitrogen or a mixture of syngas and nitrogen.

Acknowledgements

Firstly, I would like to thank my PhD supervisor Professor Thanos Megaritis for his invaluable support and guidance throughout this research work. I would also like to acknowledge the contribution of my second supervisor, Professor Hua Zhao.

The financial support of the UK Engineering and Physical Science Research Council (grant EP/H050248/1) is gratefully recognised.

Many thanks to the colleagues with whom I have shared the Engine Laboratory, but the following deserve special mention: Dr. Mohammadreza Anbari Attar, Dr. Stephen Hemmings, Dr. Yan Zhang, Mohammed Abahussain, Nehemiah Alozie and David Peirce.

Thanks are also due to the technical staff at Brunel University with particular thanks going to Ken Anstiss, Clive Barrett and Andy Selway for their continual assistance in the laboratory. The efficient ordering of laboratory equipment by the Chief Technician Christopher Allan is also recognised.

Many thanks go to Paul Hughes from MKS for the technical support and quick resolve of the FTIR issues, and Keith Hall of Hall Analytical Laboratories Ltd. for providing timely on-site repairs of the Gas Chromatograph.

Contents

List of figures

List of tables

List of abbreviations

AHRR	Apparent heat release rate
Al_2O_3	Aluminium oxide
Ba	Barium
BITDC	Before injection top dead centre
BOC	British oxygen company
BSFC	Brake specific fuel consumption
BSN	Bosch smoke number
Ca	Calcium
CA 10, 50, 90	The crank angle at which 10, 50 and 90 % of fuel mass has been burned
CAD ATDC	Crank angle degrees after top dead centre
CAD BTDC	Crank angle degrees before top dead centre
CDC	Conventional diesel combustion
CI	Compression ignition
CNG	Compressed natural gas
CO	Carbon monoxide
CO_2	Carbon dioxide
COHb	Carboxyhaemoglobin
COV	Coefficient of variation
CO_x	Carbon oxide
CR	Compression ratio
DEF	Diesel exhaust fluid
deg. CA	Degrees crank angle
DI	Direct injection
DME	Dimethyl ether
DOC	Diesel oxidation catalyst
DPF	Diesel particulate filter
ECU	Engine control unit
EGR	Exhaust gas recirculation
EOC	End of combustion
EPA	Environmental protection agency
FID	Flame ionisation detector

FTIR	Fourier transform infrared spectroscopy
GC	Gas chromatography
GHG	Greenhouse gas
H_2	Hydrogen
$H_2 + N_2$	Mixture of hydrogen and nitrogen
H_2O	Water
H_2SO_4	Sulphuric acid
HC	Hydrocarbons
HCCI	Homogenous charge compression ignition
He	Helium
HO_2	Hydroperoxyl
HSDI	High speed direct injection
HV	Heating value
ICE	Internal combustion engine
ID	Ignition delay
IMEP	Indicated mean effective pressure
K	Potassium
LFL	Lower flammability limit
LPG	Liquefied petroleum gas
LTC	Low temperature combustion
MFB	Mass fraction burned
N_2	Nitrogen
Na	Sodium
NA	Naturally aspirated
NDIR	Non-dispersive infrared
NEDC	New European Driving Cycle
NH_3	Ammonia
NMHC	Non-methane hydrocarbons
NO	Nitric oxide
NO_2	Nitrogen dioxide
NO_x	Nitrogen oxide
O_2	Oxygen

O_3	Ozone
OH	Hydroxyl
PAH	Polycyclic aromatic hydrocarbons
PCCI	Premixed charge compression ignition
PGMs	Platinum group metals
PM	Particulate matter
Pt	Platinum
RCCI	Reactivity controlled compression ignition
REGR	Reformed EGR
ROHR	Rate of heat release
RPM	Revolutions per minute
SCR	Selective catalytic reduction
SOC	Start of combustion
SOF	Soluble organic fraction
SOI	Start of injection
SOL	Solid fraction
STDV	Standard deviation
Syngas + N_2	Mixture of syngas and nitrogen
TCD	Thermal conductivity detector
TDC	Top dead centre
THC	Total hydrocarbons
UFL	Upper flammability limit
UHC	Unburned hydrocarbon
ULSD	Ultra-low sulphur diesel

CHAPTER 1

INTRODUCTION

1.1 Introduction

The diesel engine was developed in the late nineteenth century by Rudolf Diesel, who patented the first diesel engine in 1892, while the first successful engine was operated in 1897. Thermal efficiency, although remarkably high at that time, was only 26% compared to the near 40% attained by modern diesel engines. Due to their large size and weight, the early diesel engines were produced mainly for industrial and marine applications. Subsequent improvements allowed diesel engines to be used for powering road vehicles, and they became very popular especially on trucks and heavy duty vehicles. Nowadays, cars equipped with diesel engines are gaining popularity and currently approximately 50% of all new car sales in EU are diesel [1].

In developed countries, the transport sector accounts for 35% of all energy consumption [2]. Energy conservation and emissions control have long been under the spotlight as fossil fuel depletion, environmental and human health issues have come to the forefront. According to Ehsani et al. [3], if current trends of oil discovery and consumption continue, it is expected that the fossil fuels will last until approximately 2038. It is also expected that the increase in the world's population from 6 to 10 billion will induce a parallel growth in vehicles from 700 million to 2.5 billion [4]. Incremental improvement in fuel consumption and pollutant emissions has been set as a short-term goal, while the long-term goal involves innovative methods that will promote the transition to alternative-renewable fuels.

The combination of engine technologies such as exhaust gas recirculation (EGR), improved fuel systems, optimised design of the combustion chamber and alternative combustion modes, with exhaust aftertreatment methods, including the diesel oxidation catalyst (DOC), selective catalytic reduction system (SCR) and diesel particulate filter (DPF), is considered a potential solution to the emissions issue. The fuel consumption of diesel engines has been considerably improved by the introduction of the common rail system, which enables a finer fuel atomization and as a result increased combustion efficiency.

Petroleum-based transportation is well-established offering a wide range of benefits; however, a transition towards renewable fuels is essential in order to eliminate the disadvantages of using fossil fuels. Hydrogen (H_2) can be used to fuel internal combustion engines and is considered renewable when it is produced via a renewable process. Progress towards hydrogen fuelled transportation has been picking up pace since the late 1990s. Nevertheless, transition solutions such as dual fuelling, fuel blending and on-board gaseous fuel production are required, prior to the adoption of hydrogen as a transportation fuel.

Hydrogen has long been seen as a future energy carrier as its chemical compounds constitute a large part of the Earth's surface. A variety of primary resources including fossil fuel, solar, wind, hydro and nuclear power can be used for its production [5]. The combustion of hydrogen in internal combustion engines (ICEs) produces water (H_2O), nitrogen oxides (NO_x) and marginal levels of carbon oxides (CO_x) and hydrocarbons (HC). The final two chemical compounds originate from the burning of the lubricating oil [6]. Besides, NO_x production can be significantly reduced by operating the engine with a very lean air-hydrogen mixture. This way the combustion temperature is likely to remain in the zone of slow NO_x formation rate.

In automotive applications, hydrogen can be used as fuel for both Otto and Diesel engines. In an engine using the former cycle, the air-hydrogen mixture can easily be ignited by the spark plug since the minimum ignition energy of hydrogen is an order of magnitude lower than gasoline. When hydrogen is introduced in a diesel engine, the onset of combustion is achieved by a pilot diesel injection as the autoignition temperature of hydrogen is not reached in convention diesel engines. After many years of intensive research, it is now possible to develop engines fuelled by hydrogen; nevertheless, challenges associated with on-board hydrogen storage still exist.

On-board hydrogen production is deemed as a transition solution until the issues associated with hydrogen distribution and on-board storage are resolved. Realisation of on-board hydrogen production is achieved via the integration of a catalytic fuel reforming reactor into the EGR loop. A hydrogen-rich gas is generated by direct catalytic interaction of a hydrocarbon fuel with the high temperature exhaust gases expelled from the engine.

The reforming products can be used as a supplement to the engine main fuel by sending them back to the cylinder.

The main flammable gas produced from the fuel reforming process is either hydrogen or a mixture of hydrogen and carbon monoxide (syngas). The fuel reformer can be tuned accordingly in order to promote the desirable chemical reactions, which include diesel fuel steam reforming, water gas-shift, diesel fuel partial oxidation, diesel fuel complete oxidation, dry reforming reaction, autothermal reforming and hydrocarbon thermal decomposition. Recirculation of the product gas back into the intake air results in an increase in nitrogen (N_2) to oxygen (O_2) ratio, since an amount of oxygen is replaced by the nitrogen-rich reformed exhaust gases.

1.2 Aims and objectives

The aims of this dissertation were to investigate the effects of intake air enrichment with hydrogen, nitrogen, simultaneous hydrogen and nitrogen (H_2 + N_2) and simultaneous syngas and nitrogen (syngas + N_2) on the performance, emissions and combustion of an HSDI diesel engine. In real world applications, the aforementioned gases can either be stored or produced on board. In this research effort the gases were stored in bottles, which were placed close to the engine.

The first series of experiments was performed using separate hydrogen and nitrogen in order to understand the impact of the two distinct gases on the performance, emissions and combustion of the engine. In the second series of experiments, a mixture of H_2 + N_2 was used, while in the third series of experiments, the hydrogen was replaced by syngas. A more detailed explanation on the selection of the gases is given in Section 1.3. At this point, the main objectives of this study are presented:

- Demonstrate how the engine operating conditions affect the combustion, performance and emissions when bottled gases are introduced into the engine. It should be mentioned that the conditions selected (speed and load) were representative for light- and medium-duty diesel engines. Variations in injection timing and gas concentration were included in each operating condition.
- Study whether diesel combustion enriched with H_2 + N_2 can offer simultaneous reductions in NO_x, smoke and CO emissions.

- Calculate the combustion efficiency of the bottled carbon monoxide and hydrogen delivered into the engine in the different engine operating conditions and gas concentrations.
- Isolate the distinct gases (i.e. hydrogen, carbon monoxide and nitrogen) contained in the product gas to identify the effects on the combustion and emissions of the engine.
- Investigate whether the product gas-diesel mixture affects the combustion noise by comparing the pressure rise rate values.
- Investigate whether an increase in nitrogen to oxygen ratio in the intake charge affects the performance, emissions and combustion of a diesel engine. This was done by replacing an amount of the intake air with bottled nitrogen.
- Demonstrate the capability of the product gas to offer simultaneous reductions in NO_x and smoke emissions over a wide range of the engine operating conditions.

1.3 Outline of thesis

Following this introductory chapter the rest of the thesis is organised as follows:

Chapter 2 - Literature review

This chapter provides a review of emission formation in diesel engines. It also presents the European Union emission standards and the aftertreatment systems currently being used for the reduction of exhaust emissions. In addition, it provides an overview of the alternative diesel combustion modes and the injection parameters. The findings from using alternative fuels, dual fuel techniques and intake charge dilution methods in diesel engines are also discussed. Finally, the exhaust gas assisted fuel reforming technique is reviewed.

Chapter 3 - Experimental facilities, test procedure and data analysis

Chapter 3 provides a description of the experimental facilities, the measuring equipment employed throughout the experiments, the test procedure and the data analysis process. Moreover, the selection of the operating conditions, along with the parameters varied, is justified.

Chapter 4 - Enrichment of the intake air with hydrogen

The effects of the intake air enrichment with hydrogen on the performance, combustion and emissions of a diesel engine are presented in Chapter 4. The results obtained include NO_x, Bosch smoke number (BSN), carbon monoxide (CO) and total hydrocarbons (THC) as well as the brake thermal efficiency, the hydrogen combustion efficiency and a heat release rate analysis. As shown in Figure 1.1, this chapter can benefit the development of diesel engines in which diesel fuel is partly substituted by hydrogen that is either stored or produced on board. The hydrogen fuel is delivered into the engine through the intake pipe; hence, the conversion of a conventional diesel engine into a diesel-hydrogen dual fuel engine is relatively easy.

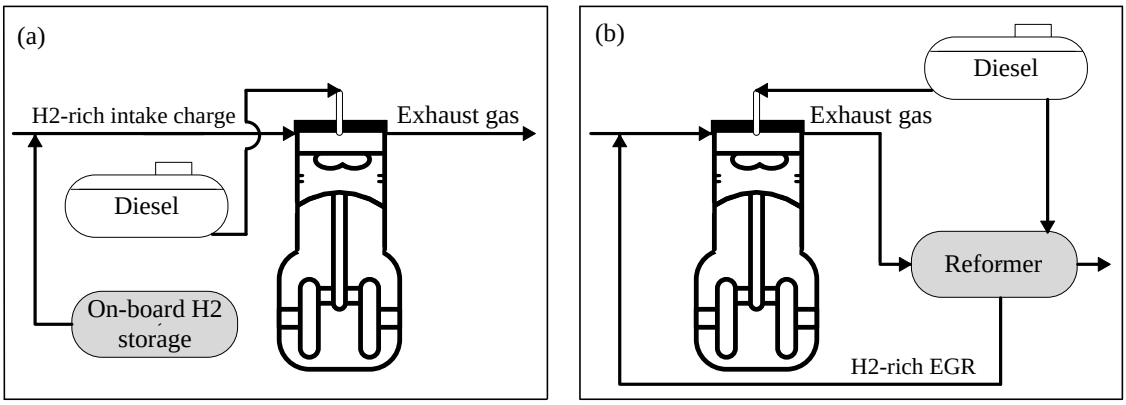

Figure 1.1: Enrichment of the intake air with hydrogen. (a) The hydrogen is stored on-board, (b) the hydrogen is generated on-board using a fuel reforming reactor.

Chapter 5 - Enrichment of the intake air with nitrogen

This chapter is devoted to presenting and discussing the findings of the enrichment of the intake air with nitrogen. An amount of intake air was gradually replaced by bottled nitrogen in order to study the effects on the performance, combustion and emissions of the engine. Figure 1.2 shows the techniques that lead to an increase in the nitrogen to oxygen ratio in the intake air. One technique is to direct the intake air through an air separation membrane, which is capable of producing nitrogen-rich air. Another technique is the supply of fuel reformed products into the engine. The concentration of nitrogen is inevitably increased as the amount of the intake air is replaced by the reformed EGR (REGR), which is rich in nitrogen.

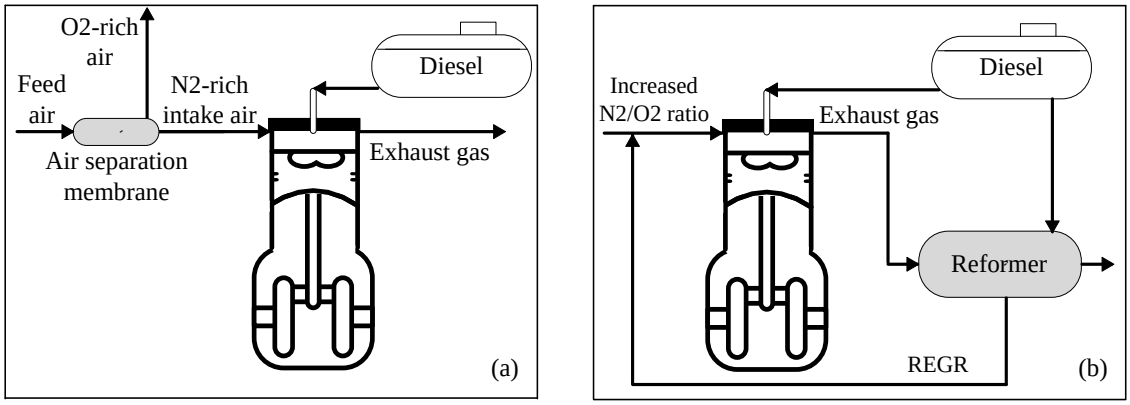

Figure 1.2: Increase in nitrogen concentration in the intake air by, (a) employing an air separation membrane, (b) integrating a fuel reformer within the EGR loop.

Chapter 6 - Enrichment of the intake air with simultaneous hydrogen and nitrogen

The objective of this chapter is to present the effects of the intake air enrichment with a mixture of H_2 + N_2 on the performance, emissions and combustion of the engine. Figure 1.3 illustrates the methods that can be employed to produce H_2 + N_2 rich intake air. Figure 1.3(a) shows a combination of the techniques already presented in Figures 1.1(a) and 1.2(a). The product gas of diesel fuel reforming may consist of H_2 + N_2, as shown in Figure 1.3(b). Carbon monoxide, at a relatively high concentration, is typically present in diesel reforming product gas; nevertheless, it can be reduced to ppm levels through the water-gas shift reaction, using a good low-temperature catalyst.

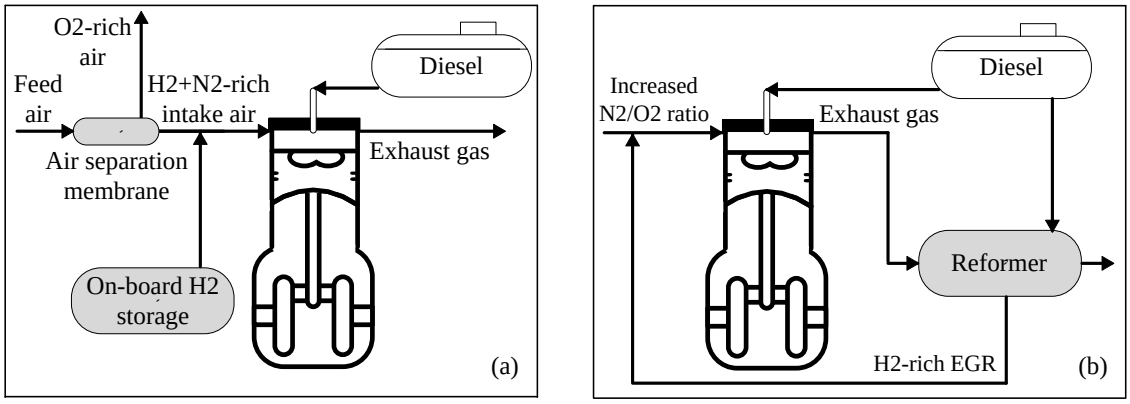

Figure 1.3: Simultaneous enrichment of the intake air with H_2 + N_2 through, (a) combination of an air separation membrane and on-board hydrogen reservoir, and (b) integration of a fuel reformer into the EGR loop.

Chapter 7 - Enrichment of the intake air with a mixture of syngas and nitrogen

The effects of the intake air enrichment with simultaneous syngas + N_2 on the performance, emissions and combustion of the engine are presented in Chapter 7. Apart from hydrogen, and depending on the reactions promoted, the reformate typically contains a significant amount of carbon monoxide, which is produced as a by-product. A bottled gas mixture with hydrogen and carbon monoxide contents resembling those of typical diesel reformer product gas was delivered into the engine. Nitrogen, drawn from a separate bottle, at the same volumetric fraction to syngas, was simultaneously admitted into the engine. Figure 1.4 shows the schematic representation of the engine with a diesel reformer integrated into the EGR loop.

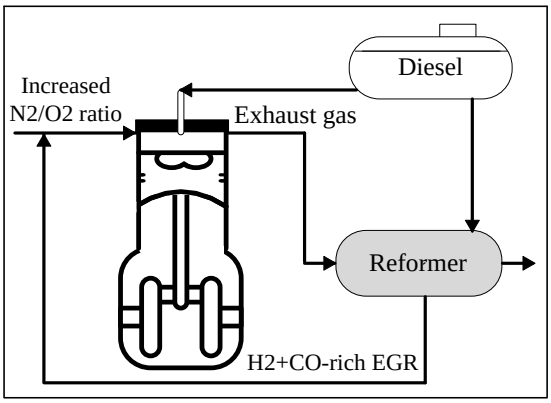

Figure 1.4: Simultaneous enrichment of the intake air with syngas + N_2 using a diesel reformer integrated within the EGR loop.

Chapter 8 - Conclusions and recommendations for future work

In addition to discussing the conclusions and the significance of this study, Chapter 8 presents the proposed future work that can be performed to take this research effort further.

CHAPTER 2

LITERATURE REVIEW

2.1 Regulated exhaust emissions from diesel combustion

Combustion is a chemical process in which the hydrogen and carbon atoms contained in a hydrocarbon fuel are oxidized releasing energy in the form of heat and light. The products of complete or ideal combustion of a hydrocarbon with air are water (H_2O) and carbon dioxide (CO_2). This type of combustion occurs under stoichiometric air-fuel ratio conditions. However, the intrinsic complexity of the combustion process, the great variability in the local equivalence ratio in diesel engines, together with the structure and function of the different components, lead to the production of additional chemical compounds such as NO_x, unburned hydrocarbons (UHCs), CO and particulate matters (PM). The adverse effects of these chemical compounds have been well documented in a number of investigations [7-9]; hence, in an effort to protect human health and the environment, air pollution limits have been established worldwide. In Sections 2.1.1 - 2.1.4, a discussion on the formation of NO_x, PM, CO and THC emissions in internal combustion engines is provided.

2.1.1 Nitrogen oxides

Nitrogen oxides are principally composed of two pollutants: nitric oxides (NO) and nitrogen dioxides (NO_2). Typically, NO comprises over 90% of the engine-out NO_x emissions. The molecular nitrogen contained in the air is oxidized to form NO when ambient air is exposed to elevated temperatures. In case nitrogen atoms are present in the fuel, the oxidation of the nitrogen-containing compounds during the combustion process is an additional source of NO. In total, there are three NO formation mechanisms in diesel engines, which are described below [10-13]:

When the combustion temperature is higher than 1527-1727 °C and the air-fuel ratio is close to stoichiometric the *thermal* or *extended Zeldovich* mechanism is the major contributor to NO_x emissions from diesel engines. The chemical reactions governing the formation of NO from nitrogen (and its destruction) are:

$$O + N_2 \leftrightarrow NO + N \quad (2.1)$$

$$N + O_2 \leftrightarrow NO + O \quad (2.2)$$

$$N + OH \leftrightarrow NO + H \quad (2.3)$$

The rate of NO formation is given by the following equation:

$$\frac{d[NO]}{dt} = k_1^+[O][N_2] + k_2^+[N][O_2] + k_3^+[N][OH] - k_1^-[NO][N] - k_2^-[NO][O] - k_3^-[NO][H] \quad (2.4)$$

where k_1^+, k_2^+, k_3^+, k_1^-, k_2^-, k_3^- are the rate constants for the extended Zeldovich mechanism ($m^3\ mol^{-1}\ s^{-1}$).

Due to the high temperature required, thermal NO only appears in significant quantities after the onset of heat release. It has been reported that the production rate doubles for every 90 °C temperature increase beyond 1827 °C [14].

The *Prompt NO* or *Fenimore* mechanism is relatively insignificant for most diesel combustion conditions. Formation of NO occurs in the flame reaction zone and is very rapid. That zone is extremely thin and residence time within the zone is short. Equation (2.5) is important for the initiation of NO under this mechanism:

$$CH + N_2 \leftrightarrow HCN + N \quad (2.5)$$

In a series of reactions that take place, the presence of O and OH strongly affect the rapid conversion to NO.

Generally, distillate fuels do not contain significant amounts of organic nitrogen; therefore, the amount of *fuel NO* in the exhaust gas of a diesel engine is negligible. Nevertheless, heavy fuel oils with residual fuel may contain significant quantities of organic nitrogen, which can contribute to NO_x emissions. In such cases, the conversion of fuel nitrogen to NO strongly depends on the stoichiometry, local temperature and level of nitrogen in the fuel-air mixture.

A complete understanding of NO_x formation mechanisms is essential in order to reduce the levels being produced and released into the atmosphere, and as a result minimize the adverse effects on human health and the environment. From the environmental point of

view, NO_x emissions react to form smog and acid rain and contribute to global warming. Concerning their impact on human health, breathing NO_x can cause respiratory problems, may damage the lung tissue and may cause premature death.

2.1.2 Particulate matter

It should be clarified that in the current research work the smoke concentration in the exhaust gas was determined by the filter paper method. In particular, a photoelectric head measured the blackening of a clean filter paper, caused by the soot (that is, combustion generated carbonaceous material) contained in the combustion products. However, for the sake of completeness a discussion on the production of PM is also provided. In fact, PM values are obtained using a different measurement method.

It is very difficult to classify PM due to the chemical and physical complexity involved. In essence, PM consists of solid carbon particles and other chemical species that agglomerate to form complicated particles. The agglomerated particles undergo the following formation sequence: the carbon formed from reactive intermediates in the fuel-rich zone is not always fully burned when moved to a region with excess oxygen. As a result, residues of fine carbon cores remain in the combustion products. The reaction rate of these fine carbon cores is reduced as they cool down. While moving through the exhaust pipe, the carbon particles agglomerate and mix with condensed heavy hydrocarbons, sulphur oxides, nitrogen oxides and metallic ash formed during the high temperature combustion [15]. The resulting particle is schematically shown in Figure 2.1.

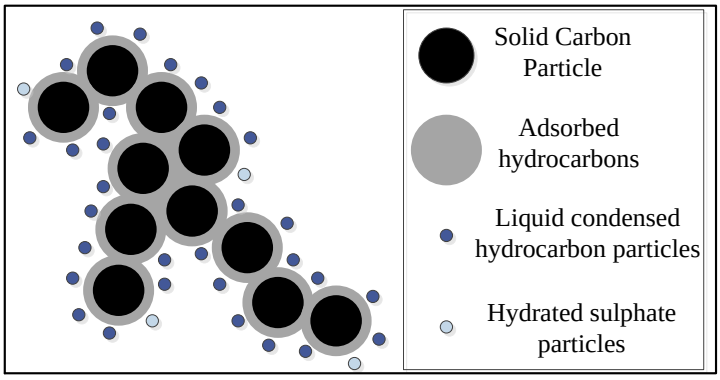

Figure 2.1: Schematic representation of diesel particulate matter.

A more detailed discussion is provided over the next paragraphs in order to further understand the formation process, their composition, the effect they have on the environment and human health as well as the treatment methods.

The particulate matter is divided into three main fractions [16]:

- Solid fraction (SOL)

The unburned carbon particles agglomerate while travelling from the cylinder to the ambient air. The oxidation rate of particles is decreased as they move away from the cylinder due to the reduction of the temperature they are exposed to. Metal ash compounds derived from lubricating oil additives, along with engine wear, is another source of solid material.

- Soluble organic fraction (SOF)

The proportion of SOF in the PM may vary considerably depending on engine load, technology and test cycle and may constitute over 50% of the total PM. As already shown in Figure 2.1, the unburned hydrocarbons adsorb or condense onto the surface of the solid fraction of a particulate matter, forming the SOF.

- Sulphate particulates

Sulphate particulates are formed through the interaction between molecules of H_2SO_4 and H_2O. Their formation strongly depends on the fuel sulphur level; thus, reduction of fuel sulphur content is the major suppression mechanism. Referring to Figure 2.1, sulphate particulates are mixed with SOL and SOF to form the final PM.

Exposure to diesel PM may result in developing asthma and/or lung cancer [17]. The size of particles has received much attention in the research carried out as it determines how deeply it penetrates into the human respiratory system. Large size particles (>10 μm) are deposited within the nose and throat, whereas small particles (<2.5 μm) can penetrate deeply into the lungs.

Measurements in the cylinder of a running engine provide useful information on the history (formation-oxidation) of the particulates at various points within the cylinder, including the diesel spray. To date, several in-cylinder particulate measurement techniques

have been used, including rapid acting valves [18], optical absorption techniques [19] and cylinder dumping [20]. Techniques that are used to measure PM in the exhaust pipe include gravimetric analysis and electrical mobility techniques.

The complexity of PM (both chemical and physical) makes the in-cylinder treatment a very challenging task since there are many mechanisms (often competing) influencing the formation-oxidation of that pollutant. Soot formation-oxidation is affected by the temperature, fuel composition, pressure within the combustion chamber, local oxygen concentration, duration of diffusion combustion and residence time, to name a few factors.

Despite the research findings on PM formation-oxidation, the current emission limits can only be met by fitting advanced emission aftertreatment technologies, such as diesel particulate filter, within the exhaust pipe. Further technological advances are required in order to achieve sufficient in-cylinder reduction of PM.

Figure 2.2 shows the soot and NO_x formation regions in the φ-T (local fuel-air equivalence ratio and flame temperature) graph obtained by performing zero-D calculations for n-hexane with 0% EGR [21].

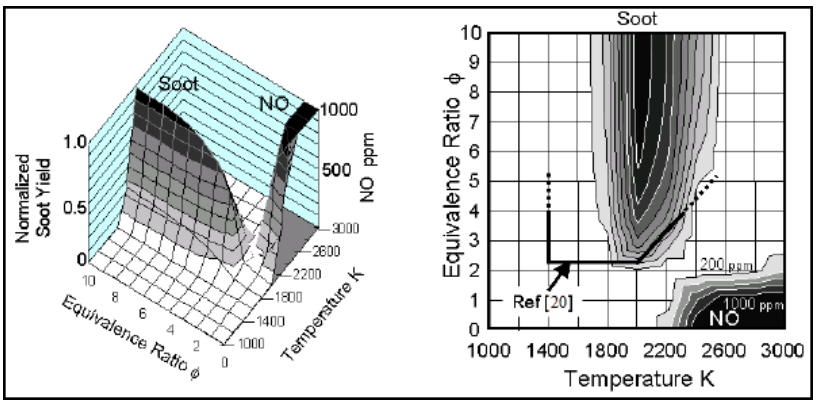

Figure 2.2: Calculated φ-T map for soot and NO formation for n-hexane, [21].

The figure clearly illustrates the strong dependence of soot and NO_x emissions on equivalence ratio and temperature. Smokeless combustion can be achieved by avoiding the soot formation peninsula, especially the area around the peak soot formation. On the left of the soot peninsula (low temperature combustion), the formation of soot is suppressed by the freezing of reactions from polycyclic aromatic hydrocarbons (PAH) to soot particles. On the right of the soot formation peninsula, the oxidation rate of soot precursors and PAH

is very high due to the increased temperature; therefore, the particles are consumed before they advance to the next particulate formation stages (that is, particle inception, surface growth, particle coagulation and agglomeration). The reduction of NO emissions can be realised by avoiding the NO formation zone, which is located at the bottom right corner of the figure.

When hydrogen is admitted into the engine, the peak combustion temperature is increased, causing an increase in NO_x and a reduction in soot formation. The former occurs mainly because the combustion temperature tends to move towards the centre of the NO_x region, whereas the latter, among other factors, is attributed to the enhanced soot oxidation as the combustion moves towards the right of the soot peninsula. In a similar way, introduction of nitrogen-rich intake air into the engine leads to NO_x reduction, since the NO_x-producing reactions freeze due to the drop of peak combustion temperature. The increase in soot is attributed to the increase in the global equivalence ratio. Enrichment of the intake air with either a mixture of H_2 + N_2 or a mixture of syngas + N_2 can lead to simultaneous reduction of NO_x and soot emissions (under certain operating conditions), provided that the NO_x and soot producing regions are avoided.

2.1.3 Carbon monoxide

In internal combustion engines, CO is produced from the incomplete combustion of the carbon-containing fuel. Oxygen depletion is the dominant factor leading to incomplete fuel oxidation. Other factors promoting the formation of CO include flame quenching on cylinder walls, non-homogenous air-fuel mixing and reduced combustion temperature and residence time. The adverse health and environmental effects of CO emissions are summarised over the next paragraphs.

When CO is inhaled it enters the bloodstream through the lungs and binds with haemoglobin to form carboxyhaemoglobin (COHb), which in turn decreases the oxygen carrying capacity and leads to tissue hypoxia [22]. The acceptable exposure to CO emissions is determined by both CO concentration and time. Permitted exposure time reduces by increasing CO emissions and vice versa. The short-term exposure limit tolerates 200 ppm for 15 minutes. Reduction of CO concentration to 30 ppm increases the exposure time to 8 hours [23]. Table 2.1 summarizes the symptoms observed after the exposure to CO emissions at a certain amount of time.

CO has not been proven to be a direct contributor to environmental pollution. However, its indirect effects on global warming are important. The presence of CO in the atmosphere affects the lifetime of strong greenhouse gases, such as methane. CO reacts with hydroxyl (OH) radicals to form a strong greenhouse gas, CO_2. Consumption of OH leads to increased methane concentration as OH radicals are very useful in removing methane from the atmosphere by reacting with it. CO street level concentration has been decreased from tens of ppm in the 1970s to a few ppm in the 1990s and even less today due to the reduction of CO emissions from vehicles [24].

Table 2.1: Symptomatology and CO exposure [23].

Symptom	**COHb concentration [%]**	**CO concentration [ppm/exposure time]**
Asymptomatic	0-20	100/8h
Mild frontal headache	10-20	100/8h to 200/4h
Headache ± tachycardia	20-30	500/2h
Steady symptom progression		200-1200
Collapse	30-40	300
Coma	50-60	
Chemical asphyxiant actions		> 1000
Death in 2h	60-70	650-1000
Death < 1h	80-90	2000
Death in few min	90-100	4000
Death in 10 min		8000
No symptoms before collapse		10,000
Fatal arrhythmia before high COHb concentration		50,000

2.1.4 Total unburned hydrocarbons

Hydrocarbon pollution is caused when unburned or partially burned fuel is emitted from the tailpipe of a vehicle. Fuel evaporation also contributes to hydrocarbon emissions in the atmosphere, but to a lesser extent. The origins of unburned hydrocarbons (UHCs) in a diesel engine can be summed up as follows [11, 25, 26]:

- Combustion chamber crevices
- Flame quenching on the combustion chamber surfaces

- Formation of liquid films on combustion chamber surfaces
- Under-mixing of fuel and air, resulting in over-rich zones that cannot burn due to local lack of oxygen (including fuel dribbling out of the injector sac volume)
- Over-mixing of fuel and air beyond lean flammability limits during ignition delay period

The composition of hydrocarbon emissions, and therefore the effects on humans and the environment, can be significantly influenced by the fuel used. Some hydrocarbons are toxic and suspected carcinogens, others are highly reactive in the smoke-producing chemistry, while others are odorants and irritants.

2.2 Legislation

In the early 1950s a California researcher realised the adverse impact of fossil fuel powered motor vehicles on air quality. Since then, much effort has been put into setting standards and developing emission control technologies.

The first emissions standard (set by the California Motor Vehicle Pollution Control Board) was first developed in 1966 and aimed at reducing the UHCs and CO exhaust pollutants emitted from the vehicles sold in California [27]. The EGR valve was developed in 1972, while the first generation catalytic converters were built 3 years later, in 1975. In 1981 sophisticated three-way catalysts, on board computers and oxygen sensors were fitted in most new cars [28].

A milestone in emission standards was the introduction of 'Tier' (United States) and 'Euro' (European Union) in 1994 and 1993, respectively. Concerning the Euro standards, the stages for light-duty diesel engines (passenger cars) are typically referred to as Euro 1 implemented in 1993, followed by Euro 2 in 1996, Euro 3 in 2000, Euro 4 in 2005, Euro 5 in 2009 and Euro 6 in 2014. It should be mentioned that the corresponding standards for heavy-duty vehicles use Roman, instead of Arabic numerals (that is, Euro I ... VI). Figures 2.3 and 2.4 illustrate the permitted particulate matter and NO_x emissions as well as the year they come into force as defined by the European Union directives [29]. Failure to meet the European or U.S emission standards results in tax penalties.

The emission levels are tested using the New European Driving Cycle (NEDC), which simulates the typical speed-time pattern of a car driven in Europe. It is composed of four

consecutive ECE-15 cycles with maximum speed 50 km/h and average speed 19 km/h and one extra-urban cycle with maximum and average speed 121km/h and 63 km/h, respectively.

Achievement of the legislated emission limits requires the combination of in-cylinder and aftertreatment emission reduction systems. The former includes application of various injection strategies (injection rate shaping, fuel injection pressure), alternative combustion concepts (HCCI, PCCI, LTC), EGR, alternative fuels and exhaust gas reforming, whereas the latter involves the installation of catalytic reduction systems within the exhaust pipe.

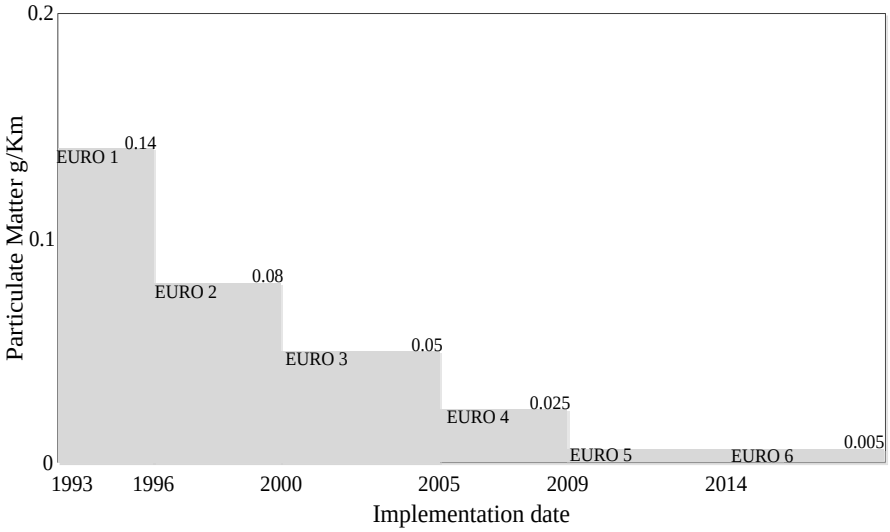

Figure 2.3: European Union Particulate matter emission standards.

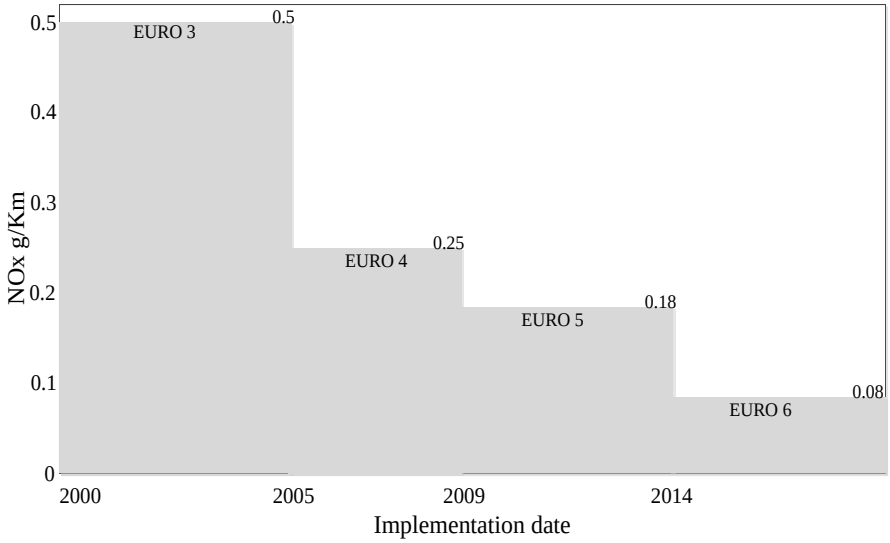

Figure 2.4: European Union NO_x emission standards.

2.3 Exhaust gas aftertreatment

Although the harmful by-products produced during the combustion process can be reduced (to a certain extent) by employing in-cylinder emission control techniques, application of aftertreatment catalysts is deemed necessary in order to reduce pollutants to legislated levels. When catalysts were first introduced, and based on the legislative emission levels at that time, an oxidation catalyst was adequate in diesel engines. A modern diesel-powered vehicle may require the combination of up to three different aftertreatment devices, which are presented below [30].

2.3.1 Diesel oxidation catalyst

The diesel oxidation catalyst is designated to convert CO, HC and SOF of particulate matters to CO_2 and H_2O. The chemical reactions involved are given below:

$$CO + \frac{1}{2}O_2 \rightarrow CO_2 \tag{2.6}$$

$$HC + O_2 \rightarrow CO_2 + H_2O \tag{2.7}$$

$$SOF + O_2 \rightarrow CO_2 + H_2O \tag{2.8}$$

The exhaust gas that flows through the small channels of the catalyst comes in contact with the platinum group metals (PGMs) that are coated on the monolith. As diesel engines spend all the operating time running on lean air-fuel ratios, there is a sufficient amount of oxygen, which is consumed by the combustion products, as shown in the equations above. Another important parameter that greatly influences the chemical reactions (2.6-2.8) is temperature. Conversion efficiency, which is a strong function of exhaust temperature, can exceed 90% at elevated temperatures.

2.3.2 Selective catalytic reduction

The selective catalytic reduction is a well proven technology for the reduction of NO_x emissions in stationary and marine diesel engines. In mobile diesel applications, EGR is typically employed to offer the required reductions. However, due to stringent NO_x limits, EGR alone is no longer capable of bringing NO_x to such low levels. Hence, incorporation of SCR systems in the exhaust pipe of diesel-powered vehicles is required in order to comply with the current NO_x limits. Traditionally, ammonia (NH_3) that is injected into the exhaust pipe evaporates and mixes with the exhaust gas and then enters the catalyst where

NO_x emissions are broken down. Nevertheless, due to toxicity and handling issues of NH_3 it is not feasible to use it in mobile diesel engines. Extensive research found urea to be an acceptable alternative to NH_3, meeting technical and commercial requirements. Figure 2.5 shows a simplified (in terms of both structure and chemical reactions) SCR system in which diesel exhaust fluid (DEF) is injected upstream of the catalyst into the exhaust pipe. DEF, also referred to as Ad-Blue, is an aqueous solution composed of 32.5% urea and 67.5% deionised water. When the exhaust gas temperature is over 160 °C, it forms NH_3 through a series of reactions in the decomposition reactor.

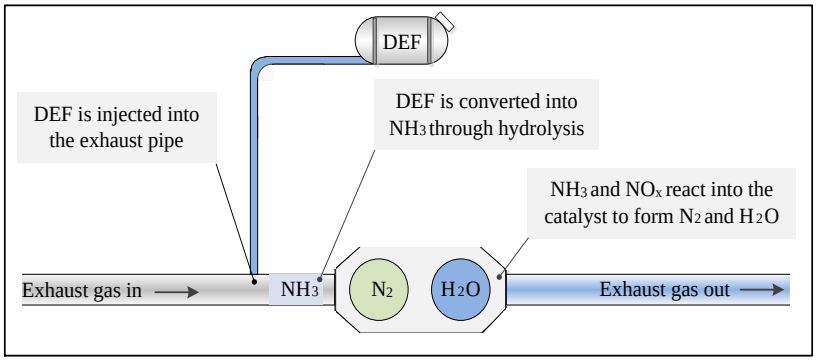

Figure 2.5: Selective catalytic reduction system.

The following urea decomposition and NO_x conversion reactions can take place:

$$CO(NH_2)_2 = 2 \cdot NH_2 + CO \quad (2.9)$$

$$CO(NH_2)_2 + H_2O = 2NH_3 + CO_2 \quad (2.10)$$

$$\cdot NH_2 + NO = N_2 + H_2O \quad (2.11)$$

$$6NO + 4NH_3 = 5N_2 + 6H_2O \quad (2.12)$$

$$4NO + 4NH_3 + O_2 = 4N_2 + 6H_2O \quad (2.13)$$

$$6NO_2 + 8NH_3 = 7N_2 + 12H_2O \quad (2.14)$$

$$2NO_2 + 4NH_3 + O_2 = 3N_2 + 6H_2O \quad (2.15)$$

2.3.3 NO_X adsorber

The NO_x adsorber is an alternative to SCR that uses a storage component such as barium (Ba), calcium (Ca), potassium (K) and sodium (Na) to trap the NO_x emitted from a lean burn internal combustion engine. When excess oxygen exists in the combustion products, NO_x is stored via the oxidation of NO to NO_2:

$$NO + \frac{1}{2}O_2 = NO_2 \quad (2.16)$$

and subsequently stored in the trap as nitrate species:

$$NO_2 + MO = MNO_3 \quad (2.17)$$

Decomposition of the stored nitrate species takes place when the engine operates either in fuel-rich conditions or at elevated temperatures:

$$MNO_3 = NO + \frac{1}{2}O_2 + MO \quad (2.18)$$

The reduction of NO over the trap is described by the following chemical equation:

$$NO + CO/HC = \frac{1}{2}N_2 + CO_2/H_2O \quad (2.19)$$

Equation (2.19) requires high temperatures otherwise a NO_x spike can occur during the regeneration [31]. Conversion efficiency of as high as 80-90% has been reported with the maximum performance typically occurring in the 350-380 °C range [32].

2.3.4 Diesel particulate filter

The DPF captures the emitted particulate matters and can demonstrate filtration efficiency in excess of 90% [33]. The operating principle is based on the separation of gas-borne particles from the exhaust gas stream by deposition on the filter walls. Figure 2.6 schematically illustrates how the DPF operates.

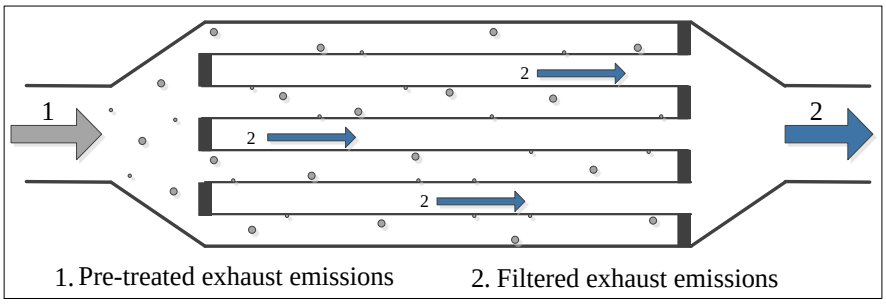

Figure 2.6: Function of the diesel particulate filter.

The structure of the filter consists of a series of dead end channels running parallel in the axial direction. The exhaust gas is forced to travel through the porous tube walls to an exit,

which results in particles being deposited on the filter walls. Frequent regeneration of the filter is required to burn off the accumulated particulates, which increase the exhaust back pressure causing adverse effects on available engine torque and fuel consumption [34].

2.4 Diesel combustion

The description of diesel combustion is essential in order to improve engine efficiency and gain insight into the emission formation and destruction mechanisms. Based on the combustion concept, various conceptual models that describe the spray formation, vaporisation, mixing, ignition and pollutant formation and destruction mechanisms have been proposed [35, 36, 37]. The conceptual model for conventional diesel combustion during the quasi-steady phase, as proposed by Dec [36], is depicted in Figure 2.7. The liquid fuel vaporises as it travels from the nozzle down the jet since it rapidly entrains in the hot in-cylinder air. This results in the formation of a sheath-like fuel-vapour/air mixture layer along the sides of the jet. The initial fuel oxidation occurs as the fuel-vapour/air flows into the jet, which is being exposed to high temperatures, while the final oxidation takes place at the border of the jet. The rate of combustion increases as more fuel-vapour/air and hot combustion products re-entrain into the penetrating jet. This actually constitutes the main idea of the two-stage fuel oxidation as shown in Figure 2.7 [37].

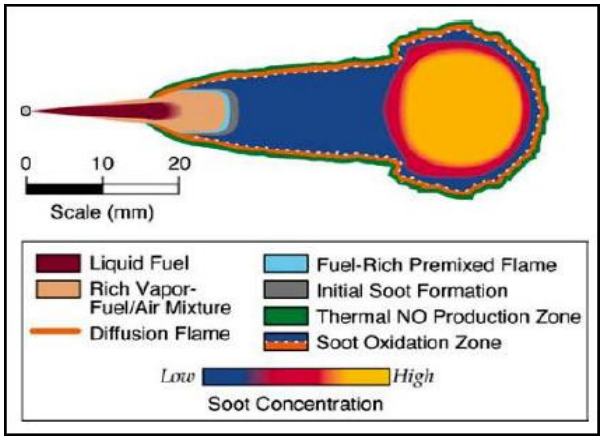

Figure 2.7: Schematic of Dec's conceptual diesel combustion model during the quasi-steady period of diesel combustion [36].

In addition to the discussion provided in the previous paragraph, a more complete picture of diesel combustion can be obtained by presenting the different stages of the combustion

process (from the start of injection (SOI) to the end of combustion (EOC)). The apparent heat release rate (AHRR), which can be evaluated by the in-cylinder pressure data, is very useful in characterising the combustion process. Figure 2.8 shows the in-cylinder gas pressure, temperature and the calculated AHRR obtained from a 5.79 litre heavy-duty diesel engine operating at 1000 revolutions per minute (rpm) and two different equivalent ratios (φ) 0.41 and 0.53 [38].

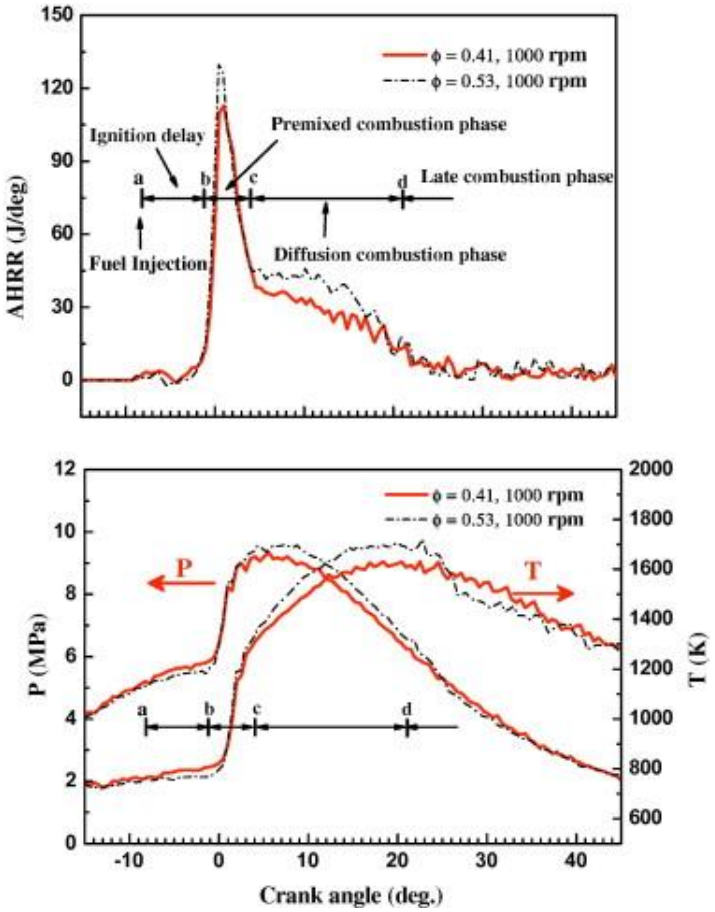

Figure 2.8: Defined phases of diesel combustion [38].

Marked on the graphs are the different combustion phases, which are detailed below:

a: *Start of fuel injection (SOI)* is taken either as the time when the injector needle lifts off its seat (when there is a needle lift indicator) or as the time the engine control unit (ECU) sends a signal to the injector (when there is no needle lift indicator).

a-b: *Ignition delay (ID)* is the time interval between SOI and start of combustion (SOC). Due to the heat absorbed by the evaporating liquid fuel, the AHRR during ID is typically negative. Some of the parameters affecting the duration of ignition delay are the engine

operating conditions, the quantity of the fuel being injected, the injection timing and the level of intake air dilution.

b-c: *Premixed combustion* refers to the phase of combustion that takes place after the ID period. A ready to ignite fuel-air mixture is formed during the ID phase and combustion starts once the autoignition temperature of diesel has been reached. As shown in Figure 2.8, the rate of pressure, temperature and apparent heat release rise is very rapid causing undesirable effects. In fact, the characteristic diesel engine noise is associated with this combustion phase. In addition, the high temperature and oxygen availability favours the production of NO_x emissions. Depending on the shape of the AHRR curve, the end of premixed combustion is defined either as the local minimum after the first spike [39, 40] or as the point at which there is a significant reduction in the gradient of the AHRR curve after the first spike [38].

c-d: *Diffusion combustion*, also referred to as mixing-controlled combustion, starts immediately after the premixed combustion and finishes at the end of fuel injection. The rate of fuel consumption is governed by the injection rate and subsequent mixing with air. Local fuel-rich mixtures during this combustion phase, along with the high in-cylinder temperature, promote the formation of soot.

d-end of combustion (EOC): *Late combustion* provides the opportunity to any remaining fuel or partially-burned products to burn at a much lower rate, provided that adequate motion still exists within the cylinder.

2.5 Alternative diesel combustion modes

Alternative diesel combustion strategies [41-44] show promising potential for the reduction of emission formation. Extensive research is being carried out in order to overcome the various issues that hinder a large-scale introduction of such combustion modes in diesel engines. Some of the challenges being faced are combustion controllability, emissions trade-off effects, fuel consumption penalties and the requirement of sophisticated fuel control units. The following section covers the workings as well as some of the findings from recent research efforts on low temperature combustion (LTC), homogenous charge compression ignition (HCCI), premixed charge compression ignition (PCCI) and reactivity controlled compression ignition (RCCI).

2.5.1 Low temperature combustion

The main objective of LTC is to alter the combustion chemistry of conventional diesel engines in order to minimise the formation of pollutants. The reduction of engine-out emissions, among other advantages, can benefit the aftertreatment devices as less complexity and cost are involved in achieving the same emission limits.

A major challenge with all LTC concepts is the difficulty in controlling the combustion process; hence, the operating range of the engine is significantly limited when adopting such combustion concepts. In addition, application of LTC typically results in trade-off effects between emission formation and fuel consumption. The above issues clearly indicate that certain challenges need to be overcome before large-scale adoption of LTC.

Feng et al. [45] studied the effects of EGR on engine combustion and emissions, using five different diesel blends. The experiments were performed on a modified compression ignition engine operated in LTC mode. It was found that an addition of EGR leads to thermal efficiency reduction, extends the ignition delay and increases the HC and CO emissions. It was also shown that the thermal efficiency decreases, start of combustion delays and maximum heat release rate increases when the initial boiling point of the fuel is reduced.

The fuel suitability in a high compression ratio engine operating at high-load conditions has been investigated by Han et al. [46]. The authors tested the suitability of four fuels (diesel, gasoline, n-butanol and ethanol) and fuelling strategies for LTC operation by examining the emission performance and the combustion controllability. When neat diesel operation was applied, LTC was enabled at 0.8 and 1.0 MPa IMEP with extremely high EGR rates required in order to combust the fuel in the LTC region. According to the authors, gasoline/diesel combustion exhibited low NO_x and soot emissions at 0.8-1.0 MPa IMEP load operation, but a further increase in load imposed problems. Operation with n-butanol revealed that high pressure direct injection of the fuel was more advantageous compared to port injection. In the latter case, premature auto-ignition of the fuel has a detrimental effect on the emission performance. Finally, it was found that ethanol/diesel combustion is suitable for high-load LTC operation as it is beneficial to both combustion control and emission.

2.5.2 Homogenous charge compression ignition

The HCCI combustion mode is a method of achieving LTC, which can simultaneously reduce NO_x and smoke emissions. Figure 2.9 shows the region, in terms of temperature and equivalence ratio, of such a combustion mode. It is clear that the NO_x and soot producing zones are largely avoided, altering this way their formation chemistry. The reduction of soot is accomplished by creating a homogenous air-fuel mixture in the combustion chamber, thus preventing the formation of local fuel-rich zones in which much of the soot is produced. The combustion temperature is located to the left of the NO_x formation zone; thus, the formation of NO_x is largely suppressed. The drawbacks associated with this combustion mode are increased CO and HC emissions as well as limited operating range. Stanglmaier and Roberts [47] found that fuel admission is critical in reducing fuel-wall wetting in HCCI engines.

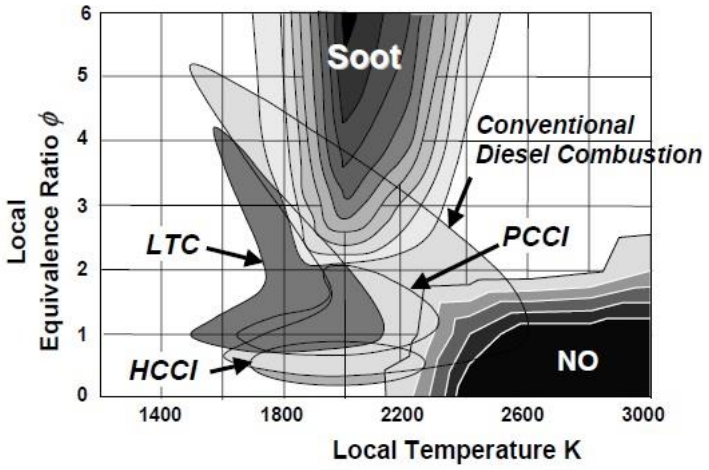

Figure 2.9: Equivalence ratio-temperature diagram of different combustion concepts [48].

Various methods have been proposed for the formation of a homogenous mixture, including port diesel injection and early direct injection. The former technique ensures the longest interval between SOI and start of ignition. Clearly, this gives the longest possible time for the mixing of diesel with air. However, this method is practically unfeasible as it suffers from poor ignition control, high HC and CO emissions and fuel consumption penalties, to name a few issues. Direct injection strategy, for early or late diesel injection, offers a good flexibility in switching combustion modes, depending on the operating conditions.

Guo et al. [49] experimentally investigated the effect of hydrogen enrichment on the combustion and emission performance of an HCCI diesel engine. Both fuels (hydrogen and diesel) were introduced into the engine through the intake port, while the intake air was diluted using EGR. It was reported that introduction of hydrogen resulted in retarded combustion phasing and reduced combustion duration. Also, it was demonstrated that the indicated specific CO and HC emissions were decreased when hydrogen was admitted into the engine. In addition, it was shown that supply of hydrogen at extra lean conditions without EGR is more effective compared to high EGR and near stoichiometric mixture. However, it was observed that hydrogen may increase the knocking tendency of the HCCI engine.

2.5.3 Premixed charge compression ignition

The PCCI is another LTC concept that can offer emissions reduction. In contrast to HCCI, in this combustion strategy, the air-fuel mixture is not entirely homogenous. In fact, it is quite difficult to obtain a fully homogenous diesel-air mixture due to the low volatility and low auto-ignition temperature of diesel. In a PCCI engine, the air-fuel mixture ignites spontaneously; thus, no flame propagation occurs as happens in a conventional diesel engine. This results in high pressure rise rates, which can reduce the engine life.

The premixed charge within the cylinder is typically achieved by early fuel injection. Certain drawbacks associated with this injection strategy, such as wall-wetting, can be detrimental to HC and CO emissions. Boot et al. [50] investigated whether uncooled EGR can reduce wall-wetting when early diesel injection is employed. The elevated by 40-60 °C intake temperature promoted better evaporation of diesel fuel. The authors reported significant smoke number reduction with simultaneous IMEP improvement. Additionally, they proposed that more research is required in order to obtain acceptable efficiency.

Based on their study, Beatrice et al. [51] reported that compression ratio (CR) is the most effective parameter in controlling the ignition delay in a PCCI engine. The CR should be carefully optimised as neither too low nor high is desirable. The former may increase the fuel consumption and cause cold engine stability issues, whereas the latter can reduce the benefits of PCCI as the combustion approaches that of conventional diesel engines. It was shown that adoption of low CR resulted in significant smoke reduction and negligible change on fuel consumption at the expense of HC and CO emissions. NO_x emissions,

which remained relatively unaffected, were controlled using EGR. The authors concluded that a CR around 15.5 is the best compromise for the engine under investigation.

Leermakers et al. [52] investigated the effects of fuel composition on PCCI combustion in a heavy-duty diesel engine. It was found that the mixing time was increased when a lower cetane number diesel was used. This resulted in less NO_x and smoke emissions at the expense of CO, HC and fuel consumption. It was also reported that in the conditions under investigation, the use of n-heptane as the diesel surrogate in modelling studies gives underestimated CO and HC emissions and overestimated NO_x emissions.

2.5.4 Reactivity controlled compression ignition

RCCI is typically realised by delivering two distinct fuels with different reactivities into the combustion chamber. The low reactivity fuel is supplied first, well before the injection of the high reactivity fuel. This technique ensures that the low reactivity fuel is thoroughly mixed with air and ignites spontaneously once the combustion of the high reactivity fuel initiates. By employing that combustion mode, increased fuel efficiency, ultra-low NO_x and PM as well as reduced heat transfer losses can be achieved.

Part of Splitter's et al. [53] study dealt with an RCCI single-cylinder heavy-duty engine operated at a fixed load and speed of 6.5 bar IMEP and 1300 rpm, respectively. Port injected E85 represented the low reactivity fuel, whereas cetane improved gasoline (direct injected into the cylinder) represented the high reactivity fuel. Under this operating mode, the authors reported a gross indicated thermal efficiency near 60% as well as near-zero NO_x and PM emissions.

Hanson et al. [54] performed experiments on a heavy-duty 2.44 litre Caterpillar 3401 single-cylinder engine operated in RCCI mode. The engine speed was varied between 800 and 1700 rpm, while the load was set at 2 and 4.5 bar gross IMEP. Throughout their experiments they employed a dual fuel and a single-fuel strategy. In the former strategy, port gasoline and direct diesel injection was used. In the latter strategy, gasoline was employed in both streams, but the cetane number of the direct injection stream was increased by adding 2-Ethylhexyl Nitrate. The authors concluded that both fuelling strategies resulted in NO_x and PM emissions below the US EPA 2010 HD on-road limits,

without fitting the engine with aftertreatment systems. They also demonstrated that both fuel strategies increased thermal efficiency.

The efficiency and emissions mapping of an RCCI light-duty diesel engine was carried out by Curran et al. [55]. The engine, operated over a wide range of speed and load conditions, was fuelled by gasoline and ultra-low sulphur diesel. Based on the operating conditions, diesel was delivered into the cylinder either through a single or a split injection and the results obtained were compared to the conventional diesel operation. According to the authors, the RCCI engine showed diesel-like thermal efficiency at lower speeds and loads, while up to 5% efficiency improvement was achieved at higher speeds and loads. In addition, the RCCI mode was reported to produce lower NO_x but higher CO and HC emissions, compared to the conventional diesel combustion (CDC).

2.6 Injection parameters

The fuel injection system plays a major role in diesel atomisation, mixture formation and flame evolution, which are very important in obtaining good combustion quality. Accurate control of the time, pressure and amount of fuel delivered into the cylinder can significantly improve the performance as well as pollutant and noise emissions of a diesel engine. Moreover, the success of alternative combustion modes and alternative fuels greatly depends on the adoption of advanced injection systems.

2.6.1 Injection timing and pressure

Diesel injection timing can easily be adjusted by triggering the injector at the desired time. The in-cylinder conditions at the time the fuel is delivered into the combustion chamber significantly affect the combustion process.

When injection timing is advanced, the fuel entering the combustion chamber is exposed to a lower temperature and pressure. This gives more time for the fuel to mix with the in-cylinder air since the onset of combustion occurs only when the in-cylinder temperature reaches the autoignition temperature of diesel. As a result, the premixed burn fraction is increased leading to high NO_x production. Soot formation, which in general is increased with diffusion burn fraction, tends to decrease as injection timing is advanced. The high combustion temperature, caused by the rapid premixed combustion, promotes the oxidation of the soot produced in the rich fuel regions. The early injection timing is

detrimental to THC emissions as the spray tip penetrates deeper (because of the lower charge density) leading to spray wall impingement. A long ignition delay may result in over-mixed regions, which are not desirable as the flame cannot propagate to fully burn the fuel.

Retardation of injection timing leads to a decrease in NO_x and THC at the expense of soot emissions. The fuel is delivered to higher in-cylinder temperature (compared to advance injection); hence, the premixed burn fraction is reduced due to the shorter ignition delay. This is actually a dominant main factor leading to the reduction in NO_x emissions. The reduction in THC emissions is attributed to the increased in-cylinder density, which leads to a decrease in spray wall impingement. The rise in soot emissions is mainly attributed to the increase in diffusion burn fraction, along with the reduction of the in-cylinder temperature. Concerning thermal efficiency, the optimum injection timing can vary depending on the operating point of the engine. In general, when diesel injection is commenced too early, the increased in-cylinder pressure forces the piston down before it reaches the TDC and thus negative work is being performed. Delayed injection can also be problematic as fuel burn during the expansion stroke limits the maximum in-cylinder pressure.

Development of the high pressure common rail fuel system brought about a revolution in diesel engines as it allows injection of high pressure fuel, currently up to 2500 bar [56]. A number of studies have shown that an increase in fuel injection pressure promotes the fuel-air mixing, which favours the reduction of pollutant emissions and fuel consumption [35, 57]. Understanding of diesel spray characteristics such as spray tip penetration, droplet size distribution and spray structure is very important in optimising the combustion process. Generally, a reduction in injector nozzle-hole is a technique that allows generation of small size fuel droplets. However, this measure can be detrimental to spray tip penetration as the spray momentum is reduced. The negative impact on spray penetration can be tackled by employing a common rail system. Combination of high injection pressures with small nozzle-holes can considerably contribute to the improvement in combustion efficiency.

In their work, Chen et al. [58] employed a common-rail high-pressure fuel injection system to study the fuel spray and atomisation characteristics of different fuels. They

concluded that droplet size is decreased as the injection pressure is increased. In particular, they showed a 50% decrease in droplet size when injection pressure was increased from 300 to 1000 bar. They also proved that at the spray periphery droplets are bigger compared to those in the centre due to pressure drop. In addition, they showed that under higher injection pressures the spray penetrates deeper, small droplets distribute in a narrower region and have less variation in their sizes. An increase in injection pressure enhances atomisation and shortens the ignition delay as a result of the better fuel-air mixing [59].

2.6.2 Multiple injection and rate shaping

The fuel can be delivered into the cylinder by adopting either a single injection event or multiple injection events. The latter can be used to reduce the combustion noise as it allows reduction of the peak heat release. For instance, a double injection strategy can give two separate heat release peaks with lower maximum values compared to the heat release value of a single injection event [60]. Moreover, the use of pilot injection has a positive impact on the formation of NO_x emissions as it reduces the ignition delay period. The corresponding increase in soot emissions can be mitigated using post injection [61]. From the above it is clear that a pilot-main-after injection strategy may contribute to simultaneous improvement of NO_x, soot and noise emissions.

Injection rate shaping is a technique that allows further optimisation of the combustion process in direct injection diesel engines. The introduction of fast response solenoid valves and piezo-electric technology in injectors enables a better control of the fuel delivery into the cylinder [62]. Simultaneous control of needle lift, injection pressure and injection timing, as shown in Figure 2.10, can influence the formation of NO_x, soot and noise emissions.

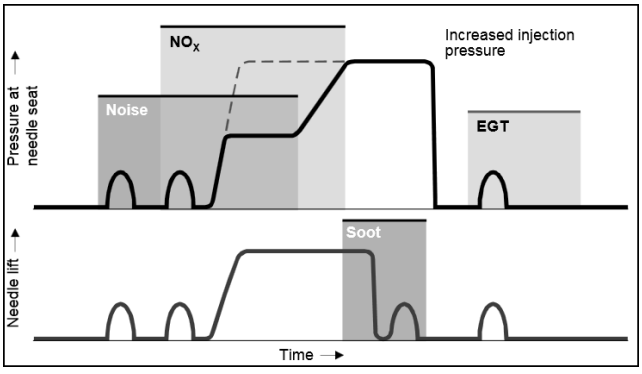

Figure 2.10: Multiple injections and injection rate shaping for future diesel engine [63].

Adoption of a steep injection rate causes a deeper spray penetration and a wider spray plume, which results in a more thoroughly mixed air with fuel [64]. After the onset of combustion, a gradual rise in injection rate results in a smaller high temperature zone, because the combustion process becomes slower. This injection technique may contribute to the reduction of NO_x emissions. The formation of soot can also be reduced [65]. It has been reported that when injection rate shaping is considered, a sharp end of injection pattern should be adopted in order to minimise the formation of soot from fuel entering into the cylinder late in the combustion process [66].

Both injection rate rise and injection pressure affect ignition delay. However, under high injection pressures the effect of injection rate shaping on ignition delay becomes small. This is due to the fact that under high injection pressure the injection rate shaping has a minor effect on the formation of the mixture as the momentum of the fuel is mainly influenced by the fuel pressure [67].

2.7 Alternative fuels and dual fuel

The objectives of using alternative fuels in the automobile sector include reduction of harmful emissions and greenhouse gases (GHG), enhancement of engine thermal efficiency, sustainability and increased independence from fossil fuels (when they come from renewable energy sources). Nevertheless, there are several factors that hinder the transition from the traditional automotive fuels (i.e. diesel and gasoline) to the proposed alternative ones, including refuelling infrastructure, transportation, storage and safety issues as well as combustion and engine related issues. Much research on alternative fuels, which aims to address the issues preventing them from a large-scale adoption by the automobile sector, is underway. The findings show that dual fuel (for instance, diesel-hydrogen and diesel-syngas) could serve as a transition solution to alternative fuels. This section provides information on the alternative fuels that are considered as potential future energy carriers.

2.7.1 Hydrogen

Chemical compounds of hydrogen such as water and hydrocarbons constitute a large part of the Earth's surface; thus, a trend towards hydrogen economy is not unexpected, taking into account its desirable properties. The use of hydrogen gas as a fuel for compression

ignition engines has been investigated by many researchers and some of the findings are presented below.

Introduction of hydrogen into the combustion chamber of a diesel engine can be realised either by port injection or direct injection. In the former method, hydrogen is typically injected into the intake pipe at a pressure slightly above atmospheric, whereas in the latter method, hydrogen is directly injected into the cylinder during the compression stroke [68]. In both methods, the combustion is typically initiated by diesel since the autoignition temperature of hydrogen (585 °C) is usually not reached.

Saravanan et al. [69] performed experiments on a single-cylinder direct injection (DI) diesel engine, modified to allow injection of hydrogen into the intake port during the suction stroke. Diesel injection was fixed at 23 degrees crank angle (deg. CA) before injection top dead centre (BITDC), while hydrogen injection timing and duration varied from 5 crank angle degrees before top dead centre (CAD BTDC) to 5 crank angle degrees after dead centre (CAD ATDC) and from 30 to 90 CAD, respectively. The authors claimed a 5.8% brake thermal efficiency increase when fuelled by diesel-hydrogen due to the enhanced combustion. They also reported simultaneous NO_x-smoke emissions reductions during the dual fuel mode. The reduction of NO_x has been attributed to the leaner equivalence ratios.

According to Shirk et al. [70], the hydrogen-assisted combustion does not affect the drivability of the vehicle. It was also demonstrated that hydrogen addition slightly reduced thermal efficiency and NO_x emissions. The results were obtained from a car equipped with a CI engine, running on a chassis dynamometer with 0%, 5% and 10% of the fuel energy derived from fumigated hydrogen.

A number of studies [71-74] have found that part substitution of diesel with hydrogen has a detrimental effect on NO_x emissions due to the high adiabatic flame temperature of hydrogen. The use of combined hydrogen and EGR has been proposed in order to mitigate the adverse effect on NO_x emissions. The latter can be employed to bring down the combustion temperature.

It has been mentioned in Section 2.1.1 that the formation of NO_x emissions is primarily associated with the combustion temperature. Introduction of hydrogen into the engine

typically causes an increase in combustion temperature with a detrimental effect on NO_x emissions. Some studies present a reduction in NO_x emissions when the main fuel is partly substituted by hydrogen [69, 75]. In essence, there are several factors that can influence the combustion temperature, which under certain conditions may have a significant effect on the high temperature zone. To name a few, the structure of the engine, the operating point, the equivalence ratio as well as the small quenching distance and the high heat capacity of hydrogen can affect the combustion temperature. Concerning the effect of hydrogen enriched combustion on carbonaceous emissions, a general agreement exists among all researchers; namely, an increase in the proportion of hydrogen in the fuel results in less carbonaceous emissions [69, 71, 76]. The reason is that under the same operating conditions the amount of carbon contained in a diesel-hydrogen mixture is always lower compared to that contained in diesel.

Hydrogen enriched combustion is capable of enhancing the function of the aftertreatment devices. Wichterlova et al. [77] demonstrated that hydrogen addition over a SCR catalyst significantly improved NO_x conversion. In their study, Bromberg et al. [78] showed that introduction of hydrogen into the exhaust stream can assist the regeneration process of the DPF. The exhaust gas temperature of a diesel engine might not be high enough to burn off the accumulated particles; hence, the oxidation of hydrogen can raise the temperature to the required levels.

2.7.2 Syngas

Syngas, or synthesis gas, is a mixture primarily made up of hydrogen and carbon monoxide at various compositions. In principle, it can be produced from any hydrocarbon feedstock. In diesel engines, on-board syngas production is achieved by injecting diesel fuel in a catalytic fuel reformer integrated within the exhaust pipe. The producer gas, which is mainly a mixture of syngas and EGR, is then sent back to the engine through the intake pipe [79].

The composition of the producer gas, which has been reported to affect engine performance and emissions, depends on the reactions promoted during the reforming process as well as the feedstock being used. Sahoo et al. [80] performed experiments with three different volumetric compositions of syngas (H_2:CO composition, 100:0, 75:25 and 50:50) in a diesel engine under dual fuel operation. It was concluded that the gaseous fuel

with 100% hydrogen content exhibited an improved engine performance at the expense of NO_x emissions, compared to the syngas that contained CO. In addition, it was found that CO and HC emissions increased as the percentage of CO in the gas mixture was increased.

In their paper, Bika et al. [81] demonstrated that part substitution of diesel fuel with syngas, in any H_2/CO proportion, resulted in a reduction in engine efficiency. It was also reported that the unburned syngas escaping in the exhaust was the main factor that led to efficiency reduction. Furthermore, it was shown that NO_2/NO ratio roughly doubled when syngas was admitted into the engine because of the increased HO_2 radicals.

Variations in flame speed are expected at different H_2/CO ratios. Dong et al. [82] used a Bunsen burner to measure the laminar flame speed of syngas over a wide range of fuel compositions and equivalence ratios. They concluded that laminar flame speed increased with the concentration of hydrogen. They also demonstrated that the laminar flame speed of an H_2/air mixture and a CO/air mixture reached its maximum value at the equivalence ratio of 1.7 and 1.6, respectively.

Supply of syngas in a compression ignition engine, produced by on-board diesel fuel reforming, can lead to a reduction in engine-out emissions. In addition, it can be used as a means of thermal efficiency improvement and combustion stability [83]. Similarly to hydrogen, syngas is beneficial to the function of exhaust aftertreatment systems when it is present in the exhaust gas.

2.7.3 Liquefied petroleum gas

Liquefied petroleum gas (LPG) is a mixture of propane and butane derived from fossil fuel sources and is the third most popular fuel being used in automobiles worldwide [84]. It has a higher specific energy density (kJ/kg) than liquid fuels (diesel and gasoline); however, the latter prevail when comparing the energy density by volume (kJ/L). The density of LPG is greater than air, posing both explosion and suffocation risks in case of leakage, as it tends to settle in low spots. Its high octane number and auto ignition temperature makes it more suitable for engines using the Otto cycle [85]. When LPG is used in compression ignition engines, an amount of diesel is required in order to initiate the combustion. A number of studies have revealed emission and performance benefits from supplying a mixture of diesel and LPG in compression ignition engines.

Fuel cost savings up to 2.3 euro/100 km have been estimated by fuelling a Volvo city bus with an LPG-diesel blend [86]. The gaseous fuel was supplied into the intake manifold of a 7.1 litre diesel engine through a retrofit system. It was also reported that dual fuelling did not significantly affect NO_x and CO_2 emissions, but it offered PM reductions, which can benefit vehicles without DPF.

A study investigating the effects on the combustion parameters from the admission of hydrogen or LPG into the intake manifold of a dual fuel diesel engine has been published recently [87]. It was shown that the peak cylinder pressure under diesel-LPG (supply of 50% LPG) operation was higher than that at the baseline operation. At the same LPG fraction, heat release rate was always lower compared to the neat diesel operation.

Saleh [88] experimentally proved that admission of propane (up to 40% gaseous fuel mass fraction) into the inlet manifold of a diesel engine increased the fuel conversion efficiency. This study also compared the fuel conversion efficiency obtained by fuelling the engine by neat propane and propane-butane blends. It was demonstrated that fuel conversion efficiency dropped with the increase in butane concentration in the gas mixture. Nevertheless, the increase in butane proportion has a beneficial effect on NO_x emissions.

2.7.4 Compressed natural gas

Compressed natural gas (CNG) can either be found above oil deposits or can be produced by the breakdown of organic matter in an anaerobic environment. It is considered a renewable energy source when it is originated from the latter process. Its density is lower than air and this makes it safe in case of leakage because it disperses and mixes readily with the ambient air. When used in compression ignition engines, the onset of combustion is achieved through the injection of diesel or a fuel having diesel-like properties.

A study aimed at evaluating the performance and pollutant emissions of a diesel and a CNG waste collection truck in the city of Milan has been presented by Fontaras et al. [89]. The authors concluded that CNG fuelled vehicles (running on the Otto cycle) are less NO_x and PM emitting, but the diesel counterparts prevail when it comes to CO, HC and GHG emissions. According to the authors, taking into account that the engine-out NO_x and PM emissions are expected to be effectively treated in Euro VI compliant engines, the diesel

ones likely to be better for the environment than CNGs. However, CNG is still an attractive fuel due to the energy security it provides.

Abdelaal and Hegab [90] performed experiments on a natural gas fuelled diesel engine and demonstrated that NO_x emissions were considerably reduced, whereas CO and HC significantly increased compared to diesel only operation. From the findings of Fontaras and Abdelaal and Hegab we may conclude that when CNG is supplied in either engine type (gasoline or diesel) the effect on NO_x, CO and HC emissions is the same.

In their study, Namasivayam et al. [91] tested three alternative pilot fuels, dimethyl ether (DME) and two water-in-biodiesel emulsions with 5% and 10% water by volume in order to assess the effects on the performance and emissions of a compression ignition engine fuelled by natural gas. It was reported that both pilot emulsions produced higher CO and HC emissions than the DME pilot. DME exhibited lower NO_x emissions apart from the high-load operation. It was also shown that the worst thermal efficiency was obtained from the DME pilot fuel.

2.7.5 Biodiesel

Biodiesel is derived from vegetable oils or animal fats that undergo a chemical process called transesterification producing methyl esters (biodiesel) and glycerin as byproduct [92]. Owing to similar properties to petrodiesel, biodiesel can be used to fuel compression ignition engines with minor modifications. It is typically blended with petroleum diesel and the properties of the mixture can significantly vary, depending upon biodiesel feedstock and the concentration of biodiesel in the petroleum diesel. The B factor is commonly used to classify such a blend and states the volume percentage of biodiesel in diesel. For instance, a B100 fuel would contain only biodiesel, whereas a B50 would be composed of 50% biodiesel and 50% petrodiesel.

Biodiesel reduces the dependence on fossil fuels as it is made from renewable sources. In addition, it reduces the net carbon dioxide emissions due to the closed loop of carbon cycle. When biodiesel is burned, the CO_2 released into the atmosphere is absorbed by the plants, which are later used for the production of biodiesel [93].

In their paper, Lapuerta et al. [94] reviewed the effect of biodiesel fuel in diesel engines. In general, they found that a wide disparity of results exists in the literature, and this is

attributed to several reasons such as: different engine technologies, operating conditions and driving cycles used as well as varying biodiesel types and measurement techniques. Despite this, they concluded that overall the following general trends hold true: Supplying biodiesel into the engine does not significantly affect thermal efficiency as the increased bsfc is in proportion to the reduction in heating value. Biodiesel contributes to a minor increase in NO_x emissions as reported in the majority of the papers. Concerning particulate emissions, many scientists agree that the engine is less PM emitting when fuelled by biodiesel mixtures; however, that finding might not hold true under cold operation. In addition, there is a general agreement among the researchers that the higher oxygen content of biodiesel contributes to a reduction in both CO and THC emissions, compared to diesel operation.

Atadashi et al. [95] provide a discussion on biodiesel biodegradability, lubricity, stability and physiochemical properties. Biodiesel can be used in sensitive environments such as marine engines as it is non-toxic and degrades in soil and water. It also features better lubricity than petroleum diesel benefiting both fuel injectors and pump, provided that a good quality biodiesel is supplied, otherwise there is a risk of clogging the injectors. In order to increase its stability, antioxidant additives might be required in case the fuel will not be used soon.

2.8 Exhaust gas assisted fuel reforming

On-board production of hydrogen using hydrocarbon fuels is deemed as a transition solution until issues with hydrogen infrastructure, distribution and on-board storage are resolved. This technique requires injection of fuel into a catalytic reformer, integrated into the EGR loop. The hydrogen-rich exhaust gas, capable of improving the combustion and emissions of the engine, is delivered back to the cylinders. In addition to hydrogen, and depending on the reactions promoted, a significant amount of CO can be produced during the reformation process. Unlike fuel cells, combustion of gaseous CO in a diesel engine does not contaminate any component of the engine.

The reactions involved in producing a hydrogen-rich or a syngas-rich gas stream are steam reforming, water-gas shift reaction, partial oxidation, endothermic dry reforming reaction, autothermal reforming and thermal decomposition of the fuel. A combination of the aforementioned reactions may take place during the fuel reforming process.

Tsolakis et al. [96] incorporated a laboratory reforming mini reactor in the exhaust system of a single-cylinder diesel engine to produce a hydrogen-rich gas. According to the authors, the reformer products contained up to 16% hydrogen. It was also indicated that the main reactions in the reformer were the complete oxidation and the steam reforming. Moreover, it was found that simulated REGR with 14% hydrogen content can benefit the trade-off between NO_x and smoke emissions in diesel engines.

In a different research paper, Tsolakis and Megaritis [97] studied the effects of supplying simulated reformer product gas in a diesel engine. It was concluded that a low level of REGR can offer simultaneous reductions in NO_x and smoke emissions. Additionally, it was found that further smoke reductions can be achieved by increasing the REGR level, but at the expense of NO_x emissions. Adjustment of fuel injection timing was proven advantageous to NO_x emissions without any detrimental effect on smoke.

Abu-Jrai et al. [98] studied the effects of simulated REGR on engine performance and SCR system. Figure 2.11 illustrates the engine-REGR-SCR system proposed by the authors. The SCR catalyst used throughout their study was a 1% Pt/Al_2O_3. Among other findings, it was shown that REGR can benefit both the engine and the SCR performance. The unburned hydrogen present in the exhaust gas enhanced the NO_x reduction performance of the catalyst.

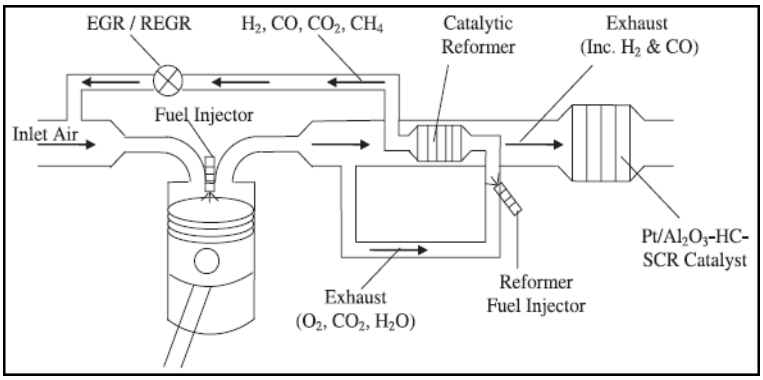

Figure 2.11: Schematic representation of the proposed engine-REGR-SCR system [98].

It has been demonstrated that the utilisation of simulated syngas is poor when the engine operates under low-load conditions [79]. This is due to the inefficient propagation of flame in the gaseous fuel when the concentration is below its lower flammability limit (LFL). In addition, under low-load operation, the amount of diesel delivered into the cylinder is

relatively small; hence, the resulting flame cannot fully burn the gaseous fuel, which burns by entraining into the liquid fuel. The poor utilisation of the gaseous fuel has a detrimental effect on thermal efficiency.

2.9 Dilution of the intake air

Dilution of the intake air is a technique that allows a reduction in engine-out NO_x emissions. To date, the most widely used method is the EGR in which an amount of exhaust gas is recirculated back to the intake pipe, resulting in a reduction in oxygen concentration in the intake air. EGR can be employed relatively easily to conventional diesel engines and is a common practice to meet the emission standards. However, there are certain drawbacks associated with EGR that can be eliminated by introducing alternative intake air dilution methods.

Enrichment of the intake air with nitrogen is a dilution method that has been proposed and implemented by various researchers [99, 100, 101]. In both EGR and nitrogen enrichment techniques, the main factor behind the decrease in NO_x emissions is the reduction in oxygen concentration in the intake air, leading to a drop in peak combustion temperature. It should be mentioned that the knowledge gained from the nitrogen enrichment studies can benefit the development of on-board reforming technology since the producer gas leads to an increase in N_2/O_2 ratio in the inlet air. The implementation of dilution techniques has an adverse effect on CO, THC and smoke emissions [102]; however, part substitution of diesel fuel with either hydrogen or syngas can reduce the levels of these emissions.

2.9.1 Nitrogen-rich intake air

Nitrogen-rich intake air can be employed to reduce the production of NO_x emissions, without causing adverse effects on engine lifespan [103]. Poola et al. [104] developed an air separation membrane that was installed on a light-duty diesel engine, achieving dilution levels similar to those of EGR. Figure 2.12 shows a typical prototype membrane module.

Li et al. [105] investigated the effects of dilution gases with various specific heats on the characteristics of combustion and exhaust emissions. Among others outcomes, it was found that oxygen reduction is the dominant factor lowering NO_x emissions, rather than gas specific heat.

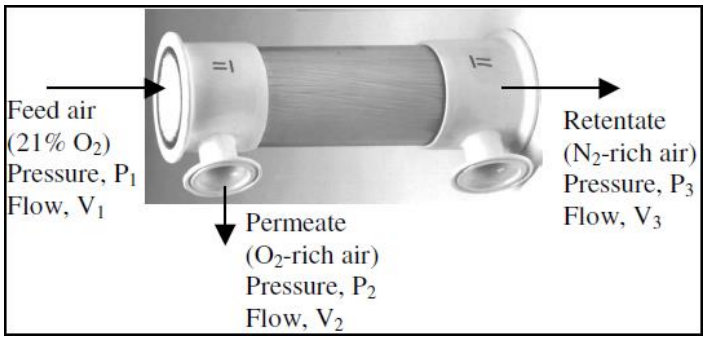

Figure 2.12: Poola's prototype membrane module [104].

The dilution gases may affect combustion and emissions in the following ways: reduce the oxygen available for the combustion, alter the specific heat capacity of the intake charge, participate in the combustion process, affect volumetric efficiency in case of temperature variations. Separate examination of the above yields that the dominant factor affecting the combustion and emissions is the reduction in oxygen concentration. When the intake air is enriched with nitrogen, the increase in heat capacity is insignificant. However, in the next few lines the effect on combustion and emissions by changing the heat capacity of the intake charge is explained. An increase in the heat capacity of the intake charge leads to a reduction in the peak combustion temperature, causing a rise in ignition delay period. Thus, the portion of the fuel burned during the premixed phase of combustion is increased, resulting in an increase in NO_x and a reduction in smoke emissions [106]. Finally, both participation of the added nitrogen in the combustion process and volumetric efficiency effects are rather insignificant.

2.9.2 Exhaust gas recirculation

EGR is a NO_x control measure applied to many types of diesel engines, including automotive light-duty, medium-duty and heavy-duty engines as well as marine low-speed two stroke engines. EGR can also be utilised in advanced combustion concepts, such as LTC, which require high EGR rates [107]. Nevertheless, combination of EGR and NO_x reduction catalysts, such as the SCR system, might be necessary in order to meet the stringent NO_x emission standards. A simple schematic representation of the EGR system is illustrated in Figure 2.13. Exhaust gas from the previous cycle is supplied back to the intake pipe, through a line equipped with a valve allowing control of the amount of EGR.

When the intake air is diluted with EGR, the reduction in peak combustion temperature is attributed to the dilution effect, added-mass effect, thermal effect and chemical effect. The dilution effect is the major contributor to NO_x reduction, because the increased non-oxygen molecules present in the combustion chamber absorb heat lowering the flame temperature. The added-mass effect occurs when by adding an inert gas the mass flow rate is increased, leading to an additional heat capacity. The thermal effect is introduced when the specific heat capacity of the diluent is higher than air. Finally, the chemical effect occurs when the diluent dissociates or participates in the combustion process.

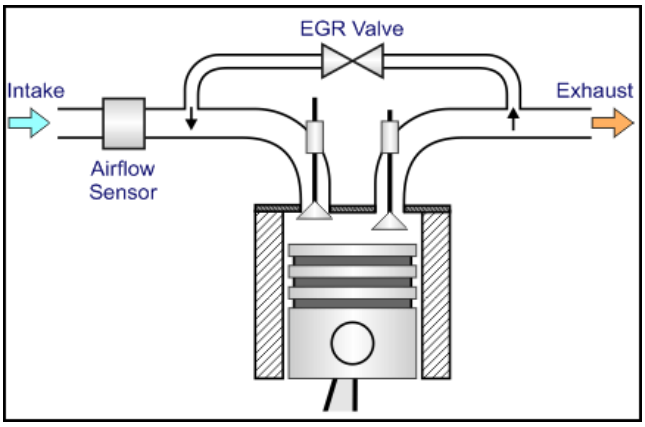

Figure 2.13: Schematic representation of EGR system [107].

Ladommatos el al. [108] conducted a set of tests on a 2.5 litre, high-speed, direct injection diesel engine in order to assess the effect of EGR on soot formation. It was found that introduction of hot EGR into the engine caused an increase in soot emissions and fuel consumption. Furthermore, it was demonstrated that the fuel consumption penalty, soot emissions and NO_x suppression are enhanced by cooling the EGR. Concerning the effect of EGR on CO and THC emissions, Feng et al. [109] reported that the levels of these emissions increase rapidly with the amount of EGR.

Singh et al. [110] experimentally investigated the effect of EGR on lubricating oil degradation and wear of a compression ignition engine. The authors compared the concentration of the metallic wear debris in the lubricating oil under normal operating conditions with that under a fixed EGR rate of 25%. It was shown that the operation with EGR resulted in a relatively higher concentration of wear metals, which indicates that EGR contributes to the wear of various engine parts. This result is supported by George et

al. [111] who revealed that the increased soot emissions of an EGR-operated engine have a detrimental effect on lubricating oil, leading to wear of engine parts.

From the above, it may be concluded that by equipping an engine with an EGR system NO_x emissions are considerably reduced at the expense of soot, CO, THC, fuel consumption and engine wear issues. It should be mentioned that an SCR system is required in order to meet the legislated stringent NO_x emission limits.

2.10 Summary

Apart from establishing a theoretical framework and gaining background knowledge on emission formation, diesel emission legislation, diesel combustion, alternative diesel combustion modes, injection parameters, alternative fuels and dual fuel, exhaust gas assisted fuel reforming and dilution techniques of the intake air, the literature review was very important in identifying gaps in knowledge that need to be filled.

As already mentioned, although there are many papers in the literature dealing with the effects of the intake air enrichment of a diesel engine with separate hydrogen, syngas and nitrogen, no papers were found examining the effects of the intake air enrichment with simultaneous hydrogen and nitrogen or simultaneous syngas and nitrogen.

Due to some discrepancies in the results reported in the literature, the experiments presented in Chapters 4 and 5 were performed to investigate the effects of introducing separate hydrogen and nitrogen in the existing engine. Moreover, together with the baseline operation, the results obtained in these two chapters were used in many instances as a basis of comparison.

CHAPTER 3

EXPERIMENTAL FACILITIES, TEST PROCEDURE AND DATA ANALYSIS

3.1 Introduction

The engine used for the experiments, the analysers, the measuring and calibration equipment, the data acquisition as well as the data processing techniques are extensively described in this chapter. In addition, the operating conditions selected and the parameters varied in each operating condition are given and explained. Finally, the measures taken in order to improve the safety of the researchers using the existing setup have been incorporated in the discussion.

3.2 Research engine

The experiments were performed using a Ford pre-production prototype diesel engine. The engine block was based on the Ford Duratorq engine, whereas the cylinder head was the same to the production Ford Zetec, equipped with two camshafts and four valves per cylinder. The specifications of the engine are summarised in Table 3.1. It should be mentioned that throughout the experiments the engine was run in naturally aspirated mode, while the EGR was not employed since the dilution of the intake air was achieved by the introduction of bottled nitrogen.

Table 3.1: Engine specifications.

Engine model and type	Ford Puma, 2.0 l, 4 cylinder, 16 valve, HSDI, turbocharged (but runs in NA mode), EGR, water cooled, fuelled by ULSD
Bore/Stroke [mm]	86/86
Compression Ratio [-]	18.2:1
Swept Volume [cc]	1998.23
Con-Rod Length [mm]	155

The engine used throughout this research effort had different air intake manifold and pistons compared to the production engines. In contrast to the design of the intake

manifold on the production engines, that aims to promote swirl, the intake manifold on the test engine had straight cylinder feeds. Concerning the pistons fitted on the test engine, they featured larger bowl volume, which resulted in a reduction in the compression ratio. For the production engines, the compression ratio is equal to 19:1, which is slightly higher than the 18.2:1 with the test engine. The piston design used on the prototype engine is illustrated in Figure 3.1.

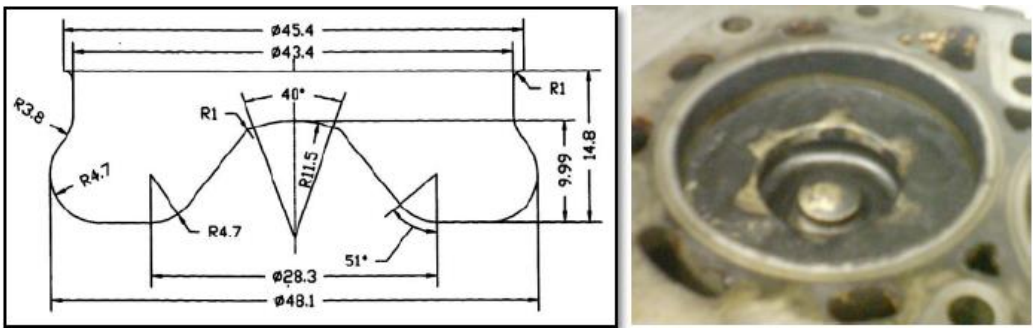

Figure 3.1: Piston bowl design [93].

At this point it would be helpful to introduce the schematic representation of the test rig as the individual parts illustrated in Figure 3.2 will be discussed in detail in this chapter.

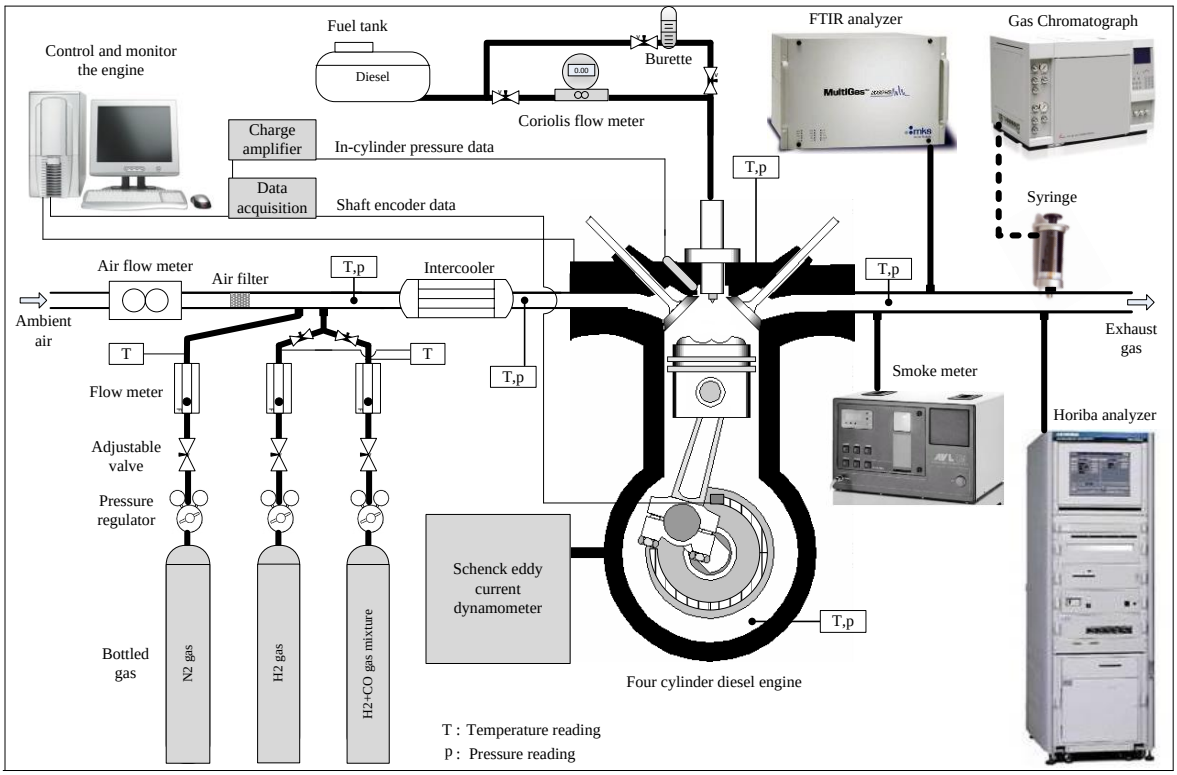

Figure 3.2: Schematic representation of the experimental setup.

The fuel injection featured a Delphi common rail system, while each injector had six holes with nominal diameter equal to 0.154 mm and 154 degree spray hole angle. The engine was cooled using two distinct circuits. One circuit was used to remove the heat from the engine by sending water through the passages in the engine block and head, whereas the other circuit picked up the heat from the lubricating oil. The coolant inlet and outlet temperatures were monitored and a signal was sent to a thermostat that controlled the coolant flow, ensuring a temperature range of 77 ± 3 °C. In order to prevent the engine from overheating, a safety cut off facility that automatically stops the engine in case the coolant temperature reaches 100 °C was in place.

3.3 Dynamometer

The output shaft of the engine was coupled to a W130 Schenck eddy current dynamometer that enabled control of the engine load and speed. The cutaway of the dynamometer is shown in Figure 3.3 and its function is explained below.

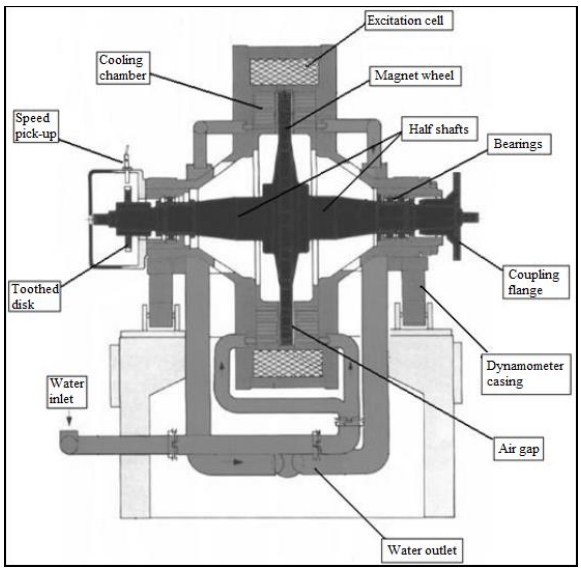

Figure 3.3: Cutaway of the eddy current dynamometer (adopted from Schenck user guide).

A magnetic field is generated by the electrical current that passes through the excitation coil. When the engine is operating, its output shaft spins the rotor of the dynamometer, causing a constant change in flux density on all stator points. As a result, the eddy currents induced cause a braking action on the rotor [112]. The torque and shaft power can be calculated from the current force and the length of the arm. The dynamometer permits the operator to keep constant either the speed or the torque of the engine. When the torque is

fixed, the engine speed can be adjusted by controlling the fuel supply to the engine, and vice versa. The heat generated during the operation is carried away by the water cooling system. The dynamometer features an emergency shutdown system.

3.4 Intake setup and instrumentation

Originally the engine was equipped with a turbocharger; nevertheless, in the current research effort that component was disengaged, resulting in a naturally aspirated operating mode. Furthermore, the EGR valve fitted on the engine was kept hermetically closed throughout the experiments. Table 3.2 presents the measuring equipment used along the engine intake, while further discussion is provided over the next paragraphs.

Table 3.2: Measuring equipment used along the engine intake.

Measuring equipment	Manufacturer	Type	Range	Error
Glass tube rotameter (H_2 measurement)	RM&C	NG	10-180[a]	± 2.0% (on the actual flow rate)
Glass tube rotameter (N_2 measurement)	RM&C	GU	a. 10-100[a] b. 30-150[a]	± 2.0% (on the actual flow rate)
Glass tube rotameter (Syngas measurement)	RM&C	NG	20-140[a]	± 2.0% (on the actual flow rate)
Intake air flow meter	Romet	RM	260-5191[a]	+0.25%
Pressure regulator	BOC	HP	0-17 bar	-
Thermocouple	NG	K	0-1100 °C	≤ ± 0.3%

[a] in litres per minute

The inlet air was initially passed through a positive displacement flow meter and then through a paper filter. The former was used to measure the volumetric flow rate of air, which was actually determined by the rate of rotor revolution, while the latter filtered the relatively big airborne particles. The bottled gases were admitted into the intake pipe through probes that were fitted perpendicular to the main air flow, downstream the paper filter. Introduction of bottled gases into the engine meant that an equivalent volume of intake air was replaced by the gas mixture. Two distinct lines were used to carry the gases from the bottles to the inlet pipe, upstream the intercooler. One of them carried the nitrogen gas, while the other carried the flammable gas; namely, hydrogen or syngas. The line used to transfer the flammable gas was equipped with a backfire arrestor and a relief

valve. Both were placed in between the pressure regulator and the glass tube rotameter. Additional safety measures included a control valve in the flammable gas line as well as hydrogen and carbon monoxide leak detectors, in both engine and control cells. Once the control valve was activated it automatically closed after 5 minutes.

The gases used throughout the experiments were supplied by the British Oxygen Company (BOC) and stored in three different 15 litre cylinders. The first two cylinders contained the hydrogen and nitrogen, while the syngas, consisted of 60% hydrogen - carbon monoxide balance, was stored in the third cylinder. Each cylinder was equipped with a pressure regulator, allowing control of the line pressure and monitor of the remaining gas. The flow rate of the admitted gases was measured by the glass tube rotameters. The gas temperature downstream the rotameters was measured and a temperature correction was applied to reduce the gas flow rate uncertainty. In addition, the inlet manifold was specially designed to allow uniform distribution of the gas-air mixture in the cylinders. The pressure in the gas lines was fixed at 3 bar as this was the pressure required to achieve the maximum flow rate of the admitted gases. Finally, the mixing quality and the concentration of hydrogen and nitrogen in the intake air were verified by the gas chromatograph, as described in Section 3.6.4.

As mentioned above, an equivalent volume of air was replaced when a bottled gas was introduced into the engine, resulting in a reduction in intake oxygen concentration. Table 3.3 illustrates the composition of the intake charge as a function of the amount of the bottled gases admitted into the engine.

Table 3.3: Intake charge composition as a function of the amount of the bottled gases.

	Bottled gas [% vol. of intake air]			**Intake charge concentration [% vol.]**			
	H2	**N2**	**Syngas**	**O_2**	**N_2**	**H_2**	**CO**
	0	0	0	21	79	0	0
H_2 addition	2	0	0	20.58	77.42	2	0
	4	0	0	20.16	75.84	4	0
	6	0	0	19.74	74.26	6	0
	8	0	0	19.32	72.68	8	0

	Bottled gas [% vol. of intake air]			Intake charge concentration [% vol.]			
	H2	**N2**	**Syngas**	**O_2**	**N_2**	**H_2**	**CO**
	0	0	0	21	79	0	0
N_2 addition	0	2	0	20.58	79.42	0	0
	0	4	0	20.16	79.84	0	0
	0	6	0	19.74	80.26	0	0
	0	8	0	19.32	80.68	0	0
H_2-N_2 addition	2	2	0	20.16	77.84	2	0
	4	4	0	19.32	76.68	4	0
	6	6	0	18.48	75.52	6	0
	8	8	0	17.64	74.36	8	0
Syngas-N_2	0	2	2	20.16	77.84	1.2	0.8
	0	4	4	19.32	76.68	2.4	1.6
	0	6	6	18.48	75.52	3.6	2.4

3.5 Diesel fuel supply and measurement

The diesel fuel was stored in a central reservoir. An electric fuel pump was used to send diesel to the high pressure pump of the engine, which was capable of increasing the pressure up to 1600 bar. The rate of fuel flow was measured either by a glass burette or a Coriolis flow meter (interchangeable operation was possible), both fitted upstream the high pressure pump. The data recorded was then processed to calculate the consumption of diesel by the engine. The engine was equipped with a common rail system, allowing multiple injections per cycle. Table 3.4 shows the basic equipment used along the diesel line.

Table 3.4: Measuring equipment used along the diesel line.

Measuring equipment	Manufacturer	Type
Glass burette	Plint & Partners Ltd	50-100-200
Coriolis flow meter	E+H	Promass 83

When the glass burette was employed, the time required by the engine to consume a given volume of fuel was measured by a stopwatch. The mass flow of diesel was calculated by multiplying the volume flow by the fuel density. This method usually leads to higher errors, compared to Coriolis, as the measurement is operator dependent.

A Coriolis flow meter is capable of providing more accurate results than the glass burette. Apart from the flow rate, Cariolis measures the density, the temperature and the viscosity of the fluid. The operating principle of a Coriolis flow meter is described below. Coriolis forces occur in an oscillating tube when a liquid or gas flows through it. The design of the tube is symmetrical and is either straight or curved. The measuring tube is subject to uniform oscillation mode by a driver. When a fluid moves inside the tube, additional twisting is imposed on the oscillation. Sensors located at the inlet and outlet ends pick up the distortion of the tube. This information is analysed by the processor, which gives the mass flow rate.

3.6 Exhaust gas analysis

Detailed exhaust gas analysis was carried out using a Horiba Mexa 7170DEGR, an MKS multigas 2030 FTIR gas analyser, an AVL 415S smoke meter and a Chrompack gas chromatograph (GC) CP 9001 equipped with a thermal conductivity detector (TCD). Table 3.5 shows the exhaust gas measuring equipment employed throughout the experiments.

Table 3.5: Exhaust gas measuring equipment employed throughout the experiments.

Measuring equipment	Manufacturer	Type
Exhaust gas analyser	Horiba	Mexa 7170
Exhaust gas analyser	MKS	2030
Smoke meter	AVL	415S
Gas chromatography	Chrompack	CP 9001

Horiba is capable of measuring CO and CO_2 through a non-dispersive infrared method (NDIR). The amount of NO emissions in the exhaust gas was determined by the chemiluminescence of their reaction with ozone, while THC emissions were measured through a flame ionisation detector (FID). Regulated emissions can also be measured by the FTIR analyser, the operation of which is based on partial absorption of an infrared beam by the species present in the exhaust gas. In addition to regulated emissions, FTIR can provide readings for unregulated emissions. In this study the FTIR was employed to measure nitrogen exhaust compounds. Besides, simultaneous operation of the two instruments enabled correlation of the regulated emissions. The Horiba, smoke meter and FTIR were supplied with exhaust gas directly from the exhaust pipe through the sample

lines. The GC required a small exhaust gas sample that was collected from the exhaust pipe using a gastight syringe.

3.6.1 Non-dispersive infrared

The principle behind NDIR, which is a type of infrared spectroscopy, is that distinct gas molecules contained in a sample will absorb infrared light at a specific wavelength. The concentration of each gas is proportional to the amount of light absorbed, and it is actually calculated by measuring the amount of light remained at a specific wavelength. A typical NDIR for CO_2 and CO measurements involves a sampling and a reference cell, the latter is filled with an inert gas such as nitrogen. An infrared beam shines through the sampling and comparison cells, band pass filters and it finally reaches the detector, as shown in Figure 3.4. Comparison of the two values acquired enables determination of CO_2 or CO levels.

In the event of exhaust gas leakage, a CO detector placed in the engine control room warns the researcher in order to prevent poisoning.

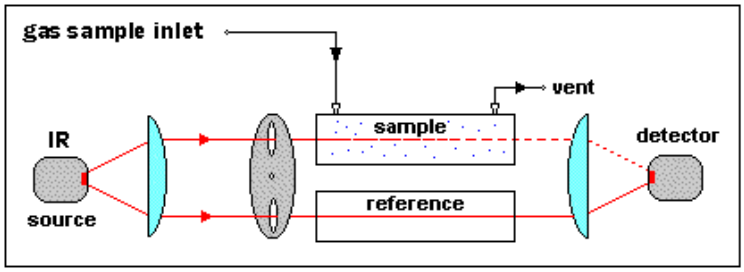

Figure 3.4: Schematic representation of the NDIR principle [113].

3.6.2 Chemiluminescence

The chemiluminescence detection method is based on the chemical reaction between NO and ozone (O_3) as detailed below:

$$NO + O_3 = NO_2^* + O_2 = NO_2 + O_2 + photon \quad (3.1)$$

The NO is contained in the exhaust gas, whereas the O_3 is produced by the instrument. When the excited NO_2 molecules return to the ground state they emit red light, which is measured by a photo multiplier after it passes through a filter to eliminate interference from other gases. Based on this technique, the amount of NO_x as well as NO_2 emissions can be determined as follows: firstly, the NO_2 is converted to NO, and then the converted molecules together with the original NO molecules in the exhaust sample react with ozone.

The signal obtained equals to the NO_x emissions (sum of NO and NO_2). The concentration of NO_2 is calculated by subtracting of the original NO from the NO_x.

It should be mentioned that for health and safety reasons, an O_3 detector was placed close to the O_3 source in order to alert the researchers in case of leakage. Repeated exposure to man-made O_3 may damage the lungs and aggravate existing respiratory conditions.

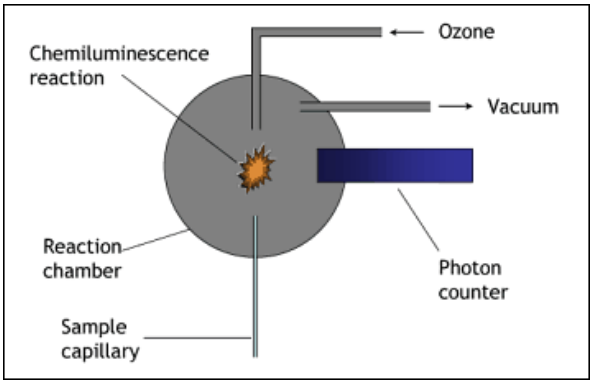

Figure 3.5: Schematic representation of a chemiluminescence detector [114].

3.6.3 Flame ionisation detector

The total hydrocarbon emissions in the exhaust gas were measured by an FID, the schematic representation of which is shown in Figure 3.6.

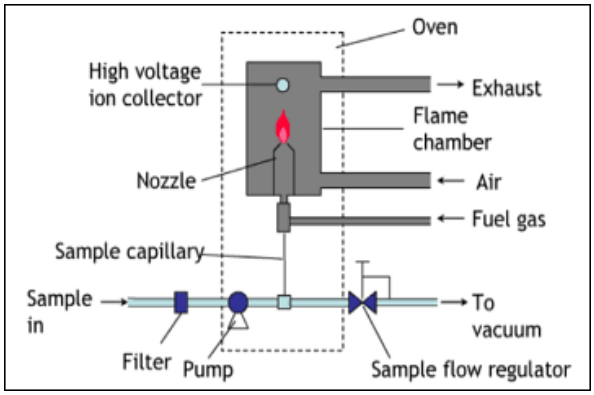

Figure 3.6: Schematic representation of flame ionisation [114].

Its operation is based on the detection of ions during the combustion of hydrocarbons in a hydrogen flame. Instead of hydrogen, a 40% H_2 - Helium (He) balance gas mixture was used during the measurements. A current that is proportional to the number of carbon atoms burned in the flame is generated between the burner and the electrode. The signal is

then processed to give the concentration of THC emissions. It should be clarified that the value given does not represent the actual volumetric concentration of hydrocarbons in the exhaust gas, but rather the amount of carbon atoms in the analysed gas.

3.6.4 Gas chromatography

A Chrompack GC equipped with a TCD was used for the measurement of the unburned hydrogen in the exhaust gas. The TCD compares the thermal conductivity of a carrier gas and a sample gas. In the current application, the sample gas (that is, the exhaust gas) was collected from the exhaust pipe using a Hamilton gastight syringe, while high purity bottled argon was used as the carrier gas. The TCD features a reference and a sample cell. The carrier gas, which passes through the reference cell, has different thermal conductivity compared to the sample and the carrier gas that passes through the sample cell. This causes a variance in the resistance of the electrically heated wires situated within the cells. Depending on the difference in the resistance, a voltage signal proportional to the concentration of the sample gas is produced. The structure of the cell is illustrated in Figure 3.7.

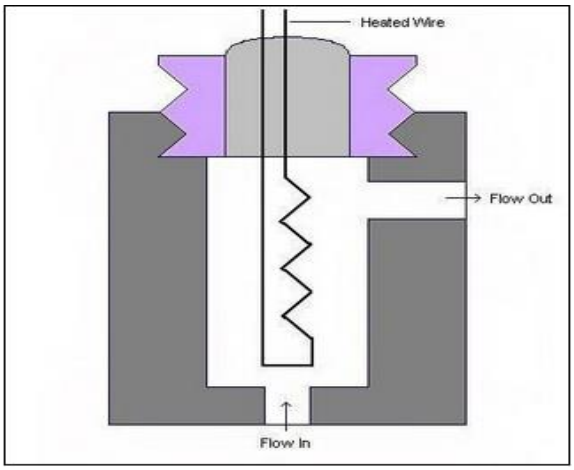

Figure 3.7: Structure of thermal conductivity detector [115].

The analyser was regularly calibrated using certified high purity BOC gases. The hydrogen concentration in the exhaust gas was always between 0 and 2%; therefore, the span gases were selected accordingly; namely, 100% N_2, 1% H_2 - N_2 balance and 2% H_2 - N_2 balance gas mixtures. The calibration was performed by injecting bottled gas into the GC in order to get the response of the detector in terms of chromatograph area given by the integrator.

Figure 3.8(a) shows the chromatograph area as a function of hydrogen concentration. A linear relationship was considered since the linear regression fit gave R^2 as very close to unity. Figure 3.8(b) illustrates the response of the detector from the calibration using 1% H_2 - N_2 balance. The little peaks between the hydrogen and nitrogen spikes correspond to oxygen, which probably entered the syringe (although sealed with a rubber bung) while transferred from the bottle to the GC injector.

Apart from measuring the exhaust gas hydrogen concentration, the GC was utilised to assess whether the bottled hydrogen and nitrogen admitted into the intake pipe was thoroughly mixed with the intake air. For this purpose two rubber-sealed access points on the inlet manifold, one at the point the intake charge enters the manifold and one in the middle of the manifold, allowed collection of hydrogen- and nitrogen-rich intake air, which was supplied into the GC. The good repeatability of the results verified that the bottled gases were thoroughly mixed with the intake air. In addition, this method enabled verification of the concentration of the bottled gases in the intake air.

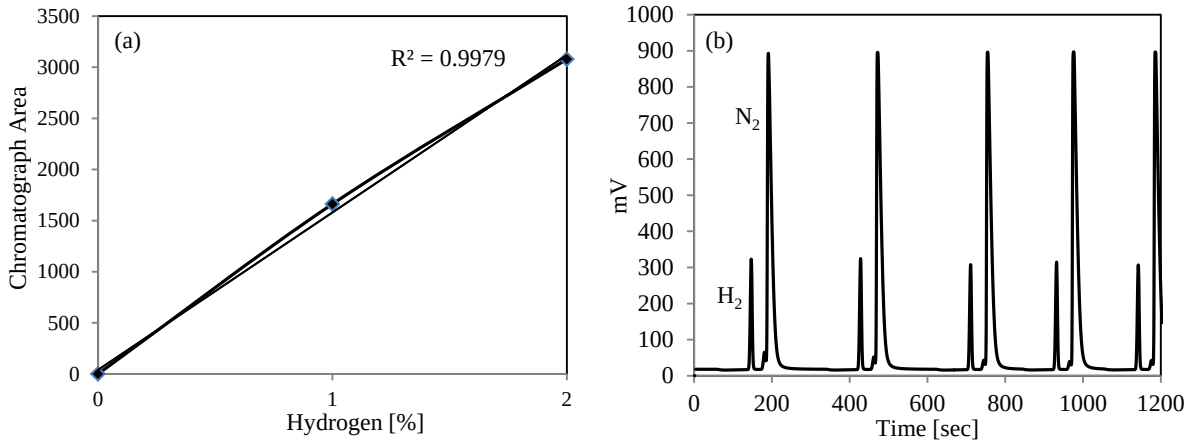

Figure 3.8: Gas chromatograph calibration: (a) Chromatograph area at different H_2 fractions, (b) Sample of chromatographic results delivered by the detector.

3.6.5 Fourier transform infrared spectroscopy

Infrared spectroscopy is an important technique traditionally used in organic chemistry. The accuracy, the fast measuring and the capability of a detailed analysis of the exhaust gases allowed this technique to gain entrance into the field of engine research.

In FTIR spectroscopy an infrared beam that passes through the gas under investigation is partially absorbed by the gas species that contained in the gas. The level of absorption at a specific wavelength depends upon the concentration of the specie. Each infrared active gas has a unique absorption spectrum, which is measured by the FTIR gas analyser and an analysis algorithm calculates the concentration of each gas using pre-loaded calibrations [116].

3.6.6 Bosch smoke number

Smoke concentration in the exhaust gas is determined by the filter paper method, Figure 3.9. A probe mounted in the exhaust line draws exhaust gas that passes through a clean filter paper. The BSN is determined according to the degree to which the filter paper is blackened. A reflectometer head is used to measure the paper blackening, with zero value corresponding to white paper and ten to completely black paper [117].

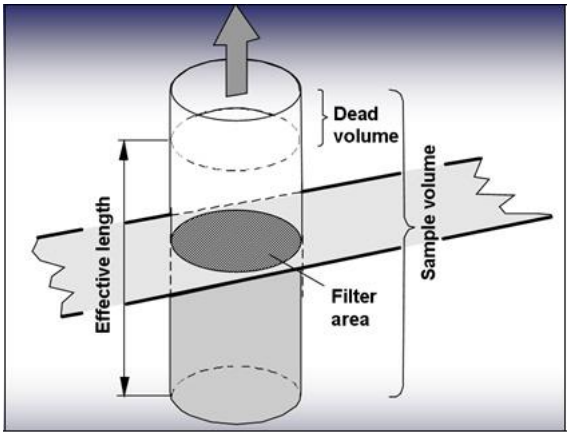

Figure 3.9: Exhaust sampling schematic (adopted from AVL user guide).

3.7 In-cylinder pressure data

The pressure data from the first cylinder was measured by a Kistler 6125A piezoelectric pressure transducer fitted into the modified glow plug hole. Figure 3.10 shows the cutaway of the cylinder head with the pressure transducer, fitted into the adapter, and the sensor that was used to dynamically determine the TDC (mounted into the injector seat).

Changes in the cylinder pressure were converted to an electrical charge (the sensitivity of the above transducer was 16 pC/bar), which was amplified using a Kistler 5001 charge amplifier and recorded by a Labview software together with the shaft encoder signal. A

heavy-duty shaft encoder (model ET758) was employed, setting the resolution to 1440 pressure data per crank shaft revolution (that is, 4 samples per crank angle degree). Table 3.6 shows the measuring equipment required to record the in-cylinder pressure data.

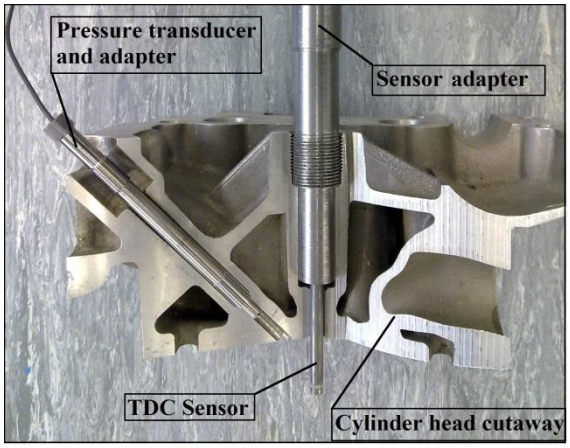

Figure 3.10: Cylinder head cross section with the pressure transducer and the TDC sensor.

Table 3.6: Measuring equipment that was used to record the in-cylinder pressure data.

Measuring equipment	Manufacturer	Type	Range	Sensitivity
Pressure transducer	Kistler	6125A	0-250 bar	-16.8pC/bar
Shaft encoder	Encoder Technology	ET758	0-8000 rpm	0.017°

Figure 3.11 illustrates the TDC sensor adopted for the dynamic determination of the TDC position. During the calibration process the following steps were performed: The injector of the first cylinder was removed and the sensor was mounted in the seat. The engine was run for a few minutes on the motored mode by deactivating the diesel injectors. The output signal of the sensor, along with the shaft encoder signal, was recorded by the Labview software and depending on the position of the maximum in-cylinder pressure a correction factor was applied accordingly.

Figure 3.11: Kistler 2629C1 top dead centre sensor.

The working principle behind the TDC sensor is the generation of a signal when the top of the piston approaches the sensor tip. The magnitude of the signal is inversely proportional to the distance between the piston and the sensor. The maximum value corresponds to the TDC position. The advantage of using such a sensor is that no correction involving the degree of the thermodynamic loss angle is required.

3.8 Fuel properties

Throughout the experiments the engine was fuelled by ULSD. Admission of hydrogen and syngas into the engine resulted in dual fuel combustion. Under this operating mode, the flow rate of ULSD was reduced to keep the speed and load constant. The composition of the bottled syngas (60% hydrogen - CO balance) resembled that of typical diesel reformer product gas. The temperature at the end of the compression stroke of the engine was always lower to the autoignition temperature of hydrogen and syngas; hence, in the dual fuel mode, the onset of combustion was initiated by diesel injection. Some useful properties of hydrogen [118] and syngas are illustrated in Table 3.7, while their effects on the performance and emissions of CI engines are discussed over the next few paragraphs.

Table 3.7: Hydrogen and syngas properties.

Property	**Unit**	**Value for H_2**	**Value for syngas**
Adiabatic flame temperature (φ=1)	[K]	2480	~ 2445
Autoignition temperature in air	[K]	858	~ 867
Density	[kg/m^3]	0.0824	0.5154
Flame velocity (φ=1)	[ms^{-1}]	1.85	1.2
Flammability limits	[% vol. in air]	4 – 75	5.45-75
Lower heating value	[MJ/kg]	119.7	20.7
Minimum ignition energy (φ=1)	[mJ]	0.02	< 0.3

The heating value of gas mixtures is determined by using the following formula [119]:

$$HV_m = \sum HV_{m,i} \times X_i \quad (3.2)$$

where HV_m is the heating value of the mixture (mass basis), $HV_{m,i}$ is the heating value of the component i (mass basis) and X_i is the composition of the gas i (mass fraction).

The flammability limits of syngas were predicted by Le Chatelier's mixing rule [120], which has been proven accurate at estimating the lower flammability limit (LFL) of gas

mixtures [121]. However, a modification of this empirical rule might be necessary when it comes to the upper flammability limit (UFL). It should be clarified that the values presented in Table 3.7 were obtained by applying Equation (3.3) without any modifications. The upper flammability limit of the mixture was calculated by substituting LFL_{mix} and LFL_i with UFL_{mix} and UFL_i, respectively.

$$LFL_{mix} = \frac{1}{\sum \frac{y_i}{LFL_i}} \tag{3.3}$$

where LFL_{mix} denotes the lower flammability limit of the mixture, y_i denotes the mole fraction of the component i taking into account only the combustible species and LFL_i denotes the lower flammability limit of the component i in volume percent.

An important advantage of the wide flammability limit of hydrogen and syngas is that they allow stable operation of the engine under lean-burn conditions. Lean operation typically results in decreased NO_x production due to the low peak combustion temperature. Also, the reaction rate, which is relatively slow in typical hydrocarbon fuels, is accelerated when hydrogen or syngas is mixed with hydrocarbons [122].

The formation of NO_x emissions strongly depends on flame temperature, an increase in which favours the reaction of atmospheric oxygen and nitrogen for the production of NO_x. Combustion of hydrogen or syngas is characterised by increased flame temperature.

In conventional compression ignition engines the maximum temperature at the end of the compression stroke does not reach the autoignition temperature of hydrogen or syngas. Therefore, the onset of combustion is typically achieved by diesel injection. This implies that in diesel and hydrogen or diesel and syngas dual fuel operation, the onset of combustion is controlled by the diesel injection timing.

When hydrogen or syngas is delivered into the cylinder through the intake pipe, the volumetric efficiency of the engine is inevitably decreased, resulting in a reduction in power density.

The high flame velocity of hydrogen may benefit the thermal efficiency of the engine. However, a drawback associated with its explosive burn is the great forces exerted on the

moving parts of the engine, owing to the high rates of pressure rise. As already presented in Table 3.7, the flame velocity of syngas is lower compared to hydrogen.

The energy required to ignite hydrogen is only 0.02 mJ, which is one order of magnitude less than the energy required by gasoline. Although this property can ensure prompt ignition, it may cause premature ignition issues, with hot spots and hot deposits serving as potential ignition surfaces [123].

The heating value of hydrogen (per unit mass) is approximately three times that of diesel; nevertheless, diesel prevails when the comparison is made on volumetric basis. When hydrogen is not produced on-board, this may pose a challenge since volume occupation is an important parameter in vehicular applications [124].

The baseline data presented throughout this study was obtained by fuelling the engine with diesel supplied by Shell. Table 3.8 summarises the properties of diesel fuel.

Table 3.8: Diesel fuel properties.

Parameter	**Unit**	**Value**
Ash content	[%]	<0.005
Autoignition temp. in air	[K]	483
Calorific value	[kJ/kg]	44800
Carbon	[%]	86.2
Carbon residue	[%]	0.2
Cetane number	[-]	52.1
Cloud point	[K]	263
Density at 288 Kelvin	[kg/m^3]	853.8
Flash point	[K]	341
Hydrogen	[%]	13.4
Oxidation stability	[g/m^3]	14
Oxygen	[%]	0
Sulphur content	[mg/kg]	10
Total aromatics	[%]	10.5
Viscosity at 313 Kelvin	[cSt]	2.5
Water content	[mg/kg]	61

3.9 Data analysis

The data recorded during the experiments was processed off-line using the methods presented in this section. The calculations were performed using dedicated software platforms developed at the Centre for Advanced Powertrain and Fuels Research (CAPF) at Brunel University. The values shown in the graphs that are presented over the next chapters correspond to test points with good combustion stability and emission repeatability.

3.9.1 In-cylinder volume

The in-cylinder pressure data provides valuable information of the combustion process, which can be used to further improve the performance and emissions of internal combustion engines. Apart from the pressure data, the geometrical parameters of the engine need to be imported into the software platform, Figure 3.12.

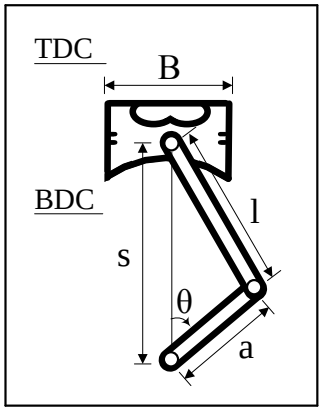

Figure 3.12: Schematic representation of piston – connecting rod – crankshaft.

The calculation process starts with the determination of the in-cylinder volume at any crank position, as shown in Equation (3.4):

$$V = V_c + \frac{\pi B^2}{4}(l + a - s) \tag{3.4}$$

where V_c denotes the clearance volume, B is the cylinder bore, l is the connecting rod length, a is the crank radius and s is the distance between the crank axis and the piston pin axis.

The distance s can be calculated as follows:

$$s = a\cos\theta + (l^2 - a^2\sin^2\theta)^{1/2} \tag{3.5}$$

Equation (3.4) can be rearranged in order to get an equation of in-cylinder volume at any crank angle θ:

$$\frac{V}{V_c} = 1 + \frac{1}{2}(r_c - 1)[R + 1 - \cos\theta - (R^2 - \sin^2\theta)^{1/2}] \tag{3.6}$$

where r_c denotes the compression ratio (defined as the maximum cylinder volume over the minimum cylinder volume) and R is the ratio of connecting rod length to crank radius l/a.

3.9.2 Apparent and cumulative rate of heat release

The gross rate of heat release and the net apparent rate of heat release can be calculated from experimental measurements by performing heat release rate analysis. The former can be determined from exhaust gas measurements, whereas the latter from the in-cylinder pressure data. Homsy and Atreya [125] developed a method for calculating heat transfer to the walls by taking the difference of the two values; namely, the gross and net apparent rate of heat release. In this work, the calculation was based on the net apparent heat release approach, which is derived from the first law of thermodynamics neglecting any blowby, crevice and enthalpy of the injected fuel effects [93, 126]. The energy balance in the combustion chamber is given in Equation (3.7):

$$\delta Q_{ch} = dU_s + \delta Q_{ht} + \delta W + \sum h_i dm_i \tag{3.7}$$

where U_s is the internal energy, Q_{ht} is the convective heat transfer to the cylinder walls, W is the work output, $h_i dm_i$ are the losses by the crevices.

Rearrangement of Equation (3.7) is represented in the following form:

$$\frac{dQ_{ch}}{d\theta} = \frac{\gamma}{\gamma - 1} p \frac{dV}{d\theta} + \frac{1}{\gamma - 1} V \frac{dp}{d\theta} + V_{cr} \frac{dp}{d\theta} + \frac{dQ_{ht}}{d\theta} \tag{3.8}$$

The final form of the formula that was used to calculate the net apparent heat release rate is given in Equation (3.9):

$$\frac{dQ_n}{d\theta} = \frac{\gamma}{\gamma - 1} p \frac{dV}{d\theta} + \frac{1}{\gamma - 1} V \frac{dp}{d\theta} \tag{3.9}$$

where Q_n denotes the net heat release, γ is the ratio of specific heats, P is the pressure and V is the volume.

Provided that the pressure and volume data was given, the only variable in the equation above was the ratio of specific heats γ. Many different ways have been proposed to calculate γ [126]; however, in this study a value of γ = 1.3 [11] was adopted and kept constant throughout the cycle.

The cumulative heat release rate, the equation of which is detailed below, equals to the sum of heat release rates at each crank angle:

$$\mathrm{CHRR} = \sum_{\mathrm{IXA}}^{\mathrm{EOC}} \frac{\mathrm{dQ_{ch}(i)}}{\mathrm{d\theta(i)}} \times \mathrm{k(i)} \tag{3.10}$$

where IXA denotes the point the heat release curve intersects the x axis, EOC denotes the end of combustion and k is the resolution of the heat release rate.

3.9.3 Mass fraction burned

The mass fraction burned is another common method that is used to define cumulative combustion, and it is expressed as the ratio of cumulative heat release to the total heat release. Equation (3.11) details its calculation:

$$\mathrm{MFB}(\theta) = \frac{\int_{\theta_{soc}}^{\theta} \frac{\mathrm{dQ_{ch}}}{\mathrm{d\theta}}\,\mathrm{d\theta}}{\mathrm{m_f} \times \mathrm{n_{comb}} \times \mathrm{LHV}} \tag{3.11}$$

where m_f is the mass of fuel, n_{comb} is the combustion efficiency and LHV is the lower heating value of the fuel.

It should be clarified that the start of combustion was taken as the point the heat release curve intersected the x axis.

3.9.4 Coefficient of variation in indicated mean effective pressure

The effect of blending gaseous with liquid fuels on the cyclic variability of the engine can be determined by the COV_{IMEP}. For this reason, data from 100 consecutive cycles was used for the calculation of the COV, which is a measure of combustion stability. The formula shown below was used to calculate this combustion parameter:

$$COV_{IMEP} = \frac{\sigma_{imep}}{\mu_{imep}} = \frac{\sqrt{\frac{1}{n}\sum_1^n \left[X_i - (\frac{1}{n}\sum_1^n (X_i))\right]^2}}{\frac{1}{n}\sum_1^n (X_i)} \quad (3.12)$$

where σ_{imep} denotes the standard deviation of IMEP, μ_{imep} indicates the mean value and n is the number of data points.

3.9.5 Brake thermal efficiency

Brake thermal efficiency is defined as the ratio of the break power to the input fuel energy and is used to evaluate how efficient the heat from the fuel is converted to mechanical energy. Equation (3.13) shows the formula used to calculate the brake thermal efficiency when a blend of diesel and hydrogen was employed [127]. When hydrogen was replaced with syngas, the equation was adapted accordingly.

$$\eta_{th} = \frac{\text{work output}}{\text{heat added}} = \frac{\dot{W}_b}{\dot{m}_{df} LHV_{df} + \dot{m}_{H_2} LHV_{H_2}} \quad (3.13)$$

where $\dot{W}_b$ is the brake power, $\dot{m}_{df}$ is the mass flow rate of diesel, $\dot{m}_{H_2}$ is the mass flow rate of hydrogen, LHV_{df} is the lower heating value of diesel and LHV_{H_2} is the lower heating value of hydrogen.

3.9.6 Energy supplied by hydrogen

The percentage of energy supplied by hydrogen was determined by Equation (3.14). The energy provided by diesel was calculated by subtracting the value obtained by Equation (3.14) from the total energy.

$$E_{H_2} = \frac{CV_{H_2} \times \left(\dot{V}_{H_2 i} - \dot{V}_{H_2 e}\right) \times \rho_{H_2}}{CV_{diesel} \times \dot{V}_{diesel} \times \rho_{diesel} + CV_{H_2} \times \left(\dot{V}_{H_2 i} - \dot{V}_{H_2 e}\right) \times \rho_{H_2}} \quad (3.14)$$

where CV_{H_2} denotes the calorific value of hydrogen (kJ/kg), $\dot{V}_{H_2 i}$ denotes the volume flow rate of hydrogen in the inlet (m^3/s), $\dot{V}_{H_2 e}$ denotes the volume flow rate of hydrogen in the exhaust (m^3/s), ρ_{H_2} is the density of hydrogen (kg/m^3), CV_{diesel} is the calorific value of diesel (kJ/kg), $\dot{V}_{diesel}$ is the volume flow rate of diesel (m^3/s), ρ_{diesel} is the density of diesel (kg/m^3).

In order to maintain the speed and load constant at a given operating condition, the amount of diesel fuel was gradually reduced as the proportion of hydrogen in the intake air was increased.

3.9.7 Combustion efficiency of hydrogen

The combustion efficiency of hydrogen was calculated using Equation ((3.15) [128]:

$$\eta_{H_2,ce} = (1 - \frac{\dot{V}_{H_2e}}{\dot{V}_{H_2i}}) \times 100 \quad (3.15)$$

where $\eta_{H_2,ce}$ is the combustion efficiency of hydrogen (%), $\dot{V}_{H_2e}$ is the volumetric flow rate of hydrogen in the exhaust (m^3/s), $\dot{V}_{H_2i}$ is the volumetric flow rate of hydrogen in the inlet (m^3/s).

3.9.8 Bottled gas flow rate

The flow rate of the bottled gases was calculated using Equation (3.16):

$$BG_{flow} = VAF \times (BG_{pc} * 10^{-2}) \quad (3.16)$$

where BG_{flow} denotes the flow rate of the bottled gas (m^3/s), VAF denotes the volumetric air flow when the engine was operated without the admission of bottled gas (baseline operation) (m^3/s), BG_{pc} denotes the desirable percentage of the bottled gas (% volume).

The volumetric air flow was calculated by the rate of rotor revolution of a positive displacement flow meter, while introduction of the desirable amount of the bottled gas into the engine was achieved by using calibrated rotameters with glass tube.

3.10 Test procedure

The experimental investigation includes results from four different operating conditions. In the first two operating conditions, the speed was kept constant at 1500 rpm, while two different loads (2.5 and 5 bar BMEP) were applied to the engine. In the next two operating conditions, same loads were applied but the speed was increased to 2500 rpm. The conditions selected are representative for low- and medium-duty diesel engines as they spend most of their running time in between these operating conditions. Therefore, the

outcomes presented in this study can provide useful guidelines to study and develop a fully integrated closed loop engine-reformer system.

Variations on injection timing and gas proportion (H_2, N_2, H_2 + N_2, Syngas + N_2) were included in each operating condition. Injection timing was swept from 3 to 12 CAD BTDC in 3 degree increments. Concerning the bottled gases, the minimum amount injected into the intake pipe was 2 per cent, whereas the maximum was 16 per cent (by volume of the total intake air). Increments of 2 per cent were employed when a single gas was delivered into the engine (i.e. H_2, N_2), while in the case of blending bottled gases together (i.e. H_2 + N_2, Syngas + N_2) 4 per cent increments were applied. It should be mentioned that the intake air was progressively replaced by the bottled gases. Table 3.9 summarizes the parameters varied at each operating condition.

Table 3.9: Test matrix with the parameters varied.

Operating condition	**1**	**2**	**3**	**4**
Speed [rpm]	1500	1500	2500	2500
Load [bar BMEP]	2.5	5	2.5	5
Start of injection [CAD BTDC]	3-12	3-12	3-12	3-12
Hydrogen [% vol.]	2-6	2-8	2-4	2-6
Nitrogen [% vol.]	2-8	2-8	2-6	2-6
Hydrogen + Nitrogen [% vol.]	4-12	4-16	4-8	4-12
Syngas + Nitrogen [% vol.]	4-12	4-12	4-12	4-12

With the pressure set at 800 bar, the diesel fuel was delivered into the cylinder using a single injection event. As already mentioned, the pressure in the gas lines was fixed at 3 bar as this was actually the pressure required to achieve the maximum flow rate of the admitted gases.

Before taking any measurements the engine would run until water temperature (77±3 °C) and emissions readings had settled to an acceptable steady state. The emission data at specified baseline points were recorded and used to check whether the engine was generating the same results every time the experiments were performed. The in-cylinder pressure data as a function of crank angle was stored in a PC for off-line analysis. Temperature and pressure readings at various points, as illustrated on the experimental

setup figure, were also provided. Every point shown in the graphs, presented in Chapters 4, 5, 6 and 7, corresponds to a test point with good combustion stability and emission repeatability. The emission data presented in this study corresponds to raw exhaust gas measurements.

CHAPTER 4

ENRICHMENT OF THE INTAKE AIR WITH HYDROGEN

4.1 Introduction

The growing market share of diesel engines coupled with stringent emission regulations has increased research efforts for the development of cleaner and more efficient compression ignition engines. The potential of both alternative powertrains [129] and renewable energy sources to reduce emissions from automobiles has been widely demonstrated. Extensive research on alternative fuels such as LPG and hydrogen [130], CNG [131] and biodiesel [132], which may serve as future energy carriers is underway, with hydrogen situated in a favourable position due to its clean combustion. As already discussed in previous chapters, hydrogen can either be stored or produced on board. The latter is likely to serve as a transition solution until issues associated with hydrogen infrastructure, distribution and storage (which are deemed as the main factors hindering the mass production of H_2-fuelled ICEs) are resolved.

A variety of methods to produce hydrogen on-board have been investigated by various authors. Tsolakis et al. [96] integrated a fuel reforming reactor within the EGR loop of a compression ignition engine to derive hydrogen from diesel fuel. Plasmatron fuel converters can also be used to produce hydrogen from hydrocarbon fuels [133]. Bari and Mohammad Esmaeil [134] employed an Epoch EP-500 oxy-hydrogen generator machine to produce a mixture of H_2/O_2 through water electrolysis, which was then sent into the inlet manifold.

The aim of this chapter is to study the effects of the enrichment of the intake air with hydrogen on the performance (hydrogen combustion efficiency and brake thermal efficiency) and emissions (NO_x, smoke, CO and THC) of the engine. The bottled hydrogen was introduced into the engine through the intake pipe, replacing an equal volume of air. In general, this technique results in a reduction in oxygen concentration (in contrast to the direct-cylinder injection); nevertheless, it is the simplest and cheapest way and can be used in conjunction with the hydrogen production techniques described above and the on-board hydrogen storage.

4.2 Methodology

A detailed schematic representation of the hydrogen line is illustrated in Figure 4.1. Section 3.4 provides an extended discussion of the intake set up; however, the figure below aims to give a more complete picture of the hydrogen supply line.

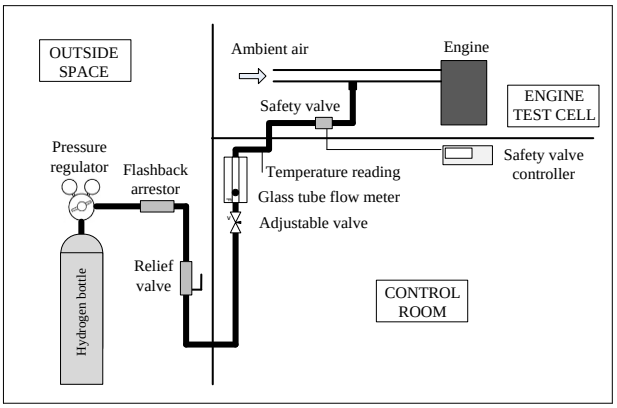

Figure 4.1: Detailed schematic representation of hydrogen supply into the intake pipe.

As the hydrogen was conveyed from the bottle towards the intake pipe, it initially passed through the pressure regulator, which had a twofold function. On the one hand, it allowed control of the line pressure, and on the other, it showed the gas pressure in the bottle, which was an indication of the remaining hydrogen. The next device was the flashback arrestor, which was used to stop the flame in case it would flash back into the hydrogen line. The relief valve that was placed after the flashback arrestor ensured that the line pressure did not exceed a certain value. The hydrogen flow rate was measured by a rotameter with a glass tube, equipped with an adjustable valve. The line temperature was measured using a K-type thermocouple. Whenever the temperature was not equal to 25 ^{o}C (the calibration temperature of the flow meter), a correction factor was applied to the actual reading of the flow meter. In order to enhance safety, an additional valve, which was programmed to close after 5 minutes once activated, was fitted downstream the thermocouple.

The volume fraction of hydrogen in the intake air ranged from 2% to 8%, in 2% steps. In order to keep the speed and load constant, diesel fuel flow was gradually reduced as the concentration of hydrogen in the intake air was increased. Hence, as the proportion of the bottled hydrogen in the intake air was increased, so was the energy provided by hydrogen.

Table 4.1 shows the volume fraction of hydrogen and the corresponding energy fraction it constitutes, whereas Figure 4.2 presents the same information diagrammatically.

Table 4.1: Tabulated energy supplied by hydrogen.

H_2 supply [%vol.]	Intake air [%vol.]	Energy from H_2 [%], 1500 rpm		Energy from H_2 [%], 2500 rpm	
		2.5 bar BMEP	5 bar BMEP	2.5 bar BMEP	5 bar BMEP
0	100	0	0	0	0
2	98	13.65	9.51	11.73	7.92
4	96	27.62	19.00	24.47	15.90
6	94	45.15	28.83	-	25.34
8	92	-	39.13	-	-

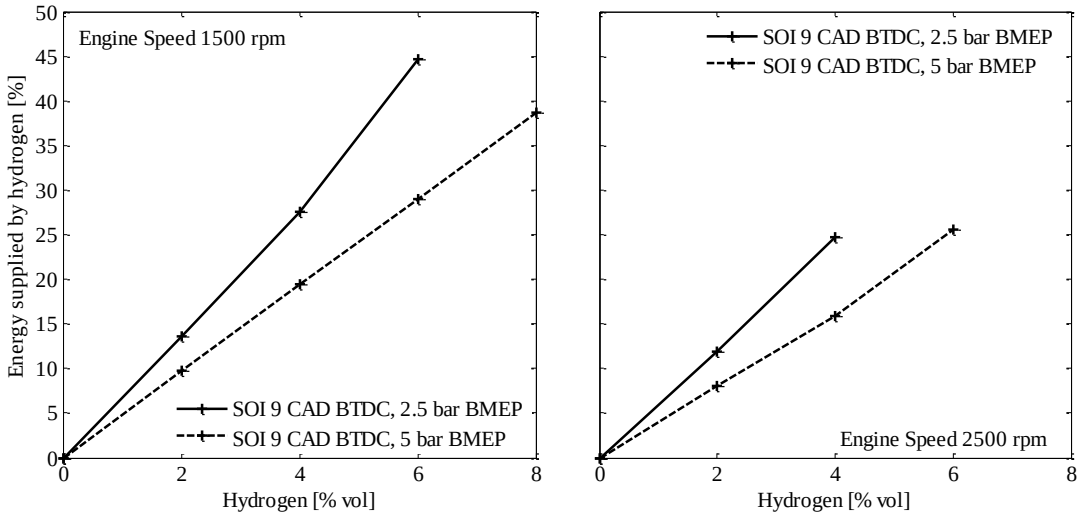

Figure 4.2: Diagram of the energy supplied by hydrogen.

At a fixed engine speed, the load was adjusted by changing the flow rate of diesel fuel. Thus, the medium-load operating condition was achieved by increasing the amount of diesel fuel, keeping the hydrogen flow rate constant. This clearly led to a reduction in the energy supplied by hydrogen.

4.3 Results and discussion

The effects of hydrogen-rich intake air on the performance, combustion and emissions of a diesel engine are presented in the following sections. In particular, the results obtained include the NO_x, BSN, CO and THC emissions as well as the brake thermal efficiency, the

hydrogen combustion efficiency and a heat release rate analysis. The engine was tested at 1500 and 2500 rpm, while each speed included two different loads, 2.5 and 5 bar BMEP. SOI was swept from 12 to 3 CAD BTDC in 3 degree increments.

4.3.1 Effect of hydrogen-rich intake air on NO_x-smoke trade-off

Figures 4.3 and 4.4 show the trade-off between the NO_x and smoke emissions when hydrogen-rich air was introduced into the engine. In particular, the NO_x-BSN values obtained under low-speed operation are illustrated in Figure 4.3, whereas Figure 4.4 depicts the emission values collected under high-speed run. The graphs with the letter (a) denote the low-load operation, whereas the letter (b) indicates the medium-load run. It should be mentioned that due to the zero BSN values obtained under low-speed low-load operation, a secondary y-axis is used in Figure 4.3(a) in order to better illustrate the results obtained.

Under low-speed low-load operation, the introduction of hydrogen hardly affected the NO_x emissions. The already low smoke emissions, obtained under the baseline operation, became zero, or at least below the detection limit of the smoke meter. The smoke emissions at SOI 3 and 6 CAD BDTC were the same; thus, only three smoke lines appear in the figure. The reduction in fuel carbon to hydrogen ratio was possibly the dominant smoke reduction mechanism in this case as the temperature change in the combustion chamber (which is reflected in the NO_x emissions) was likely to be small.

Under low-speed medium-load operation, the expected effect of hydrogen combustion on NO_x emissions was revealed. The admission of hydrogen resulted in increased NO_x emissions due to the higher adiabatic combustion temperature of hydrogen, compared to the baseline operation. The rate of increase was 10-15% when the hydrogen concentration was anywhere between 2% and 4%, while it reached 29% at higher hydrogen percentages. As expected, smoke emissions gradually decreased as the amount of hydrogen introduced into the engine was increased. A considerable increase in NO_x emissions without a significant drop in BSN was recorded when the admitted hydrogen was equal to 8%. Bearing the NO_x-smoke trade-off in mind, this suggests the maximum hydrogen concentration under this particular operating condition should be limited to 6%.

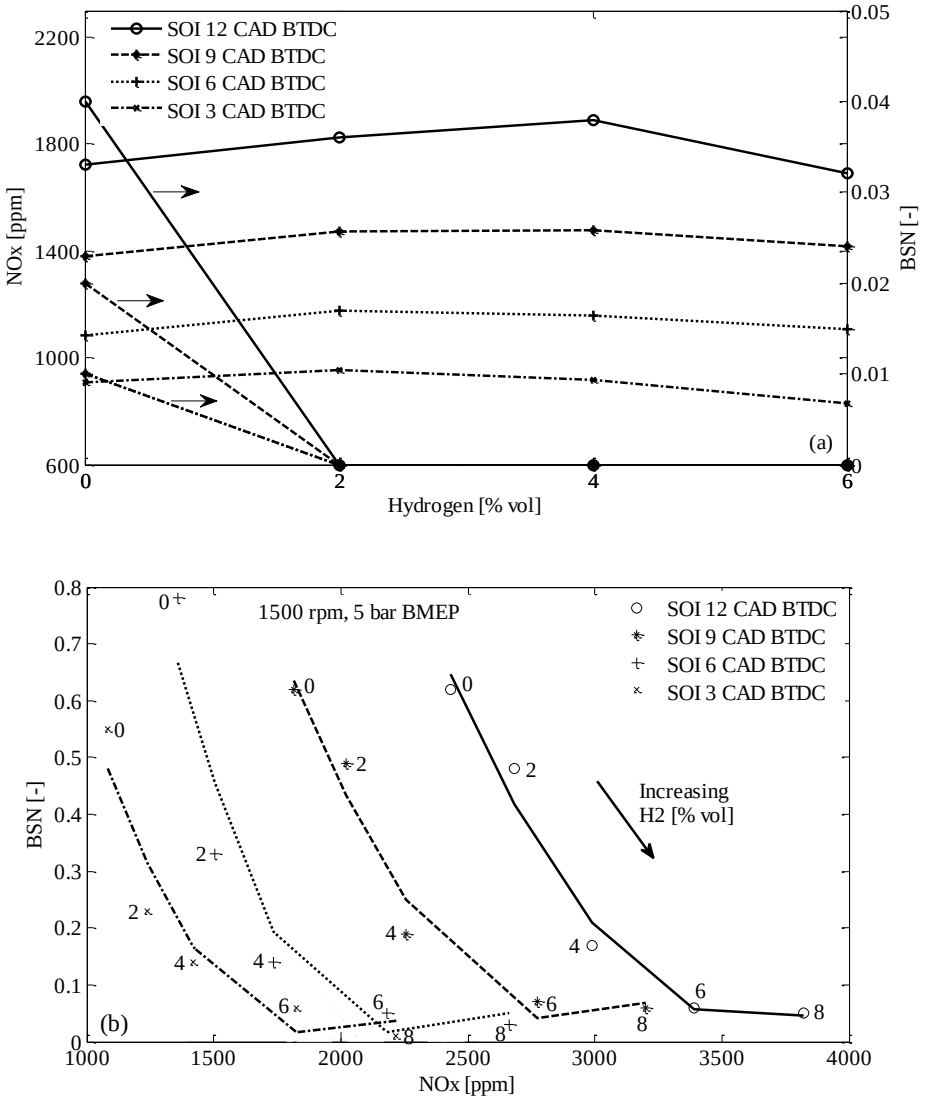

Figure 4.3: Effect of intake air enrichment with hydrogen on the trade-off between NO_x and smoke. Engine speed: 1500 rpm, load: (a) 2.5 bar BMEP, (b) 5 bar BMEP.

The results from the high-speed run are illustrated in Figure 4.4. Comparison between low- and high-speed operations (in identical load conditions) indicated that under high-speed, NO_x emissions were shifted to lower values, although combustion temperature was possibly higher. This trend is probably attributed to the less residence time, which has a large effect on NO_x formation. An increase in smoke (compared to low-speed operation) was not unexpected since the high-speed operation was achieved by delivering a higher amount of diesel into the engine. Besides, referring to Figure 4.2, it is revealed that the percentage of energy provided by diesel fuel was higher at high-speed run compared to low-speed, in identical load conditions.

Figure 4.4(b) reveals that the rate of BSN drop was considerably increased when the concentration of hydrogen was over 2%. Overall, the NO_x-smoke trend obtained under low-speed medium-load operation (Figure 4.3b) was maintained under high-speed medium-low operation (Figure 4.4b).

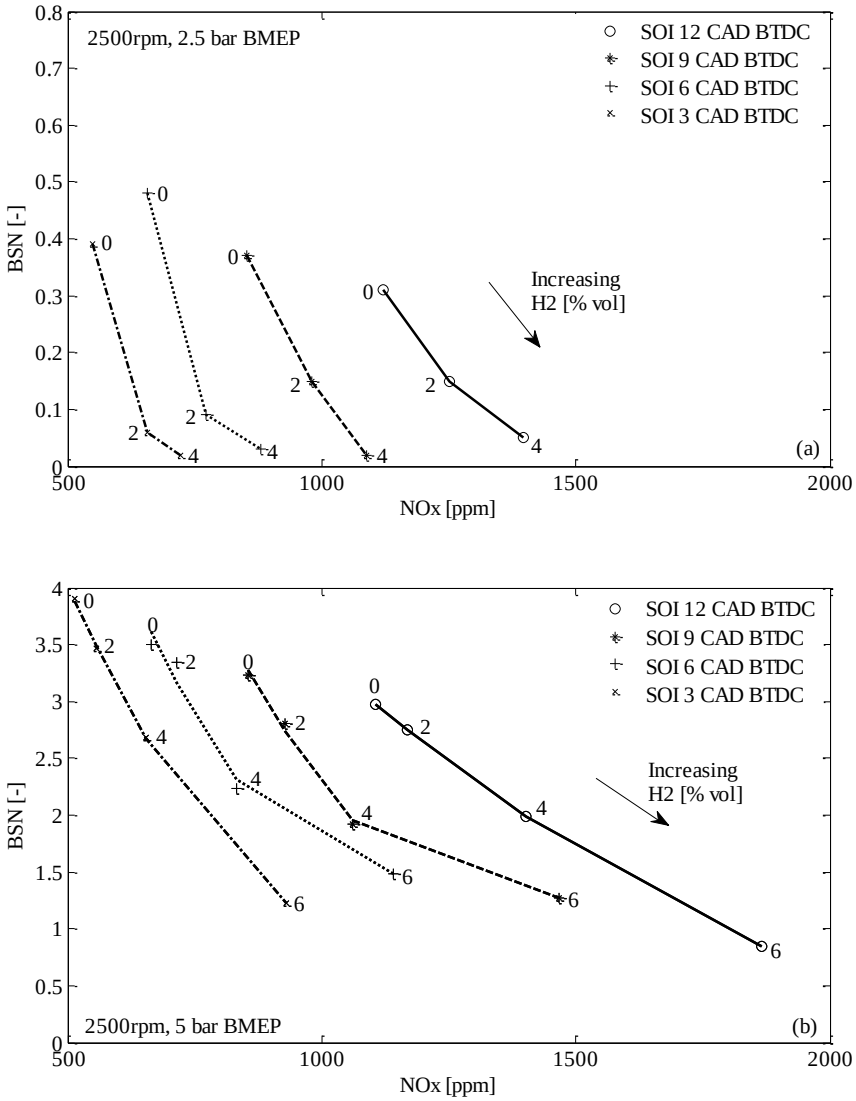

Figure 4.4: Effect of intake air enrichment with hydrogen on the trade-off between NO_x and smoke. Engine speed: 2500 rpm, load: (a) 2.5 bar BMEP, (b) 5 bar BMEP.

Enrichment of the intake air with hydrogen affects smoke in various ways. Firstly, a diesel-hydrogen mixture inherently contains less carbon, which is the main soot component. Secondly, the high in-cylinder temperature arising from the combustion of hydrogen enhances soot oxidation and thirdly, the OH radicals produced from the reaction of hydrogen with oxygen promote the oxidation of soot [11, 135, 136]. It has been reported

that particle size and mass distribution are not significantly affected by the admission of hydrogen into a diesel engine [137].

In Figure 4.3(a), NO_x emissions remained relatively unaffected irrespective of the amount of hydrogen supplied into the engine. Hence, it would be interesting to compare the in-cylinder pressure and the rate of heat release, obtained under this particular operating condition, with a case in which hydrogen admission led to an increase in NO_x emissions. Figure 4.5 shows a comparison between the in-cylinder pressure data recorded under low-speed low-load and low-speed medium-load operation and the corresponding calculated rate of heat release. In Figure 4.5(a), admission of hydrogen into the engine caused a slight drop in the in-cylinder pressure, compared to the baseline operation. It is therefore clear that under this operating condition the combustion of hydrogen did not contribute to an increase in the in-cylinder temperature, which would lead to an increase in the production of NO_x emissions. Under low-speed medium-load operation, fuelling on a diesel-hydrogen mixture resulted in higher in-cylinder pressure as compared to the baseline operation, Figure 4.5(b). It can therefore be deduced that the in-cylinder temperature, the dominant NO_x formation factor, reached a higher peak value. Also, in the same figure, the premixed burn fraction was increased by the admission of hydrogen.

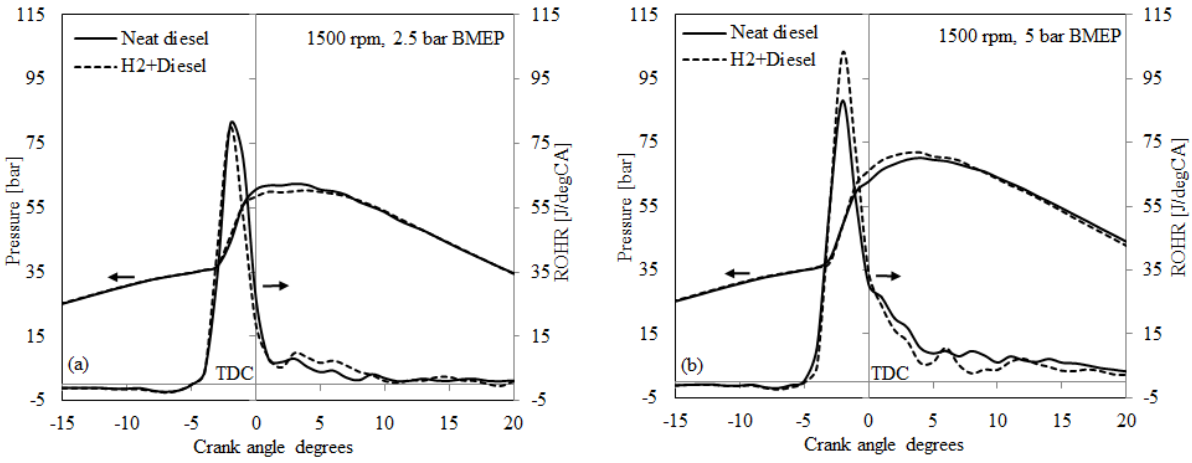

Figure 4.5: Effect of intake air enrichment with hydrogen on the pressure and heat release rate. Engine conditions: speed 1500 rpm, load (a) 2.5 and (b) 5 bar BMEP, hydrogen concentration 4% vol., SOI 9 CAD BTDC.

4.3.2 Effect of hydrogen-rich intake air on CO emissions

In general, compression ignition engines do not suffer from high CO production because of their lean operation. Introduction of hydrogen into the engine causes a further reduction in CO emissions as the carbon content of the fuel is reduced compared to the baseline operation.

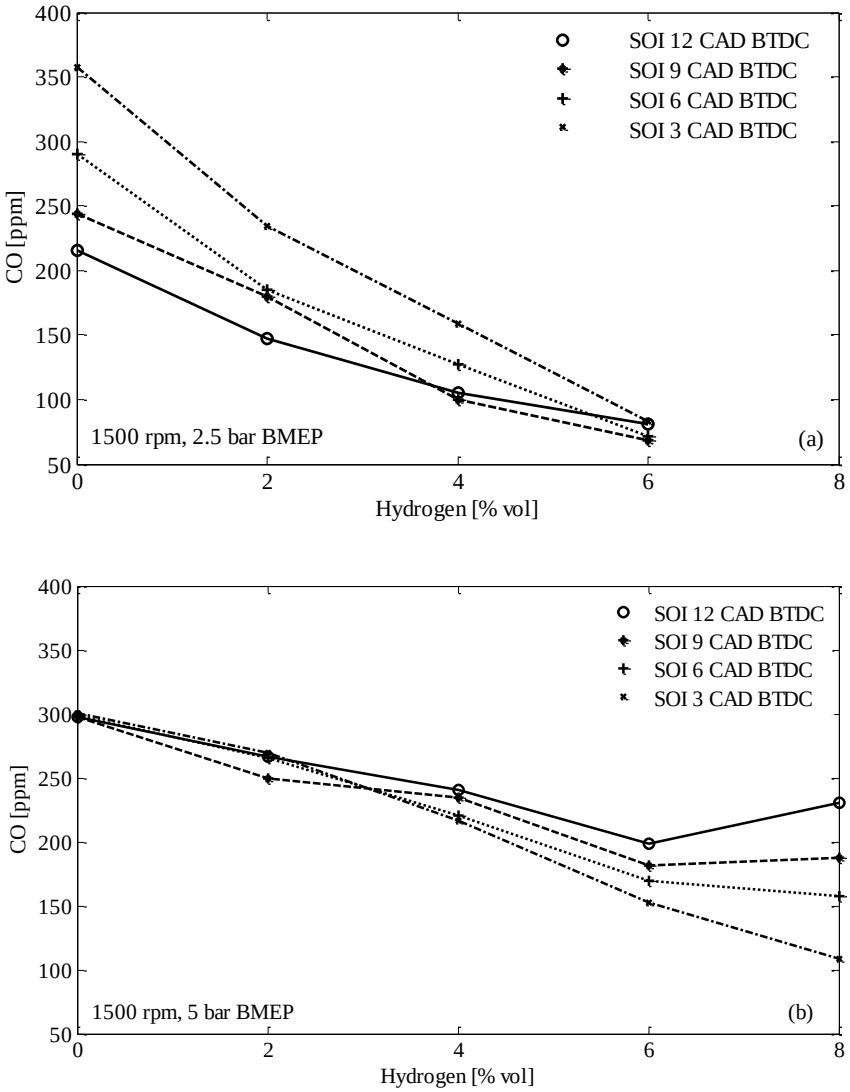

Figure 4.6: Effect of intake air enrichment with hydrogen on the CO emissions. Engine speed: 1500 rpm, load: (a) 2.5 bar BMEP, (b) 5 bar BMEP.

Figures 4.6 and 4.7 depict the CO emissions as a function of the amount of hydrogen delivered into the engine. In the majority of the points tested, an increase in the percentage of hydrogen led to a reduction in CO emissions. The higher CO emissions recorded in a

few operating points (compared to the previous points in which the amount of hydrogen was lower), might have been caused by diesel misfire, as the admission of hydrogen imposed reductions in both oxygen concentration and diesel fuel. For instance, under the following operating point: 1500rpm - 5 bar BMEP - SOI 12 CAD BTDC - 8% hydrogen fraction, the COV_{imep} was found to be 2.6%. When diesel injection was commenced anywhere between 3 and 9 CAD BTDC (keeping the engine speed, load, and hydrogen fraction constant), the COV_{imep} was found to be 1.6%. The increase in the COV_{imep} when diesel injection was commenced at 12 CAD BTDC was probably caused by diesel misfiring. It should be mentioned that under the baseline operation the COV_{imep} did not significantly change with diesel injection timing.

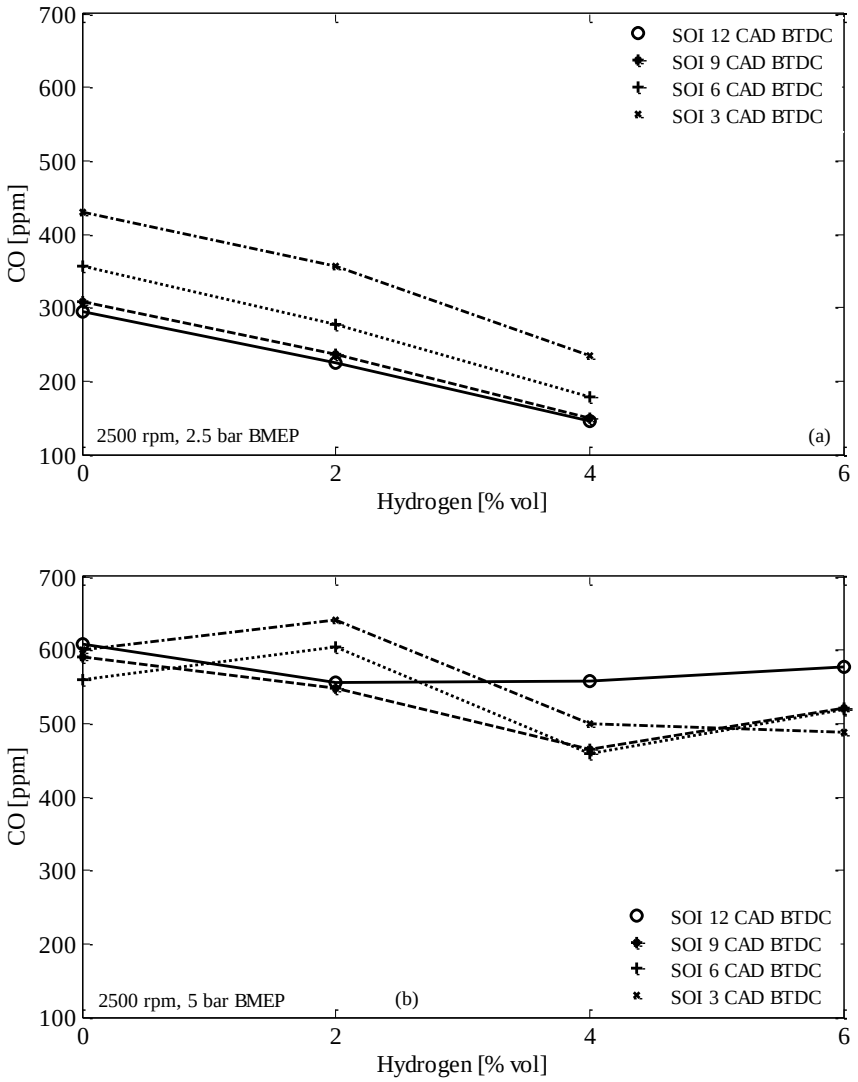

Figure 4.7: Effect of intake air enrichment with hydrogen on the CO emissions. Engine speed: 2500 rpm, load: (a) 2.5 bar BMEP, (b) 5 bar BMEP.

4.3.3 Effect of hydrogen-rich intake air on unburned hydrocarbon emissions

Hydrocarbon emissions are derived from diesel fuel and lubricating oil and are commonly expressed as either total hydrocarbons (THC) or as non-methane hydrocarbons (NMHC). The latter refers to the portion of THC that does not include methane. In heavy-duty diesel engines, NMHC can be obtained by subtracting 2% from the measured THC value. In a conventional compression ignition engine fuelled by diesel, the concentration of gaseous hydrocarbons in the exhaust typically ranges from 20 to 300 ppm [138]. This range can be verified by examining Figures 4.8 and 4.9.

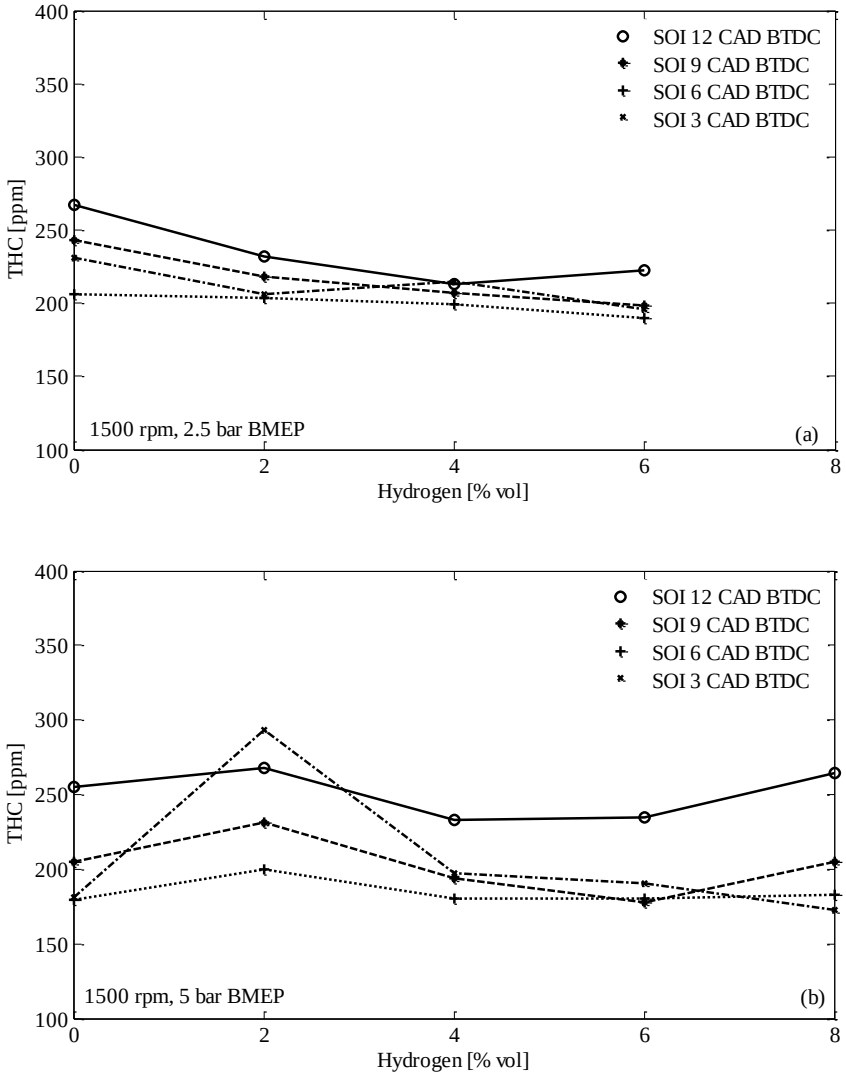

Figure 4.8: Effect of intake air enrichment with hydrogen on the unburned hydrocarbons. Engine speed: 1500 rpm, load: (a) 2.5 bar BMEP, (b) 5 bar BMEP.

Comparison of the baseline operations at the different speeds and loads tested revealed that the high-speed medium-load operation produced the lowest THC emissions. From this finding, it can be concluded that the in-cylinder temperature has a significant impact on the oxidation of hydrocarbons. Another important finding is that, in the majority of the test points, THC emissions increased with advancing the diesel injection timing because the spray tip penetrated deeper (due to low charge density) leading to spray wall impingement.

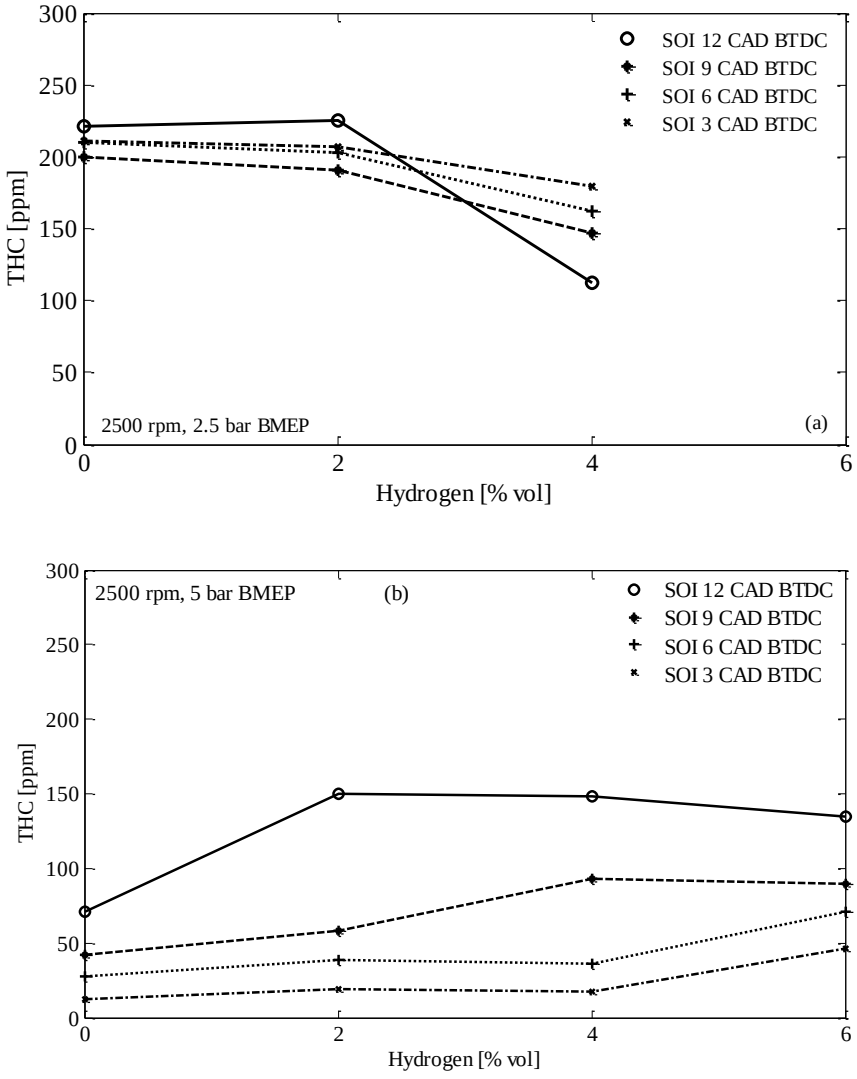

Figure 4.9: Effect of intake air enrichment with hydrogen on the unburned hydrocarbons. Engine speed: 2500 rpm, load: (a) 2.5 bar BMEP, (b) 5 bar BMEP.

Enrichment of the intake air with hydrogen led to higher, lower, or unchanged THC emissions compared to the baseline operation. For instance, in Figure 4.9(b), THC emissions increased with increasing the percentage of hydrogen. In essence, the hydrogen-

air mixture has a lower density compared to air which, in conjunction with the high amount of diesel required in this operating condition, may have led to spray wall impingement.

In Figure 4.8(a), the small diesel quantity delivered into the cylinder, together with the excess air, probably compensated for the reduction in the intake charge density; hence, the introduction of hydrogen did not negatively affect the THC emissions.

4.3.4 Hydrogen combustion efficiency

In a hydrogen-based economy the concentration of hydrogen in the atmosphere would potentially increase (although it currently exists in trace levels), incurring negative consequences in the environment [139]. It is therefore important to optimise the combustion process of the hydrogen dual fuel engines, in order to minimise the unburned hydrogen emitted in the atmosphere. Clearly, any unburned hydrogen in the exhaust is an indication of either incomplete combustion or charge flowing past the exhaust valve during the valve overlap period, both leading to a reduction in the engine thermal efficiency. However, in a diesel-hydrogen dual fuel engine the unburned hydrogen can be utilised in the regeneration process of the DPF. Moreover, it can be used to enhance the performance of the NO_x aftertreatment system [140, 141]. This could evidently improve both fuel economy and CO_2 emissions by reducing the burden on the aftertreatment systems.

In the current experimental setup, the unburned hydrogen was measured using a gas chromatograph (TCD), as described in Section 3.6.4. The instrument was calibrated using certified high purity bottled hydrogen the concentration of which was between 0% and 2%. The combustion efficiency of hydrogen, depicted in Figures 4.10 and 4.11, was calculated based on Equation (3.15).

Before taking any measurements from the dual fuel mode, it was considered necessary to check whether the hydrogen measured in the exhaust gas was exclusively originated from the bottle supply, and that there was no contribution from diesel reactions, which according to Bond et al. [142] produce marginal hydrogen emissions. Exhaust samples from the baseline operation were injected into the GC, which did not respond at all. Thus, it was presumed that the baseline operation was not producing hydrogen, or the amount produced was very low and could not be detected from the GC.

In order to interpret the results the flammability limit of hydrogen needs to be introduced. As already shown in Chapter 3, the LFL of hydrogen is 4% at temperature and pressure 25 ^{o}C and 1 bar, respectively. Nevertheless, in a diesel engine combustion chamber, both pressure and temperature are considerably higher resulting in different LFL. In fact, LFL increases with pressure, whereas an increase in temperature leads to a reduction in LFL [143].

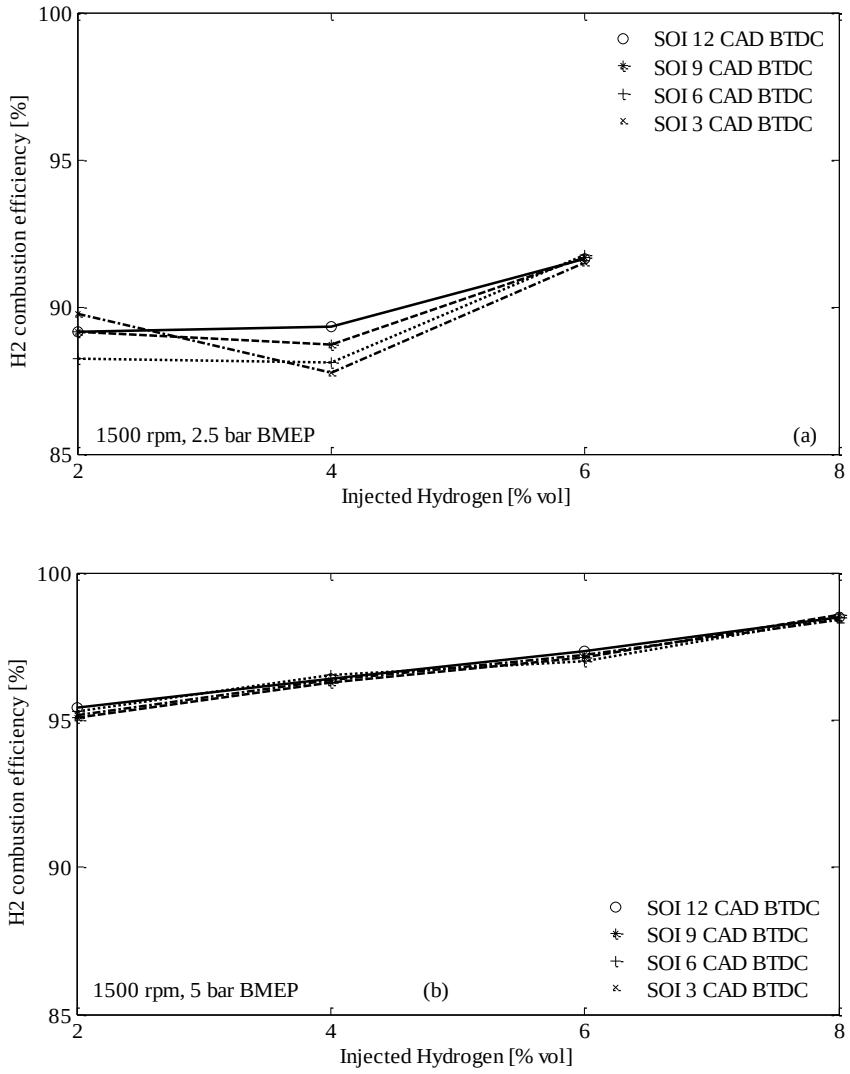

Figure 4.10: Hydrogen combustion efficiency. Engine speed: 1500 rpm, load: (a) 2.5 bar BMEP, (b) 5 bar BMEP.

Under low-speed low-load operation and a hydrogen percentage over 4% (above the LFL), the combustion efficiency of hydrogen was over 90%, Figure 4.10(a). In general, when the concentration of hydrogen is below the LFL, the flame cannot propagate into the

hydrogen-air mixture because it is too lean. Hydrogen burns together with diesel fuel by entraining into the diesel vapour [128]. In the same figure, the combustion efficiency of hydrogen slightly deteriorated when the hydrogen concentration was increased from 2% to 4% with diesel injection commenced after 9 CAD BTDC.

In Figure 4.10(b), the combustion efficiency of hydrogen was gradually increased by increasing the proportion of hydrogen. The dominant factors that contributed to the enhancement of hydrogen combustion efficiency are: the exposure of hydrogen to higher in-cylinder temperatures, leading to a reduction in the LFL, and the larger amount of diesel delivered into the combustion chamber.

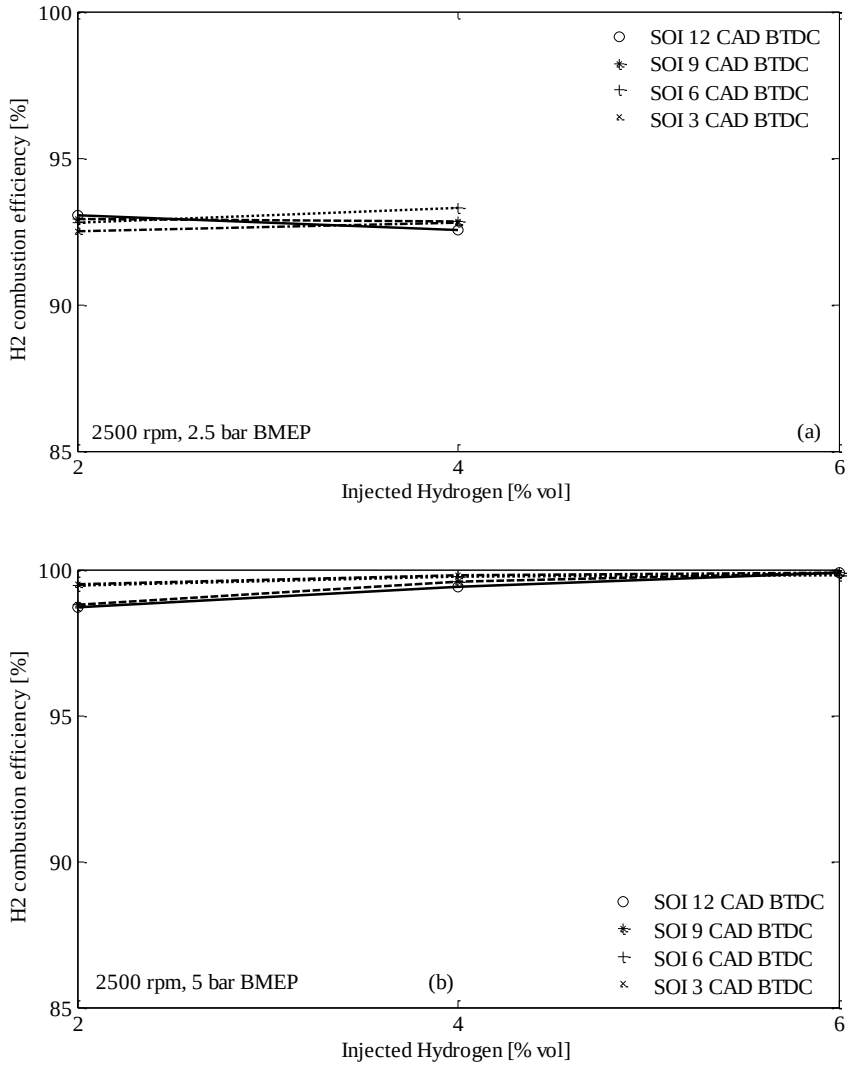

Figure 4.11: Hydrogen combustion efficiency. Engine speed: 2500 rpm, load: (a) 2.5 bar BMEP, (b) 5 bar BMEP.

Under high-speed operation, the combustion efficiency of the bottled hydrogen was further improved, as shown in Figure 4.11. The graphs reveal that under high-speed low-load operation, the combustion efficiency varied from 92.5% to 93.3%, while under high-speed medium-load operation, the percentage of the bottled hydrogen that was utilised during the combustion process varied from 98.7% to 99.9%, depending on the hydrogen fraction and the SOI selected.

4.3.5 Effect of hydrogen-rich intake air on brake thermal efficiency

Figures 4.12 and 4.13 depict a brake thermal efficiency comparison between the hydrogen rich combustion and the baseline operation. All the values presented in the graphs correspond to SOI 9 CAD BTDC. The fuel consumption tests were repeated four times and the values reported are mean values, while the error bars correspond to the ± standard deviation of the calculated brake thermal efficiency.

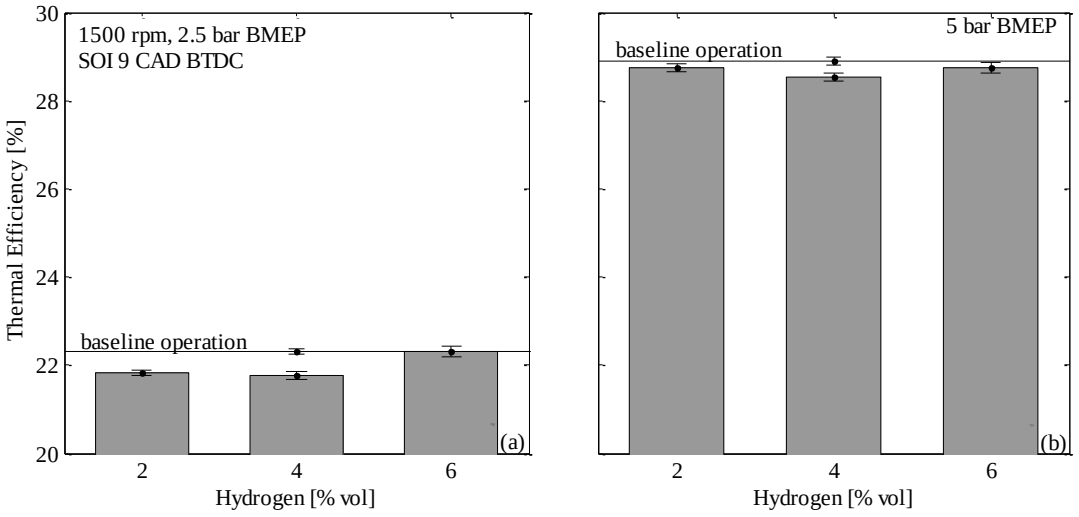

Figure 4.12: Brake thermal efficiency. Engine speed: 1500 rpm, load: (a) 2.5 bar BMEP, (b) 5 bar BMEP, SOI 9 CAD BTDC.

Overall, under low-speed operation, enrichment of the intake air with hydrogen caused a reduction in brake thermal efficiency, apart from the operation under low-load - 6% hydrogen concentration. Despite the 8% loss of the admitted hydrogen, the thermal efficiency was not affected. A further investigation to understand the reason behind that trend would be interesting. Under high-speed operation, a slight efficiency improvement was achieved but remained within the uncertainty limits of the brake thermal efficiency.

As discussed in Section 4.3.4, hydrogen combustion efficiency increased with the load and speed. The largest efficiency loss (around 0.5%) was observed under low-speed low-load operation when the concentration of hydrogen was below 4%. With reference to Figure 4.10(a), around 10% of the admitted hydrogen was not utilised in this particular operating condition, and this was probably the main reason for the drop in thermal efficiency.

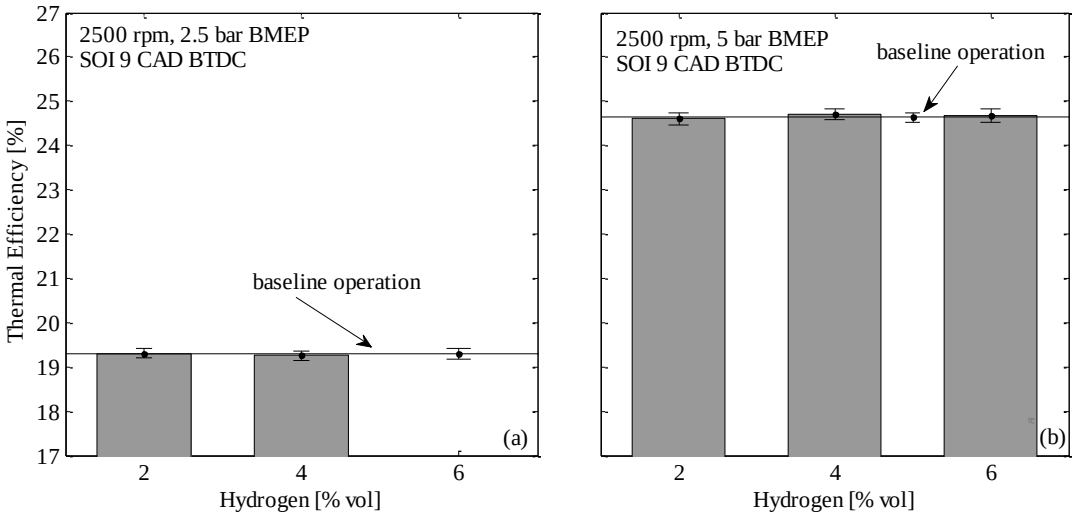

Figure 4.13: Brake thermal efficiency. Engine speed: 2500 rpm, load: (a) 2.5 bar BMEP, (b) 5 bar BMEP, SOI 9 CAD BTDC.

4.4 Summary

The effects of hydrogen enrichment of the intake air on the performance and emissions of an HSDI diesel engine were investigated. The concentration of hydrogen in the intake air was varied from 2% up to 8% (v/v of the total intake charge), in 2% steps. The main findings from this chapter can be summarised as follows:

- In the majority of the conditions tested, part substitution of diesel fuel with hydrogen reduced smoke at the expense of NO_x emissions. Under low-speed low-load operation, enrichment of the intake air with hydrogen was found to have an insignificant effect on NO_x emissions.
- A considerable increase in NO_x without a significant drop in BSN was recorded under low-speed medium-load operation and hydrogen fraction equal to 8%. Bearing the NO_x-smoke trade-off in mind, this suggests the maximum hydrogen concentration under this operating condition should be limited to 6%.

- The high-speed operation resulted in lower NO_x emissions compared to the low-speed (at identical load, hydrogen concentration and start of diesel injection). The reduction of residence time was probably the dominant factor that led to lower NO_x values.
- The CO emissions were reduced as the amount of hydrogen supplied into the engine was increased due to the reduction in the fuel carbon to hydrogen ratio.
- The THC emissions increased with advancing injection timing because the spray tip penetrated deeper into the cylinder, due to the low charge density, leading to spray wall impingement.
- Enrichment of the intake air with hydrogen can lead to higher, lower or unchanged THC emissions compared to the baseline operation. For instance, under high-speed medium-load operation, the THC emissions increased with increasing the percentage of hydrogen. In essence, the hydrogen-air mixture has a lower density compared to air which, in conjunction with the high amount of diesel required in this operating condition, may have led to spray wall impingement. Under low-speed low-load operation, the introduction of hydrogen did not negatively affect the THC emissions, as the small diesel quantity delivered into the cylinder, together with the excess air, probably compensated for the reduction in the intake charge density.
- Hydrogen combustion efficiency improved with increasing the speed, load and hydrogen proportion. In general, unburned hydrogen in the exhaust gas originates from incomplete combustion of hydrogen and charge flowing past the exhaust valve during the valve overlap period. The latter can be eliminated by injecting hydrogen after the closure of the exhaust valve.
- Overall, under low-speed operation, enrichment of the intake air with hydrogen caused a reduction in brake thermal efficiency. Under high-speed operation, a slight efficiency improvement was achieved but remained within the uncertainty limits of the brake thermal efficiency.

CHAPTER 5

ENRICHMENT OF THE INTAKE AIR WITH NITROGEN

5.1 Introduction

Stringent NO_x emission requirements forced the introduction of aftertreatment and in-cylinder NO_x reduction technologies such as SCR systems and EGR, respectively. The integration of aftertreatment systems within the exhaust pipe is associated with increased cost, complexity and fuel consumption penalties; hence, in-cylinder techniques are typically employed in order to mitigate the performance demands of the aftertreatment systems.

EGR is a well-established intake air dilution technique in which exhaust gas from the previous cycle is delivered back into the engine. Although EGR can contribute significantly to the reduction of NO_x emissions, it has been found that it has, among other drawbacks, a detrimental effect on engine lifespan [110, 111]. Alternative intake air dilution techniques, which aim to minimise the drawbacks associated with EGR, have been proposed and studied by various researchers [99,100]. The findings from the enrichment of intake air with nitrogen are promising, and it is very likely that this technique will be adopted by the automobile industry after it undergoes certain improvements.

The outcomes of this chapter will enhance the understanding of the effects an air separation membrane (producing nitrogen-rich combustion air) has on the emissions, combustion and performance of a diesel engine. They can also benefit the development of a fuel reforming catalytic reactor since the introduction of product gas into the engine leads to an increase in the nitrogen to oxygen ratio in the intake air.

5.2 Methodology

Figure 5.1 shows the schematic representation of the line that was used to carry nitrogen from the bottle into the intake pipe. In contrast to the hydrogen line, which has been presented in the previous chapter, the measures required to eliminate the risk of accident are less strict. For instance, a flashback arrestor is not required in pipes carrying inert gases.

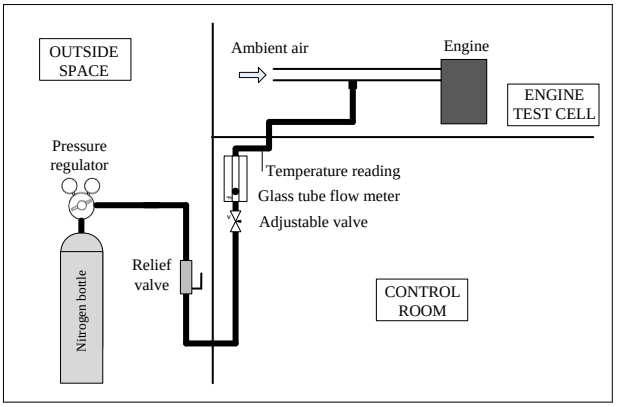

Figure 5.1: Detailed schematic representation of N_2 supply into the intake pipe.

A detailed description of the bottled gas flow, from the bottle through the various components fitted along the gas line into the intake pipe, has already been provided in Section 4.2. At this point, only a brief description of the nitrogen line is provided since the setup of hydrogen and nitrogen lines was similar. The nitrogen flow, control and monitor were achieved by fitting four components along the nitrogen line: a pressure regulator, a relief valve, a glass tube rotameter with an adjustable valve and a thermocouple. The pressure regulator was used to control the line pressure and to track the gas pressure in the bottle. The relief valve, which was fitted after the pressure regulator, ensured that the line pressure did not exceed a certain value. The nitrogen flow rate was measured by the glass tube rotameter, whereas a K-type thermocouple was employed to measure the nitrogen temperature. In case it was different to the calibration temperature of the flow meter, a correction factor was applied to the actual reading of the flow meter.

In this study, an amount of the intake air was gradually replaced by nitrogen in order to examine the effects on the performance, combustion and emissions of the engine. Table 5.1 shows the percentage of the bottled nitrogen supplied into the engine (volumetric basis of the total intake air) and the corresponding inlet oxygen concentration.

Table 5.1: Concentration of oxygen in the intake air as a function of the bottled nitrogen.

N_2 addition [%]	**Inlet O_2 concentration [%]**
2	20.58
4	20.16
6	19.74
8	19.32

The amount of bottled nitrogen delivered into the engine was calculated using Equation (3.16). In addition, the volumetric air flow in the intake was measured by a positive displacement flow meter. The volumetric nitrogen flow was calculated based on the measured air flow. Further details are provided in Chapter 3.

5.3 Results and discussion

The rest of this chapter is devoted to presenting and discussing the findings of the enrichment of the intake air with bottled nitrogen. Under low-speed operation (1500 rpm), up to 8% (volumetric basis) of the intake air was replaced by bottled nitrogen, whereas under high-speed operation (2500 rpm), the bottled gas was limited to 6%, as 8% would require a high flow rate of nitrogen.

5.3.1 Effect of nitrogen-rich intake air on NO_x-smoke trade-off

In general, nitrogen enrichment causes a remarkable reduction in NO_x emissions. However, the reduction in the concentration of oxygen, together with the decrease in peak combustion temperature, results in an increase in smoke levels. Figure 5.2(a) reveals that when 8% of the inlet air was replaced by bottled nitrogen, NO_x emissions were reduced by 71%, while Figure 5.2(b) shows that under medium-load operation, NO_x reduction reached 90% at the same nitrogen fraction. In both loads, the values were compared to the corresponding baseline operation. Reduction of oxygen concentration typically leads to longer duration of combustion, which contributes to the formation of smoke.

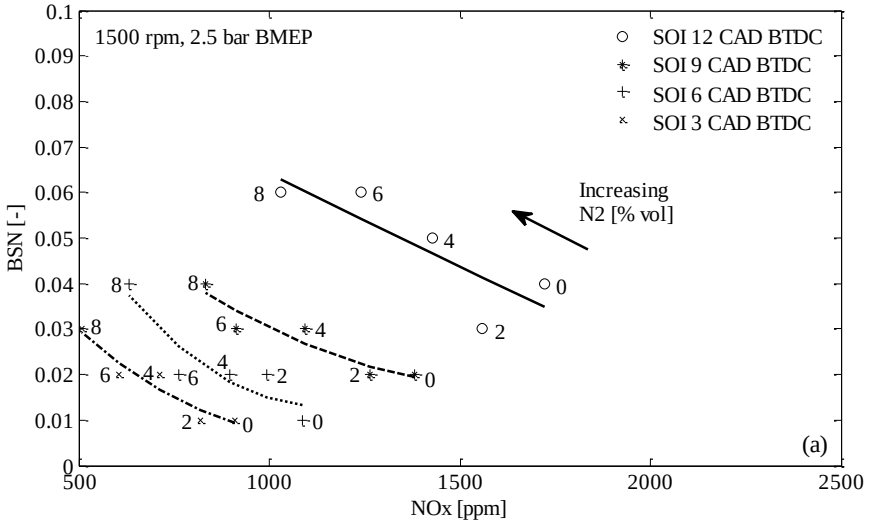

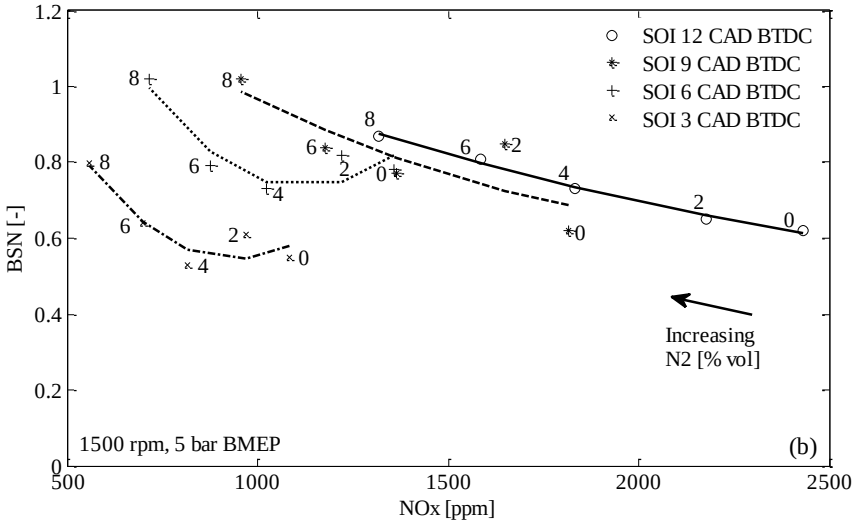

Figure 5.2: Effect of nitrogen-rich intake air on the trade-off between NO_x and smoke. Engine speed: 1500 rpm, load: (a) 2.5 bar BMEP, (b) 5 bar BMEP.

Figures 5.2(b) and 5.3(a) show that introduction of bottled nitrogen up to 4% did not significantly affect BSN when diesel injection was commenced at 3 or 6 CAD BTDC. In both figures, the optimum diesel injection timing, in terms of NO_x and smoke emissions, under the nitrogen-rich mode was at 3 CAD BTDC. Typically, the value of BSN increases as the injection timing is retarded; nevertheless, under certain operating conditions, commencement of diesel injection at 3 CAD BTDC resulted in a reduction in smoke emissions. It should be mentioned that this was a repeatable trend of the engine used to perform the experiments.

Figure 5.3(b) reveals that nitrogen enrichment was very detrimental to smoke emissions when the engine was operated under high-speed medium-load. Replacement of 6% of the intake air with bottled nitrogen led to an increase of over 100% in BSN, compared to the baseline operation. An increase in fuel consumption is expected since a rise in smoke emissions is typically associated with poor utilisation of the fuel. The relatively high equivalence ratio, together with the high in-cylinder temperature, promotes the formation of smoke. According to Kennedy [144], soot production is initiated from the pyrolysis of fuel droplets exposed to high temperature. Finally, under this particular operating condition, the inherent effect of retarding diesel injection on smoke emissions was revealed.

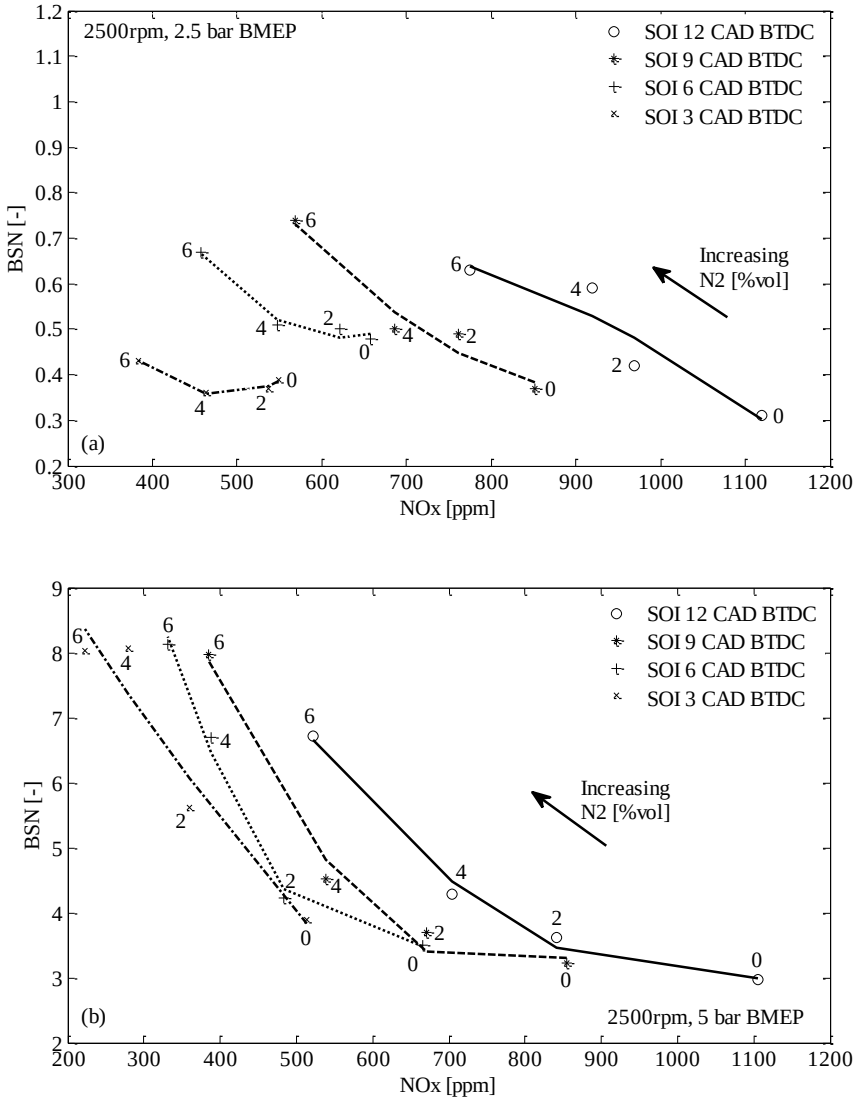

Figure 5.3: Effect of nitrogen-rich intake air on the trade-off between NO_x and smoke. Engine speed: 2500 rpm, load: (a) 2.5 bar BMEP, (b) 5 bar BMEP.

5.3.2 Effect of nitrogen-rich intake air on CO emissions

CO levels in the exhaust of a modern conventional diesel engine typically range from approximately 10 to 500 ppm [138]. Dilution of the intake air with nitrogen results in an increase in CO emissions because it lowers the peak combustion temperature and influences the local equivalence ratio. Figures 5.4 and 5.5 demonstrate the concentration of CO in the exhaust gas as a function of the bottled nitrogen supplied into the engine under low- and high-speed operation, respectively. Under low-speed operation, enrichment of the intake air with over 2% nitrogen led to a considerable increase in CO emissions.

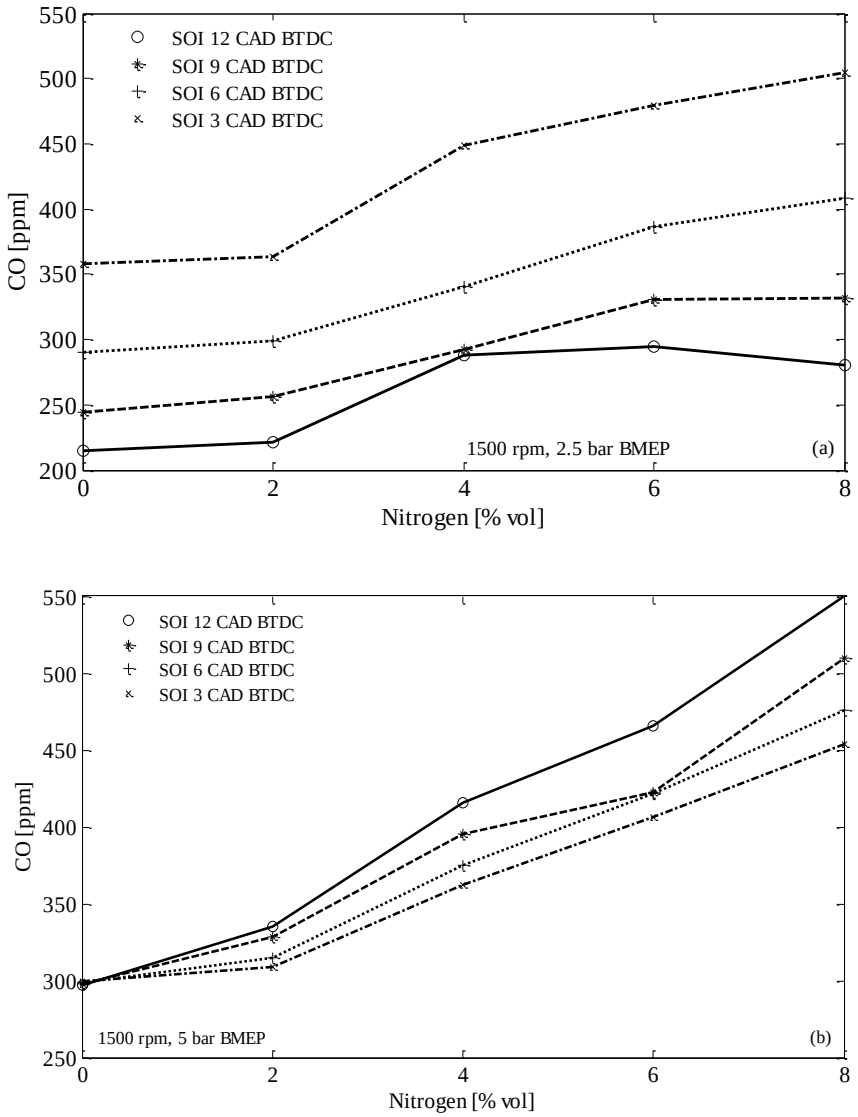

Figure 5.4: Effect of nitrogen-rich intake air on the CO emissions. Engine speed: 1500 rpm, load: (a) 2.5 bar BMEP, (b) 5 bar BMEP.

In the majority of the points tested, CO emissions increased with retarding the injection timing. As diesel injection was commenced closer to the TDC, the time the in-cylinder gases were exposed to temperatures above the CO oxidation threshold was reduced, since the downward movement of the piston (during the expansion stroke) increased the cylinder volume with a simultaneous decrease in both pressure and temperature.

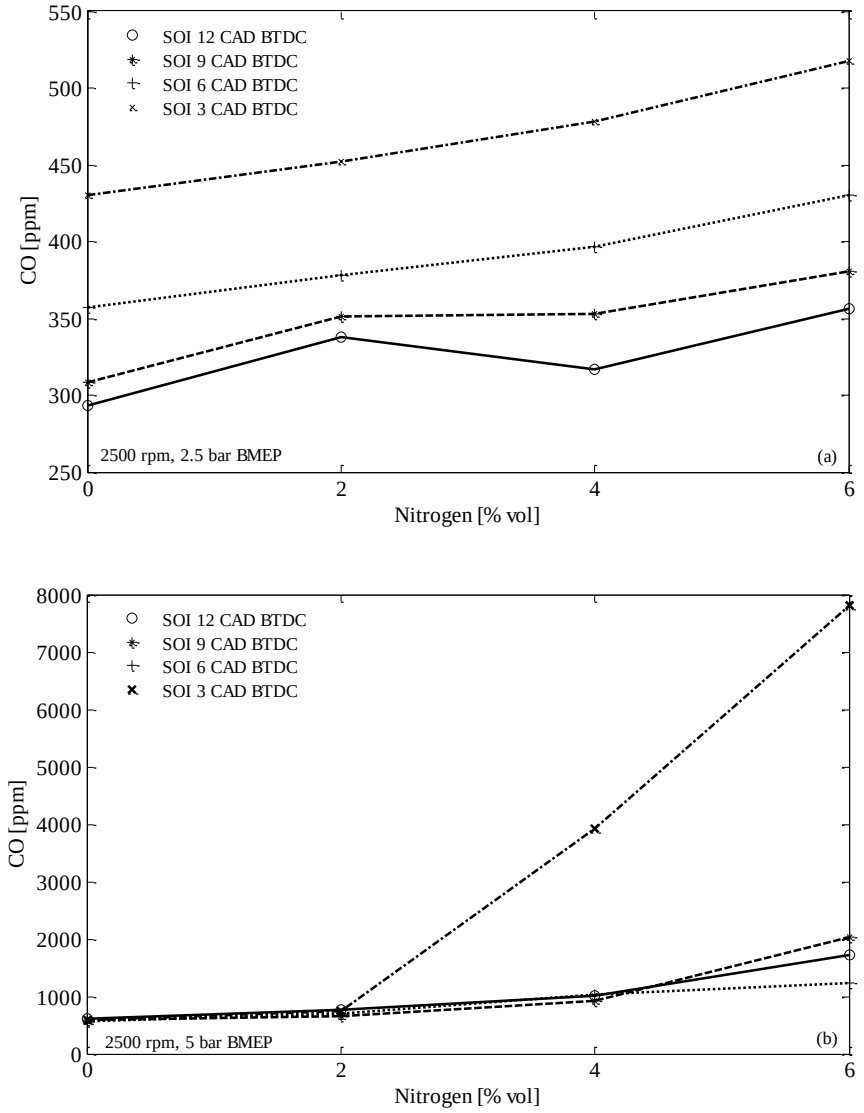

Figure 5.5: Effect of nitrogen-rich intake air on the CO emissions. Engine speed: 2500 rpm, load: (a) 2.5 bar BMEP, (b) 5 bar BMEP.

5.3.3 Effect of nitrogen-rich intake air on the maximum in-cylinder pressure

Figures 5.6 and 5.7 illustrate the maximum in-cylinder pressure at the extreme start of injection timings adopted throughout the experiments; that is, 12 and 3 CAD BTDC. In general, admission of a diluent gas in the intake pipe affects the heat capacity of the intake charge, the oxygen concentration and the reaction rates, which become slower.

Enrichment of the intake air with nitrogen resulted in a rather small change in heat capacity. For instance, replacement of 8% of the intake air with bottled nitrogen caused only a 0.012 kJ/kgK increase in heat capacity, compared to neat air. At the same fraction

of bottled nitrogen, the concentration of oxygen in the intake air dropped to 19.32%; thus, it is more likely that the oxygen reduction effect influenced the combustion process to a greater degree.

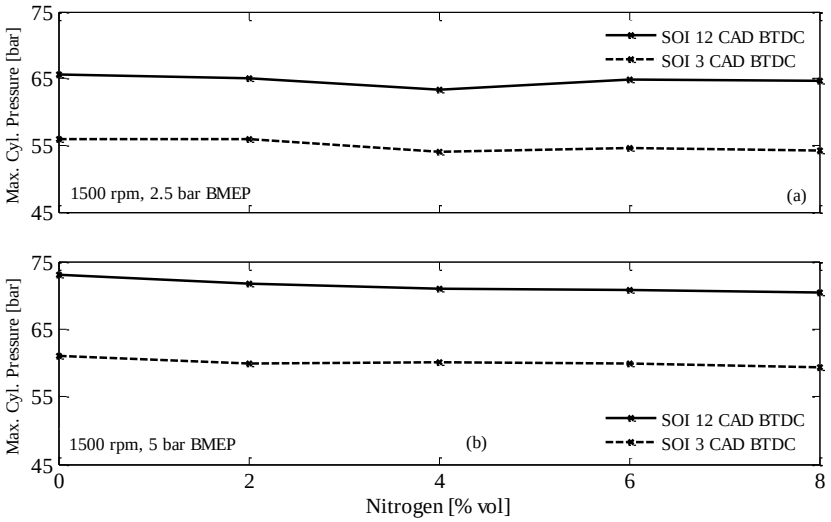

Figure 5.6: Effect of nitrogen-rich intake air on the maximum in-cylinder pressure. Engine speed: 1500 rpm, load: (a) 2.5 bar BMEP, (b) 5 bar BMEP.

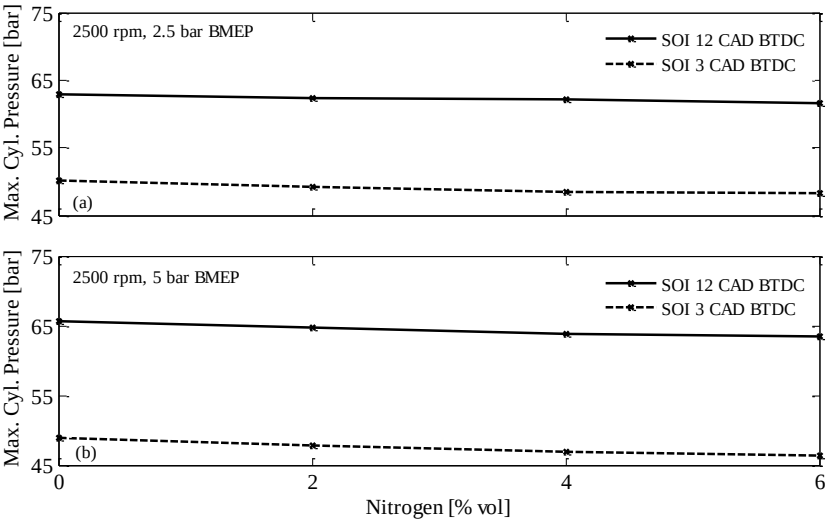

Figure 5.7: Effect of nitrogen-rich intake air on the maximum in-cylinder pressure. Engine speed: 2500 rpm, load: (a) 2.5 bar BMEP, (b) 5 bar BMEP.

Overall, at fixed SOI, the maximum in-cylinder pressure decreased with the reduction in oxygen concentration. In the majority of the test points, retardation of fuel injection from

12 to 3 CAD BTDC resulted in approximately a 10 bar drop in the maximum in-cylinder pressure. The reduction in the in-cylinder pressure that was caused by both the enrichment of the intake air with nitrogen and the retardation of diesel injection can be linked to the decrease in NO_x formation, as presented in Section 5.3.1.

At the same load and nitrogen fraction, the in-cylinder pressure recorded under high-speed operation was lower compared to low-speed. This, together with the less residence time available, were the main factors that led to the reduction in NO_x emissions under high- speed operation, as already presented in Section 5.3.1.

5.3.4 Effect of nitrogen-rich intake air on ignition delay

The ignition delay is defined as the time interval between the SOI and the SOC. In this study, the SOC was considered as the crank angle at which the heat release became positive. The ignition delay is influenced by the diesel spray characteristics (fuel pressure and droplet diameter), in-cylinder conditions (temperature and density) and oxygen concentration of the intake charge (degree of dilution) [145, 146]. In this study, only the final two parameters were varied, while the diesel spray characteristics were kept fixed. The effect of in-cylinder temperature on ignition delay was investigated by changing the start of injection, whereas variations on the oxygen concentration of the intake air were achieved by adjusting the amount of bottled nitrogen.

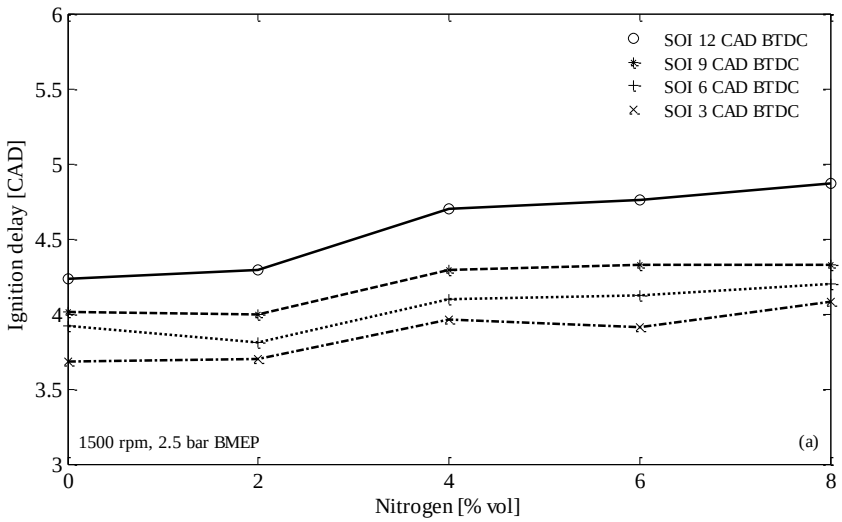

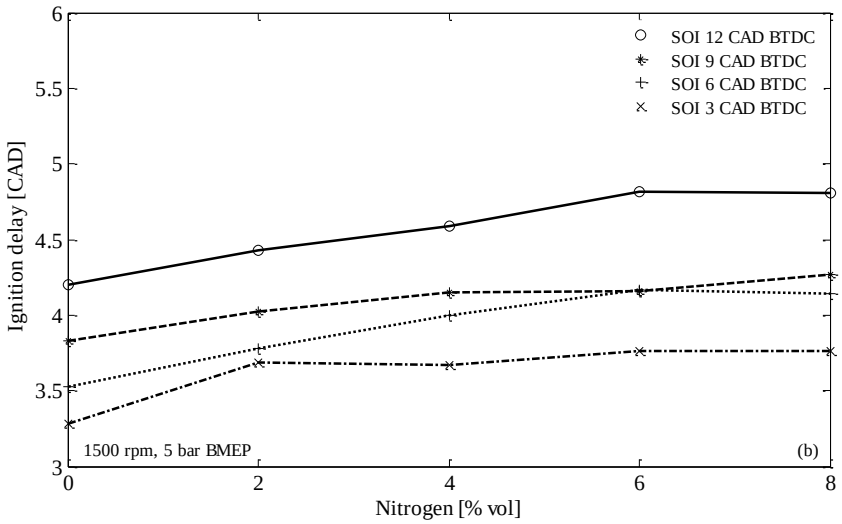

Figure 5.8: Effect of nitrogen-rich intake air on the ignition delay. Engine speed: 1500 rpm, load: (a) 2.5 bar BMEP, (b) 5 bar BMEP.

Figures 5.8(a) and 5.8(b) show that a reduction in oxygen concentration led to an increase in ignition delay. The temperature of the bottled nitrogen was the same as the ambient air, while its effect on the intake charge density was insignificant. Enrichment of the intake air with 8% bottled nitrogen resulted in a reduction in the intake charge density by approximately 0.01 kg/m^3. This clearly indicates that the increase in ignition delay, when the intake air was enriched with bottled nitrogen, was exclusively caused by the reduction in oxygen concentration.

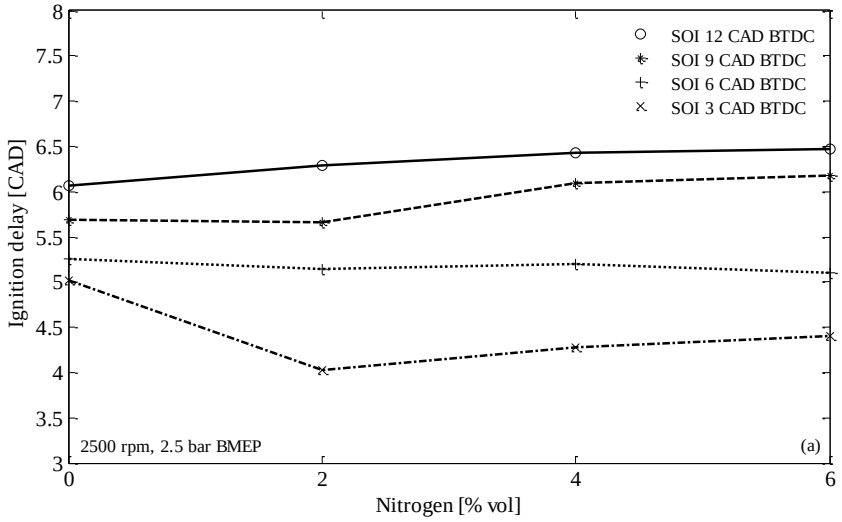

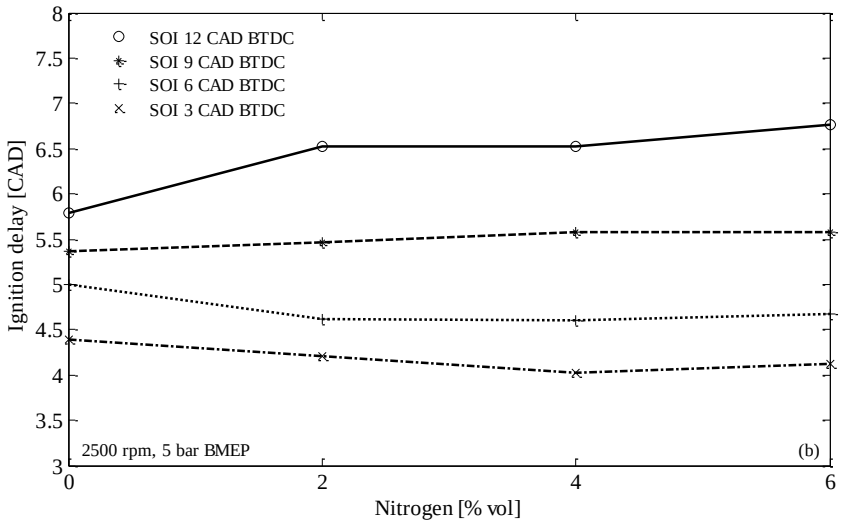

Figure 5.9: Effect of nitrogen-rich intake air on the ignition delay. Engine speed: 2500 rpm, load: (a) 2.5 bar BMEP, (b) 5 bar BMEP.

Another parameter that typically influences the ignition delay is the in-cylinder temperature during the diesel injection, as discussed in the first paragraph of this section. From Figures 5.8 and 5.9, it is clear that retardation of diesel injection led to a shorter ignition delay because the fuel was delivered at a higher in-cylinder temperature.

Under high-speed operation, Figures 5.9(a) and 5.9(b), enrichment of the intake air with nitrogen unexpectedly resulted in a reduction in ignition delay when the injection of diesel was commenced at 6 or 3 CAD BTDC. Taking into account that the in-cylinder temperature was reduced by the admission of nitrogen (reflected in NO_x emissions), it may be concluded that the fuel was ignited by hot spots on the piston as it was relatively close to the injector tip. Nevertheless, this is just a speculation that requires further investigation using optical diagnostics.

5.3.5 Effect of nitrogen-rich intake air on brake thermal efficiency

Figures 5.10 and 5.11 illustrate the brake thermal efficiency at the different bottled nitrogen percentages used to enrich the intake air. The fuel consumption tests were repeated four times and the values reported are mean values, while the error bars correspond to the ± standard deviation of the calculated brake thermal efficiency. Equation (5.1) details the formula used to calculate the brake thermal efficiency:

$$\eta_{th} = \frac{\text{work output}}{\text{heat added}} = \frac{\dot{W}_b}{\dot{m}_{df} LHV_{df}} \tag{5.1}$$

where $\dot{W}_b$ denotes the brake power, $\dot{m}_{df}$ denotes the mass flow rate of diesel and LHV_{df} denotes the lower heating value of diesel.

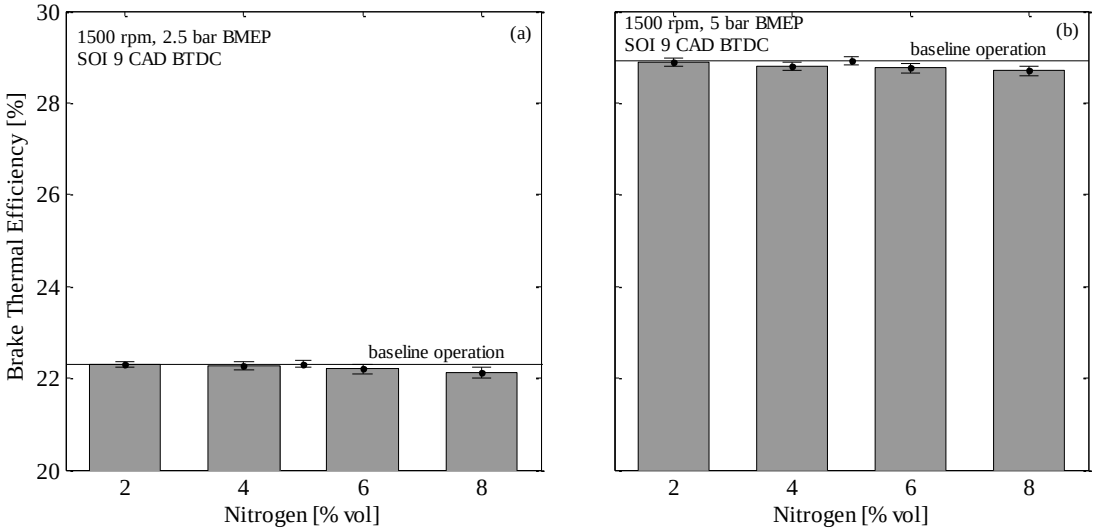

Figure 5.10: Effect of nitrogen-rich intake air on the brake thermal efficiency. Engine speed: 1500 rpm, load: (a) 2.5 bar BMEP, (b) 5 bar BMEP.

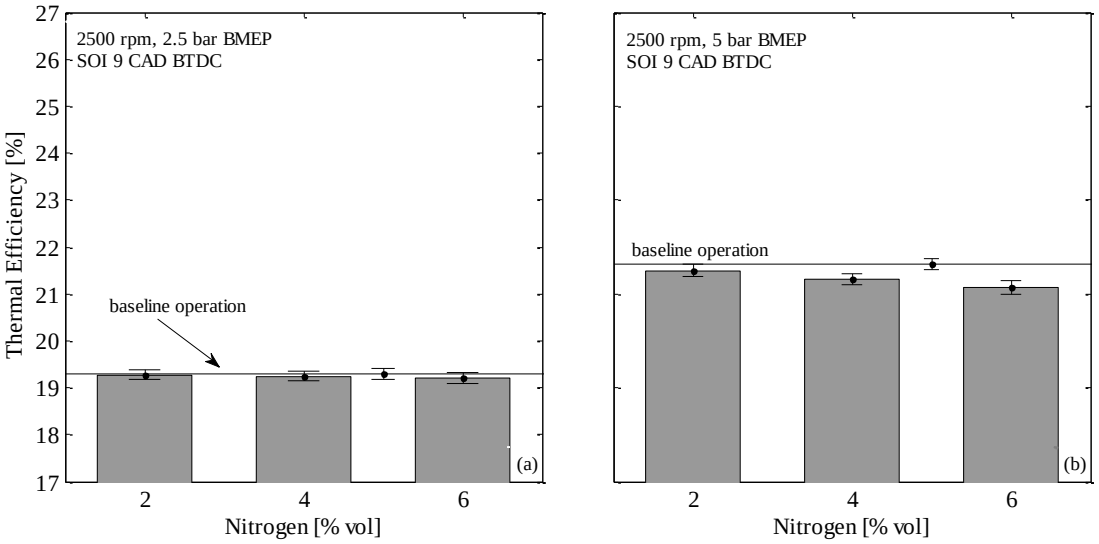

Figure 5.11: Effect of nitrogen-rich intake air on the brake thermal efficiency. Engine speed: 2500 rpm, load: (a) 2.5 bar BMEP, (b) 5 bar BMEP.

In general, an increase in the proportion of nitrogen in the intake air leads to a thermal efficiency drop. The increase in carbon-containing emissions in the exhaust gas, originating from the incomplete combustion of diesel, as presented in Sections 5.3.1and 5.3.2, is associated with poorer utilisation of diesel fuel, which causes a reduction in brake thermal efficiency.

In all the operating conditions tested, it was found that dilution of the intake air with up to 2% bottled nitrogen had a very small impact on brake thermal efficiency. Operation under high-speed medium-load and introduction of 6% bottled nitrogen, resulted in a significant reduction in brake thermal efficiency. This was not unexpected, as this particular operating point was the most BSN and CO emitting, as shown in Figures 5.3(b) and 5.5(b), respectively.

5.4 Summary

The results obtained from the enrichment of the intake air of the engine with bottled nitrogen were presented and discussed in this chapter. The concentration of the bottled nitrogen varied from 2% up to 8% (v/v of the total intake charge), in 2% steps. The main effects on the emissions, performance and combustion can be summarised as follows:

- Enrichment of the intake air with nitrogen resulted in a reduction in NO_x formation. However, the reduction in the concentration of oxygen in the intake air, together with the reduction in peak combustion temperature, had a detrimental effect on smoke and CO emissions.
- Under high-speed medium-load operation, nitrogen enrichment was very detrimental to smoke emissions. In particular, at 6% bottled nitrogen, BSN more than doubled compared to the baseline operation. The reduction of oxygen concentration led to local fuel-rich zones, a lower peak combustion temperature and poor oxidation of diesel fuel. These factors contributed to the formation of smoke, which was not burned off later on as the in-cylinder temperature remained relatively low due to the dilution of the intake air.
- The CO emissions increased with the percentage of the admitted nitrogen. In the majority of the points tested, retarded SOI resulted in higher CO emissions.

- At a fixed start of injection, the maximum in-cylinder pressure decreased with the reduction in oxygen concentration.
- In the majority of the test points, retardation of fuel injection from 12 to 3 CAD BTDC resulted in approximately a 10 bar drop in the maximum in-cylinder pressure.
- Enrichment of the intake air with nitrogen resulted in longer ignition delay as compared to the baseline operation. Retardation of SOI shortened the ignition delay because the fuel was delivered in a higher in-cylinder temperature.
- Brake thermal efficiency reduced with the increase in the proportion of nitrogen. This was not unexpected taking into account that carbonaceous emissions increased when the intake air was diluted with nitrogen.

CHAPTER 6

ENRICHMENT OF THE INTAKE AIR WITH SIMULTANEOUS HYDROGEN AND NITROGEN

6.1 Introduction

Overcoming the trade-off between NO_x and smoke emissions in diesel engines requires investigation of novel systems, which can potentially serve the automobile industry towards further emission reduction. Enrichment of the intake air with a H_2 + N_2 gas mixture, which can be obtained from a diesel fuel reforming system, can lead to new generation low polluting diesel engines.

Reduction of diesel exhaust emissions can be achieved either with in-cylinder emissions suppression techniques [147], or with aftertreatment technologies [148]. The existence of inverse correlation between emissions, especially NO_x and smoke, makes the in-cylinder emission control a very challenging task, taking into account the low emission limits that are in force. Hence, novel solutions are required in order to simultaneously reduce the levels of the different pollutants leaving the cylinder.

Some parameters affecting the formation of emissions, which can be adjusted relatively easy through the ECU are injection timing, injection pressure and EGR volume fraction. Buyukkaya and Cerit [149] performed experiments on a low heat rejection diesel engine and found that retardation of injection timing lowered NO_x emissions at the expense of PM. The same NO_x-smoke trend was obtained either by decreasing the injection pressure or by increasing the proportion of EGR in the intake air [150]. The latter resulted in a reduction in oxygen concentration in the intake air, which led to a decrease in NO_x and an increase in PM [151].

Various techniques that simultaneously suppress the formation of NO_x and smoke emissions have been investigated, but only few of these techniques have been applied to mass production. Mkilaha et al. [152] modified a four cylinder indirect injection diesel engine to deliver compressed air into the pre-chamber during combustion. At no load conditions, the NO_x and PM emissions reduced simultaneously. It was concluded that NO_x

reduction was caused by flame quenching, while the drop in PM was caused by the enhanced mixing of diesel with air.

Many studies have shown that adoption of dual fuel is a feasible solution to the reduction of emissions. This technique can affect various combustion parameters such as flame propagation, ignition delay, adiabatic flame temperature, flammability limits, reduction in intake charge oxygen concentration and combustion duration, which influence engine emissions and performance.

Papagiannakis and Hountalas [153] investigated the effects of blending diesel with natural gas on the performance and emissions of a DI diesel engine. It was shown that in most of the operating points tested, admission of natural gas resulted in simultaneous reductions in NO and PM. It was also reported that fuel consumption, CO and HC emissions deteriorated under the dual fuel operation. In a different study, it was demonstrated that operation with combined hydrogen and EGR can also offer simultaneous reductions in NO_x and smoke emissions [154].

Roy et al. [155] combined in-cylinder and aftertreatment emission reduction techniques in a single-cylinder naturally aspirated DI diesel engine. The formation of NO_x emissions was suppressed using EGR, whereas the increased PM emissions, associated with EGR, were treated by a cyclonic separator fitted into the exhaust pipe. The particles were subject to centrifugal forces enabling the separation of soot from the exhaust gas. Nakatani et al. [156] reported a more than 80% reduction in both NO_x and PM emissions by developing an aftertreatment system called DPNR (Diesel Particulate - NO_x Reduction System).

Johnson [157] presented a review on NO_x control and PM reduction technologies. Diesel particulate filter is the technology currently used to remove PM from the exhaust gas, whereas NO_x emissions are treated with the aim of the SCR system. The integration of both systems in the exhaust pipe allows simultaneous NO_x and PM aftertreatment. Yoshinobu et al. [158] proposed an electrochemical reduction system to reduce NO_x and smoke emissions from diesel engines. They claimed NO_x and PM reductions over 90%.

The objective of this chapter is to present the effects of $H_2 + N_2$-enriched intake air on the emissions, combustion and performance of an HSDI diesel engine. Bottled gases, simulating diesel fuel reforming product gas, were introduced into the engine through the

inlet pipe. Carbon monoxide, at a relatively high concentration, is typically present in diesel reforming product gas; nevertheless, it can be reduced to ppm levels through the water-gas shift reaction using a good low-temperature catalyst. The effects of syngas + N_2-enriched intake air, aiming to build on the knowledge obtained in the previous and current chapter, are presented in Chapter 7.

6.2 Methodology

A detailed description of the hydrogen and nitrogen lines has already been provided in Chapters 4 and 5. In fact, admission of a H_2 + N_2 mixture into the engine was achieved by using both lines simultaneously. Figure 6.1 shows the schematic representation of the two lines used to carry the bottled gases into the intake pipe.

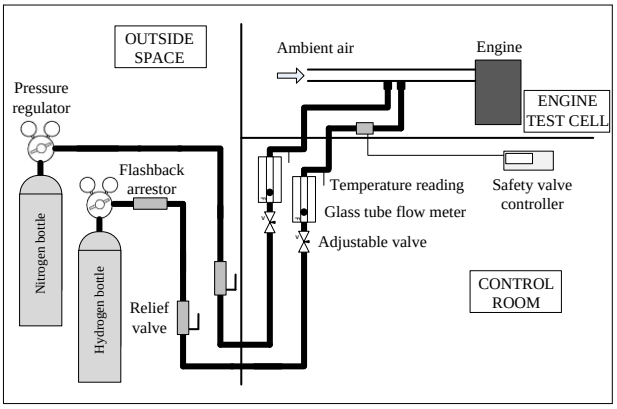

Figure 6.1: Detailed schematic representation of simultaneous hydrogen and nitrogen supply into the intake pipe.

6.3 Hydrogen and nitrogen enrichment

This chapter extends beyond the enrichment of the intake air with separate hydrogen and nitrogen (presented in Chapters 4 and 5, respectively) by supplying the two gases into the engine simultaneously in order to assess the effects on the emissions, performance and combustion. The study aims to simulate the supply of oxygen-free reformer products into the engine. Depending on the reactions promoted, hydrogen can be the main combustible product of diesel fuel reformation, while nitrogen simulates the reduction in oxygen concentration in the intake air; that is, increased nitrogen to oxygen ratio. Table 6.1 illustrates the intake charge composition at the various H_2 + N_2 fractions used.

Table 6.1: Intake charge composition.

Bottled H_2 + N_2 [%vol. of intake air]	**Intake charge composition**		
	[%N_2]	**[%O_2]**	**[%H_2]**
0	79	21	0
2+2	77.84	20.16	2
4+4	76.68	19.32	4
6+6	75.52	18.48	6
8+8	74.36	17.64	8

A review of the effects of enriching the intake air with separate hydrogen and nitrogen on the combustion of a diesel engine has already been provided in Chapter 2; however, a brief discussion is also provided in the following paragraph.

Nitrogen does not participate in the combustion process but the displacement of intake air oxygen lowers the combustion temperature; hence, NO_x emissions reduce at the expense of CO, smoke and THC. The high adiabatic flame temperature of hydrogen contributes to the increase in NO_x formation; however, the combustion of hydrogen produces zero CO, smoke and THC emissions. Enrichment of the intake air with simultaneous H_2 + N_2 allows realisation (under certain operating conditions) of the benefits the two gases offer; namely, simultaneous NO_x, BSN and CO reduction. It is anticipated that H_2 + N_2 rich intake air could lead to new advances in diesel engines with the reforming-based H_2 + N_2 serving as the enabling technology for developing new frontier emission reducing engines.

6.4 Results and discussion

The results obtained from the H_2 + N_2 rich combustion are presented in this section. Along with the regulated emissions, the effects of H_2 + N_2 enrichment on nitrogen exhaust compounds such as NO, NO_2, NH_3 and N_2O are provided. In addition, a combustion analysis aims to clarify how a H_2 + N_2 gas mixture affects various combustion parameters such as the in-cylinder pressure, the rate of heat release and the mass fraction burned. A brake thermal efficiency comparison between the baseline and the H_2 + N_2 rich operation is also presented.

6.4.1 Effect of hydrogen- and nitrogen-rich intake air on the NO_x-smoke trade-off

As already mentioned, N_2-rich intake air reduces the formation of NO_x emissions at the expense of smoke, whereas hydrogen enrichment typically causes the opposite effect. Simultaneous H_2 + N_2 enrichment can allow realisation of the benefits the two gases offer; namely, simultaneous NO_x and smoke emission reduction. In this section, among other results, it is shown that under low-speed low-load operation, enrichment of the intake air with simultaneous H_2 + N_2 can break the trade-off between NO_x and smoke emissions. Figures 6.2 and 6.3 show the NO_x-BSN values recorded when the intake air was enriched with a mixture of H_2 + N_2. It should be clarified that due to the zero BSN values in Figure 6.2(a) a secondary y-axis was adopted to better illustrate the results.

Figure 6.2(a) reveals that introduction of bottled H_2 + N_2 up to 4% caused a minor reduction in NO_x emissions. An increase in the volume of the admitted gas mixture beyond 4% led to a substantial suppression in the formation of NO_x emissions. As already presented in Chapter 4, under low-speed low-load operation, the combustion of a H_2-diesel blend hardly affected the levels of NO_x emissions; therefore, it is speculated that the drop in NO_x when the intake air was enriched with a mixture of H_2 + N_2 (running the engine at the same operating conditions) was caused by the reduction in the amount of oxygen in the intake air. A comparison with the neat diesel operation showed a 71.5% reduction in NO_x formation when a 12% H_2 + N_2 gas mixture was used. It is worth mentioning that at 12% H_2 + N_2 (6% H_2 + 6% N_2) proportion, in three out of four different injection timings, NO_x emissions were slightly lower compared to the NO_x values obtained at 6% nitrogen admission, Figure 5.2(a). The lower percentage of oxygen in the former case (18.48% as compared to 19.74% in the latter) possibly compensated for the admission of hydrogen. Concerning the BSN values, the reduction of carbon to hydrogen ratio in the H_2-diesel blend, compared to the baseline operation, resulted in a reduction in BSN that became finally zero (or below the detection limit of the smoke meter). It should be noted that the BSN lines at SOI 3 and 6 CAD BTDC coincide.

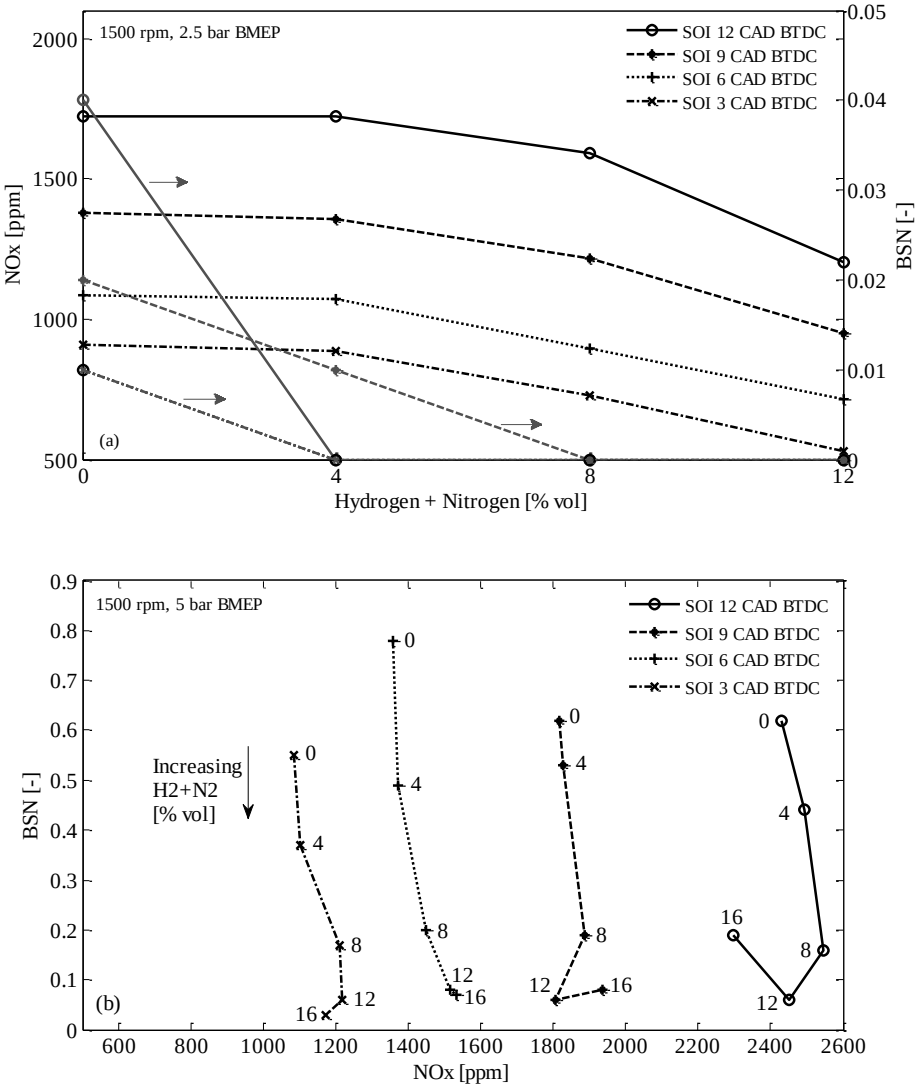

Figure 6.2: Effect of simultaneous H_2 + N_2 enrichment on the NO_x-BSN trade off. Engine speed 1500 rpm, load: (a) 2.5 bar BMEP, (b) 5 bar BMEP.

Figure 6.2(b) shows that under low-speed medium-load operation, BSN values significantly decreased by the introduction of a H_2 + N_2 gas mixture into the engine. At the same operating condition, substituting up to 8% of the inlet air with H_2 + N_2 caused an increase in NO_x emissions at a rate of 0.6-9%, depending on the injection timing and the fraction of the gas mixture. When the admitted gas mixture was over 8%, the effect of H_2 + N_2 enrichment on NO_x emissions varied, depending on the SOI selected. However, of interest is the following operating point: 16% H_2 + N_2 gas mixture - start of injection 12 CAD BTDC in which the emission data revealed an unexpected trend. The reduction in NO_x in conjunction with the increase in BSN was probably caused by diesel misfire. In

general, when injection timing is advanced, diesel is injected at lower in-cylinder temperature. This condition, together with the reduction in diesel quantity and the replacement of an amount of oxygen, may have led to poor fuel oxidation, reflected in emissions with increased BSN (partially oxidised fuel) and reduced NO_x (lower temperature due to less fuel being utilised). The correctness of this speculation can be verified by examining Figures 6.7 and 6.13(b), which show the in-cylinder pressure and the CO emissions under this particular operating condition.

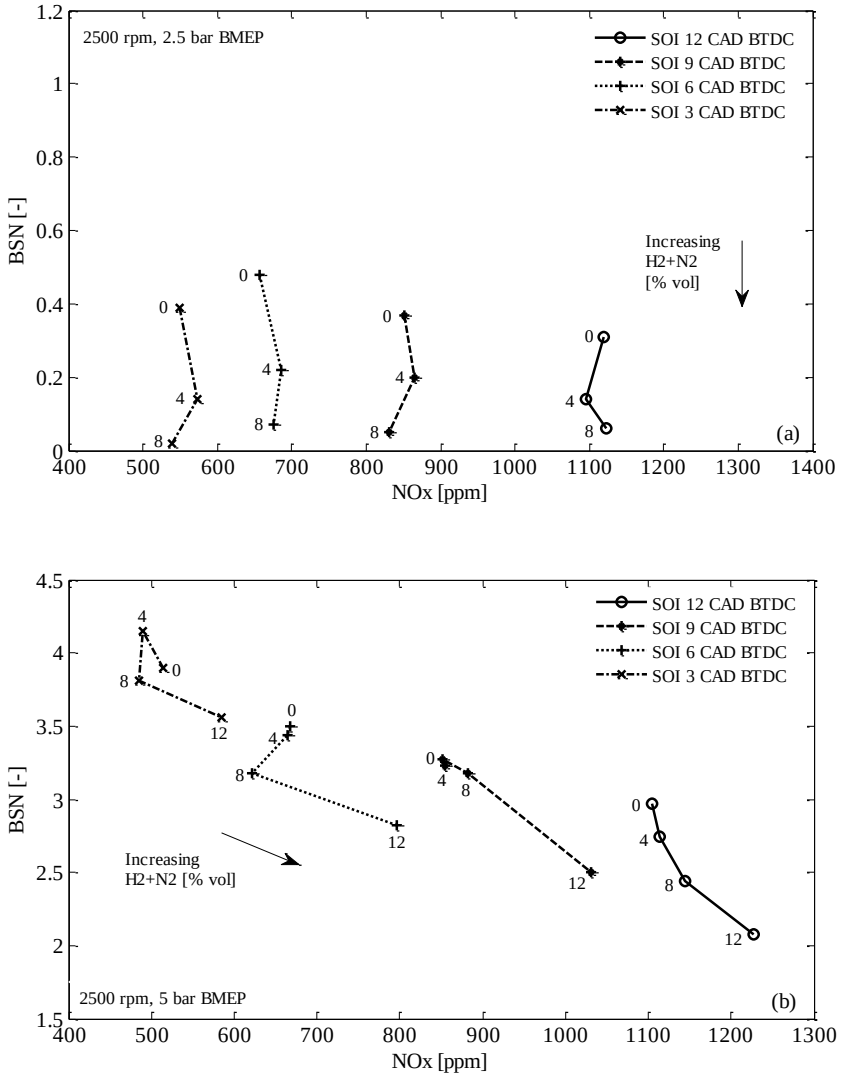

Figure 6.3: Effect of simultaneous H_2 + N_2 enrichment on the NO_x-BSN trade off. Engine speed 2500 rpm, load: (a) 2.5 bar BMEP, (b) 5 bar BMEP.

Under high-speed low-load operation, enrichment of the intake air with a mixture of H_2 + N_2 exhibited a considerable reduction in smoke and relatively unaffected NO_x emissions,

Figure 6.3(a). It is speculated that a change in the proportion of H_2 + N_2 could lead to a simultaneous decrease in NO_x and BSN. Reduction in hydrogen supply (for instance a gas mixture consisted of either 6% N_2 + 2% H_2 or 5% N_2 + 3% H_2), would probably result in a reduction in NO_x formation.

Under high-speed medium-load operation, the rate of NO_x formation exhibited a significant increase when the admitted H_2 + N_2 mixture was over 8%. Below this gas mixture proportion, the effect of H_2 + N_2 on NO_x emissions varied, depending on the injection timing. When diesel injection was commenced either at 12 or at 9 CAD BTDC, an increase in the amount of H_2 + N_2 resulted in increased NO_x emissions. Start of diesel injection either at 6 or at 3 CAD BTDC, led to a reduction in NO_x formation as the proportion of H_2 + N_2 increased. Smoke emissions reduced at almost all the points tested as the amount of H_2 + N_2 increased.

6.4.2 Combustion analysis

To examine the effect of H_2 + N_2 enrichment on the in-cylinder pressure and the rate of heat release (ROHR) six points were selected from Figures 6.2 and 6.3. Figures 6.4(a) and 6.4(b) correspond to 1500 rpm low- and medium-load operation, respectively, while Figure 6.4(c) shows the data recorded in 2500 rpm 5 bar BMEP operation. All the data illustrated in Figure 6.4 corresponds to a fixed start of diesel injection, 6 CAD BTDC.

Figure 6.4(a) shows a case in which an increase in the amount of H_2 + N_2 resulted in a reduction in NO_x emissions. In this figure, the comparison was made between the data collected at 8% and 12% H_2 + N_2 fraction. The smaller premixed burn fraction obtained at 12% H_2 + N_2 justifies the drop in NO_x emissions. A higher proportion of premixed burning often correlates with higher NO_x emissions [30]**.** Referring to **Figure 6.2**(a), BSN was maintained at zero levels in both 8% and 12% H_2 + N_2 fractions, although at 12% H_2 + N_2 the combustion temperature was lower (reflected in the lower NO_x value), and the amount of fuel burned during the diffusion combustion phase was higher, Figure 6.4(a). From this it can be concluded that under this operating condition, the reduction of fuel carbon to hydrogen ratio was the dominant factor that led to BSN reduction. Comparison of the heat release when the introduction of different H_2 + N_2 amounts (12% and 16% H_2 + N_2) did not significantly affect NO_x and BSN values revealed a distinct similarity between the two curves, Figure 6.4(b). Finally, Figure 6.4(c) shows a case in which an increase in the

amount of the gas mixture (from 8% to 12% H_2 + N_2) led to an increase in NO_x emissions and a reduction in BSN. Again, higher NO_x were emitted from the combustion with the larger premixed burn fraction.

The reduction in smoke emissions is attributed to the following reasons: Reduction in carbon to hydrogen ratio as the amount of hydrogen is increased, better soot oxidation when the combustion temperature is increased, enhancement of soot oxidation from the production of OH radicals and reduction of the amount of fuel burned late in the expansion cycle [11, 135, 136, 159].

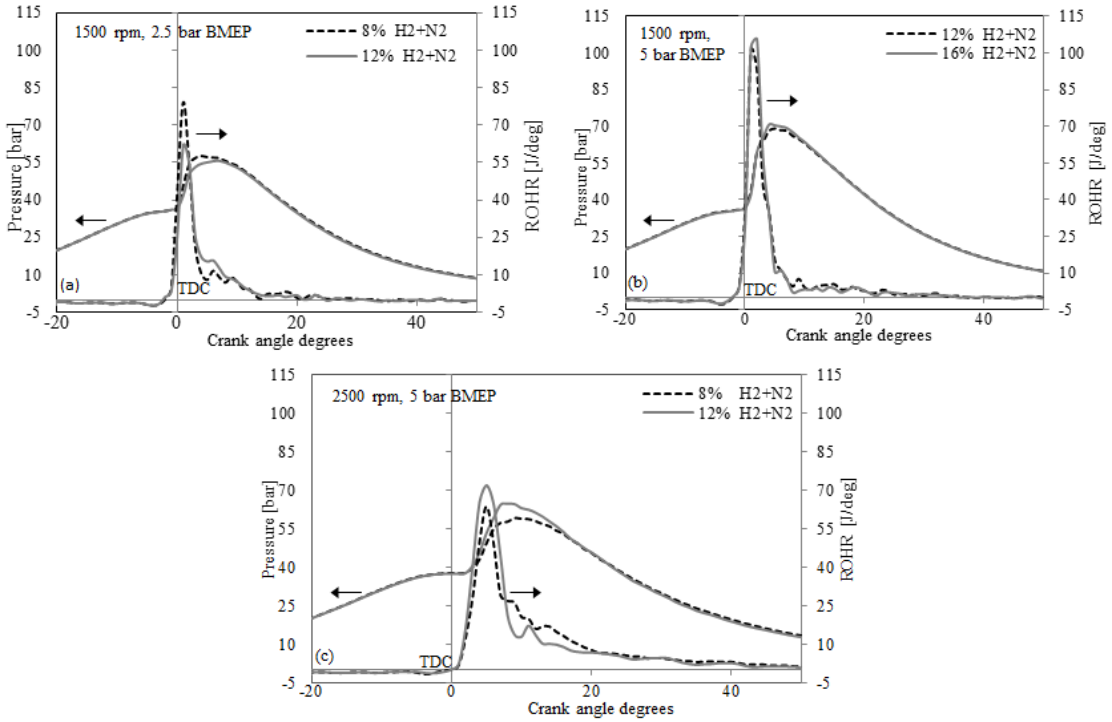

Figure 6.4: Effect of simultaneous H_2 + N_2 enrichment on the in-cylinder pressure and rate of heat release: (a) 1500 rpm, 2.5 bar BMEP; (b) 1500 rpm, 5 bar BMEP; (c) 2500 rpm, 5 bar BMEP.

Figure 6.5 depicts the 10, 50 and 90 % mass fraction burned points (obtained from the integration of heat release rate) for the cases presented in Figure 6.4. The start of combustion, taken as the point the heat release curve intersects the x-axis, is also indicated on the graphs.

Under low-speed operation, an increase in the amount of the gas mixture introduced into the engine did not significantly affect the MFB patters, as shown in Figures 6.5(a) and

6.5(b), whereas under high-speed operation, a distinct change on combustion duration was observed, Figure 6.5(c). In particular, a shorter 50% and 90% MFB was obtained by increasing the proportion of H_2 + N_2 from 8% to 12%. Peirce et al. [160] conducted experiments on a compression ignition engine fuelled by diesel and biodiesel and proved that the fuel which is burned faster is the most NO_x emitting one. The same holds true when diesel is partly substituted by hydrogen [161]. Referring to Figure 6.3(b), it is clear that the admission of 12% H_2 + N_2 gas mixture led to higher NO_x emissions compared to the 8% H_2 + N_2. Under this operating condition, an increase in the amount of hydrogen resulted in more explosive burn, which is reflected in the shorter duration of combustion.

Taking into account the results presented in the previous paragraph, it can be concluded that enrichment of the intake air with a H_2-containing gas mixture does not always contribute to faster combustion, which is typically associated with enhanced thermal efficiency. This along with the incomplete hydrogen combustion and the dilution effect usually lead to a reduction in thermal efficiency.

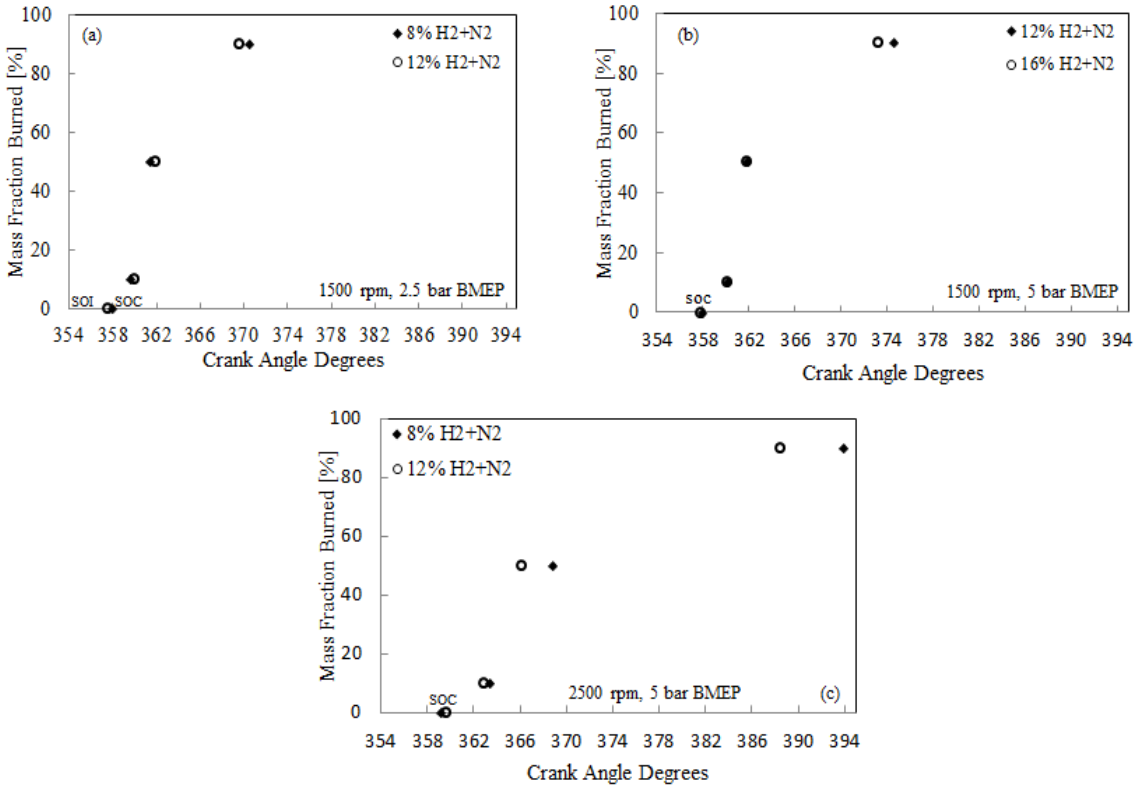

Figure 6.5: Comparison of mass fraction burned at different amounts of H_2: (a) 1500 rpm, 2.5 bar BMEP; (b) 1500 rpm, 5 bar BMEP; (c) 2500 rpm, 5 bar BMEP.

In Figure 6.6, it is shown that when the premixed burn fraction was over 70%, an increase in the proportion of H_2 + N_2 unexpectedly caused a reduction in ignition delay. Typically, substitution of an amount of intake air with either a flammable or an inert gas leads to an increase in ignition delay. Under high-speed operation, the expected effect of intake air dilution on ignition delay was revealed; namely, an increase in the amount of H_2 + N_2 introduced into the engine led to a longer ignition delay. In contrast to low-speed operation, under high-speed operation, the premixed burn fraction was below 65%. From the above analysis, it can be deduced that the ignition delay is not prolonged with the dilution of the intake air when the premixed burn fraction is over 70%.

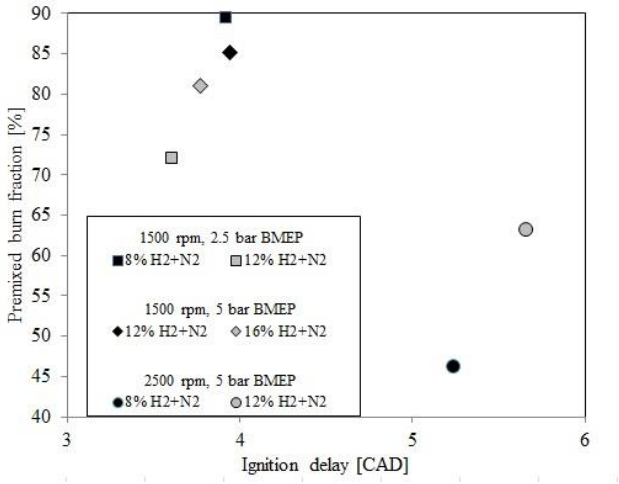

Figure 6.6: Premixed burn fraction as a function of ignition delay.

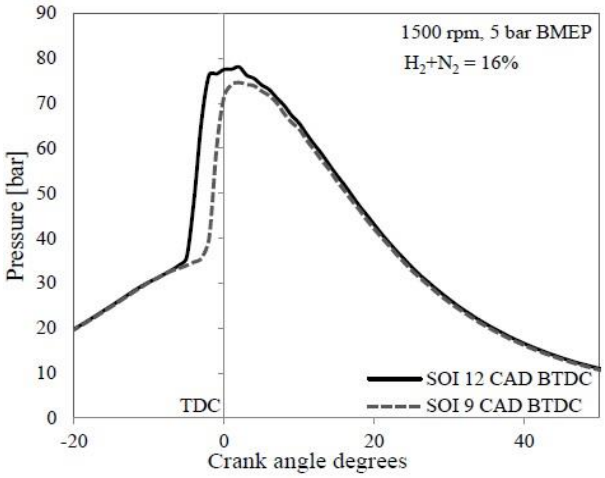

Figure 6.7: Comparison of the in-cylinder pressure data. Engine speed: 1500 rpm, load: 5 bar BMEP, SOI: 12 and 9 CAD BTDC, H_2+N_2 vol. fraction 16%.

Figure 6.7 shows the in-cylinder pressure data that correspond to the following operating conditions: low-speed medium-load, 16% H_2 + N_2 gas mixture, commencement of diesel injection at 9 and 12 CAD BTDC. This figure verifies the assumption made in Section 6.4.1; namely, when diesel injection was commenced at 12 CAD BTDC the engine probably misfired. Comparison of the two curves (the dotted curve corresponds to SOI at 9 CAD BTDC) shows that the peak of the solid curve is not as smooth as the dotted curve. This abnormality implies an issue with the combustion, which is reflected on the emission values, see Sections 6.4.1 and 6.4.6.

6.4.3 Effect of hydrogen- and nitrogen-rich intake air on nitric oxide and nitrogen dioxide

The FTIR analyser is capable of measuring, among other chemical species, the nitrogen compounds in the exhaust gas. In this chapter, apart from the regulated emissions, a discussion on NO, NO_2, N_2O and NH_3 emissions is also provided.

During the combustion process NO_2 is produced through the oxidation of NO by oxidative radicals, while it has been demonstrated that the type of the fuel used and the engine operating conditions affect the conversion [11, 162]. The production of HO_2 radicals, occurring at low temperatures through the reaction of H atoms with oxygen, enhances the conversion of NO to NO_2 [81].

Figures 6.8 and 6.9 show the NO and NO_2 emissions produced under low-speed low-load and high-speed medium-load operation, respectively. In the four different operating conditions tested, the maximum NO_2 fraction was measured under low-speed low-load, whereas the minimum under high-speed medium-load operation. This is not unanticipated since the amount of fuel supplied into the engine was increased by increasing either the speed or the load, leading to a reduction in A/F ratio; namely, reduction in oxygen concentration in the combustion products. Figure 6.8 shows an important trend concerning the effect of fuel type on NO oxidation. When a H_2 + N_2 gas mixture, at any percentage, was supplied into the engine, the amount of NO_2 increased compared to the neat diesel operation, although the admission of H_2 + N_2 replaced an equivalent volume of air. In particular, under the baseline operation, the NO_2 fraction was around 6%, whereas under H_2 + N2 rich intake air operation, the NO_2 value varied from 11% up to 27%. It is worth

mentioning that downstream a diesel oxidation catalyst the NO_2/NO ratio may increase [163].

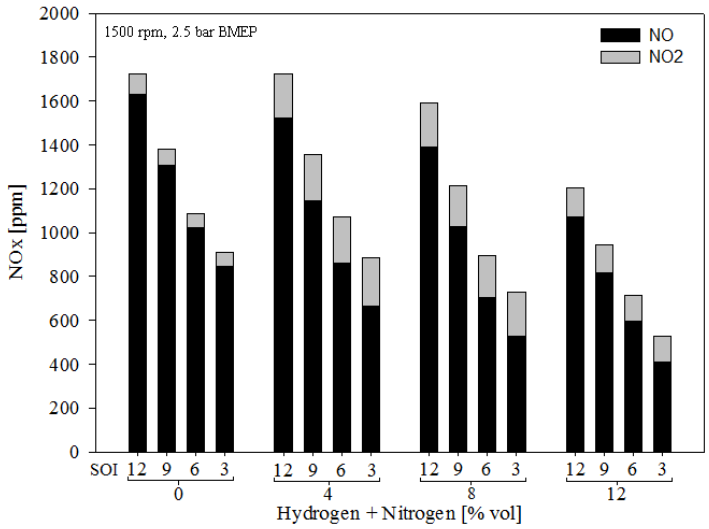

Figure 6.8: NO-NO_2 fraction. Engine speed 1500 rpm, load 2.5 bar BMEP.

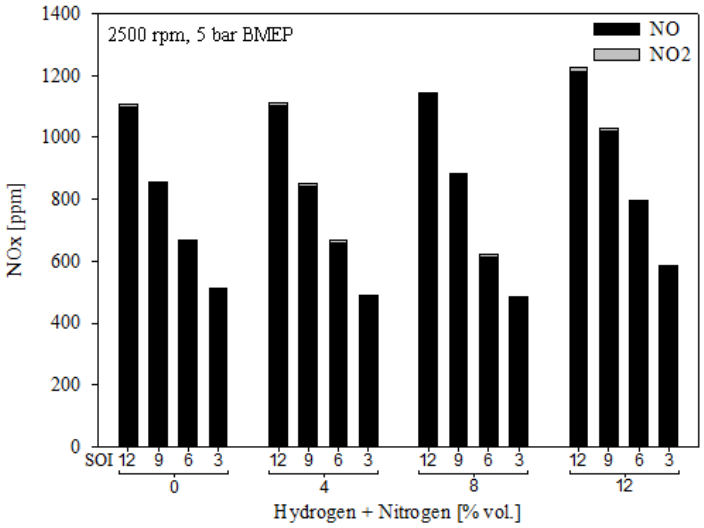

Figure 6.9: NO-NO_2 fraction. Engine speed 2500 rpm, load 5 bar BMEP.

6.4.4 Effect of hydrogen- and nitrogen-rich intake air on nitrous oxide

N_2O is a greenhouse gas and air pollutant and has been found that this chemical compound exists in the treated exhaust gases of automobiles [164, 165]. Figure 6.10 demonstrates that raw exhaust gases contained marginal N_2O emissions that showed a declining trend as the proportion of H_2 + N_2 in the intake air was increased. Only the results obtained under low-speed low-load operation are illustrated, since the emission levels were the same in all the

operating conditions tested. Lipman and Delucchi [166] reported zero N_2O emissions from cars without a catalytic converter; however, the installation of a catalytic converter may promote the formation of nitrous oxide.

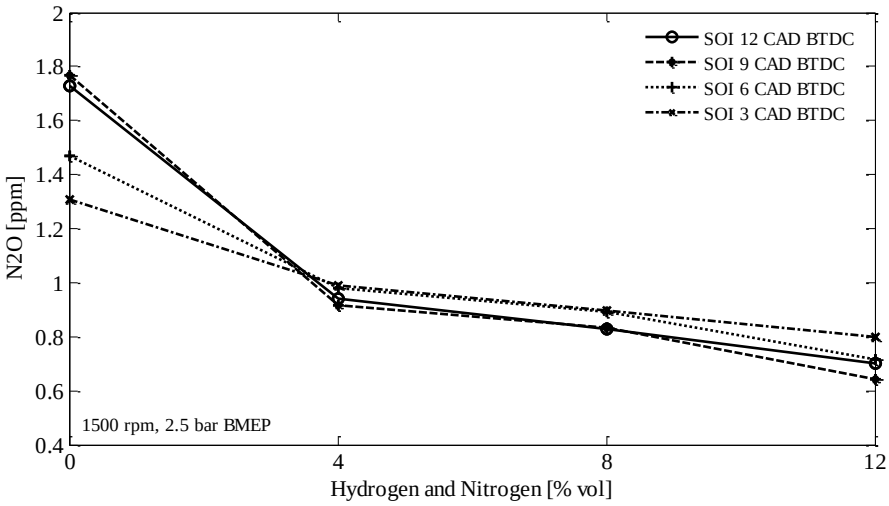

Figure 6.10: N_2O emissions. Engine speed 1500 rpm, load 2.5 bar BMEP.

6.4.5 Effect of hydrogen- and nitrogen-rich intake air on ammonia emissions

Under both baseline and H_2 + N_2 rich intake air operation, no ammonia emissions were detected in the exhaust gas. In fact, the FTIR analyser showed negative ammonia values, which were possibly caused by both a small electrical noise and interfering effects, Figure 6.11. Similarly to Figure 6.10, only the data collected under low-speed low-load operation are presented since the ammonia levels were the same in all the operating conditions tested.

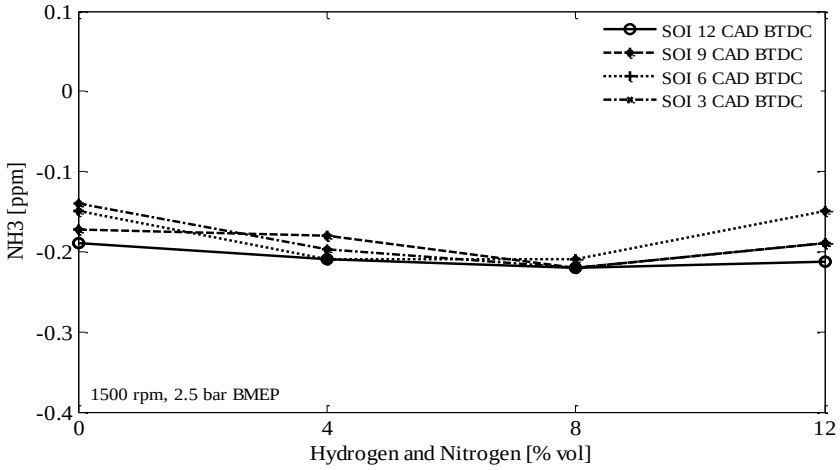

Figure 6.11: Ammonia emissions. Engine speed 1500 rpm, load 2.5 bar BMEP.

6.4.6 Effect of hydrogen- and nitrogen-rich intake air on CO emissions

Under low-load operation (cond. 1 and 3), enrichment of the intake air with simultaneous $H_2 + N_2$, resulted in a considerable reduction in the levels of CO emissions, Figures 6.12(a) and 6.13(a). A comparison between the CO emitted under the baseline and the $H_2 + N_2$ rich intake air operation (at the maximum $H_2 + N_2$ amount; namely, 12% in low-speed and 8% in high-speed operation), showed up to 273% and 77% reduction in CO emissions under low- and high-speed operation, respectively.

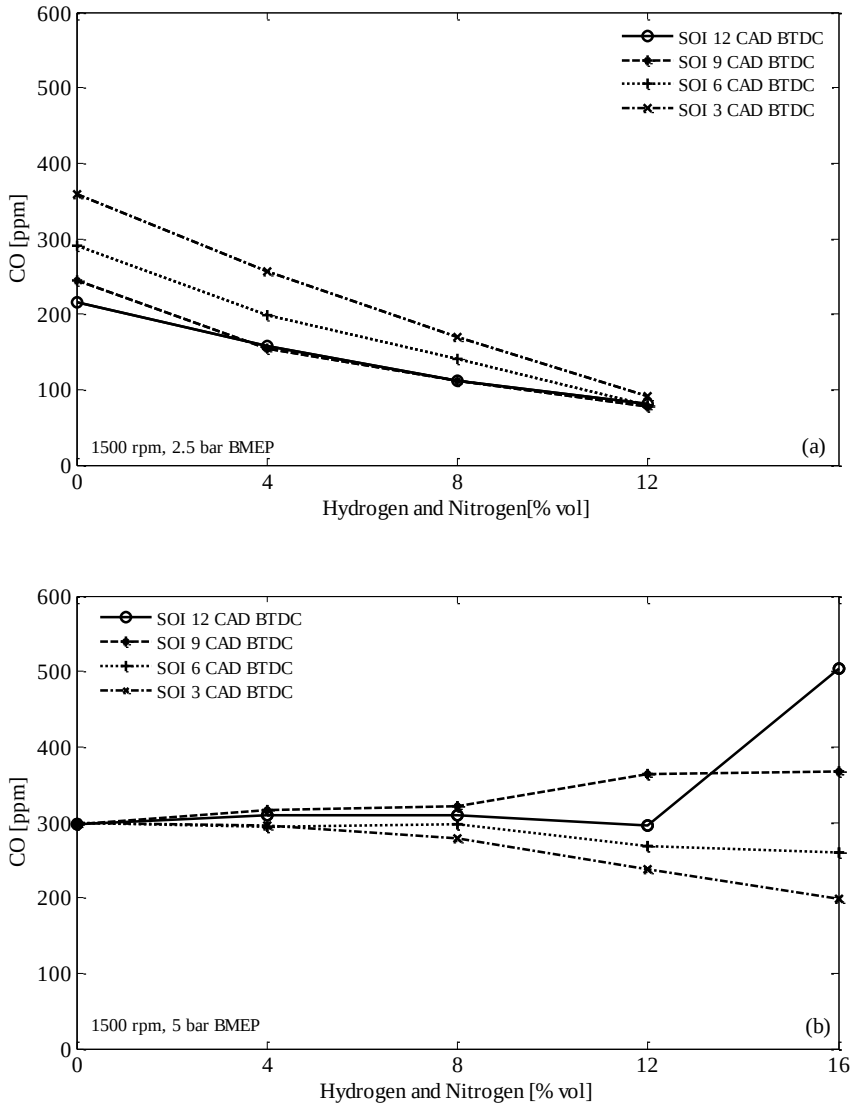

Figure 6.12: Effect of simultaneous $H_2 + N_2$ enrichment on the CO emissions. Engine speed: 1500 rpm, load: (a) 2.5 bar BMEP, (b) 5 bar BMEP.

The CO values obtained under medium-load operation are illustrated in Figures 6.12(b) and 6.13(b). In contrast to low-load operation, in the majority of the test points CO emissions were not reduced when $H_2 + N_2$ rich intake air was introduced into the engine.

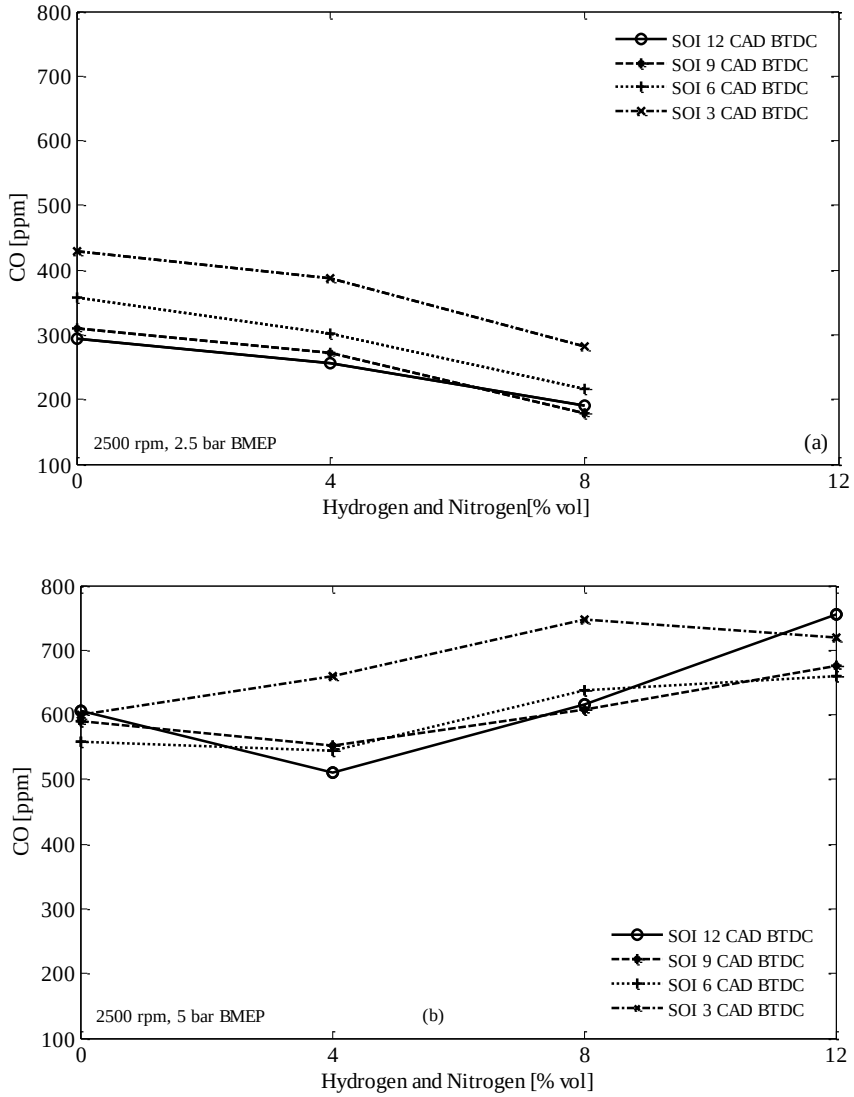

Figure 6.13: Effect of simultaneous $H_2 + N_2$ enrichment on the CO emissions. Engine speed: 2500 rpm, load: (a) 2.5 bar BMEP, (b) 5 bar BMEP.

Under low-speed medium-load run, admission of $H_2 + N_2$ up to 8% had an insignificant effect on CO emissions, Figure 6.12(b). Over 8% $H_2 + N_2$ caused an increase in CO emissions when diesel injection was commenced at 9 CAD BTDC, while the levels of CO reduced at SOI 3, 6 and 12 CAD BTDC. Referring to the same figure, an unexpected CO value was observed in the following operating point: SOI 12 CAD BTDC, $H_2 + N_2$ 16%.

Bearing in mind the data presented in Sections 6.4.1 and 6.4.2, the relatively high CO value at this operating point was probably caused by diesel misfire. Concerning the high-speed medium-load operation, up to 4% H_2 + N_2 admission, resulted in a reduction in CO emissions when injection was commenced anywhere before 3 CAD BTDC. Over 4% H_2 + N_2 led to an increase in CO levels compared to the baseline values, Figure 6.13(b).

6.4.7 Effect of hydrogen- and nitrogen-rich intake air on brake thermal efficiency

A brake thermal efficiency comparison is illustrated in Figures 6.14 and 6.15. The results revealed that the engine was more fuel efficient under low-speed operation (1500 rpm). Taking into account that thermal efficiency is improved as the peak in-cylinder pressure occurs closer to TDC [106], it is not unexpected that the operation under 1500 rpm was more fuel efficient compared to the operation under 2500 rpm, Figure 6.4.

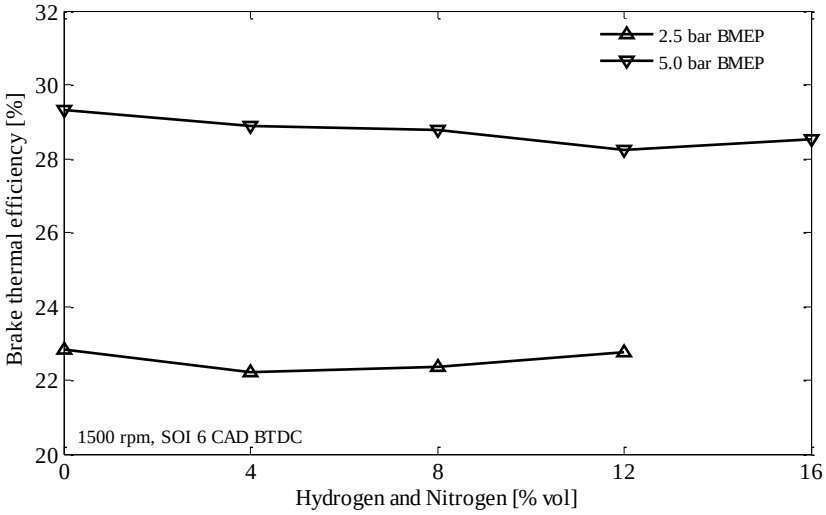

Figure 6.14: Effect of simultaneous H_2 + N_2 enrichment on the brake thermal efficiency. Engine speed 1500 rpm, load 2.5 and 5 bar BMEP, SOI 6 CAD BTDC.

In Chapter 4, it was shown that under high-speed medium-load operation the combustion efficiency of hydrogen was over 98.7%. Figure 6.15 exhibits that under high-speed medium-load operation, thermal efficiency gradually reduced as the concentration of H_2 + N_2 in the intake air was increased. This suggests that under this operating condition, the major contributor to the reduction in thermal efficiency was the incomplete utilisation of diesel fuel (due to the dilution of the intake air), since almost all the hydrogen supplied into the engine was burned during the combustion process.

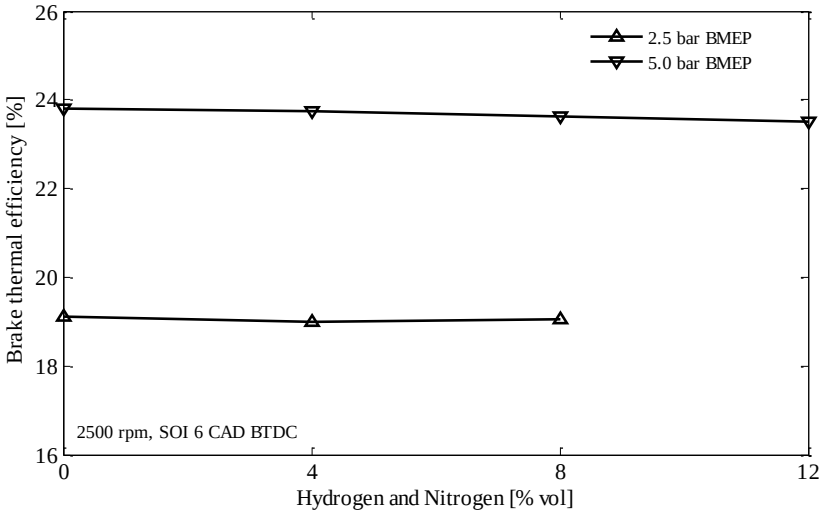

Figure 6.15: Effect of simultaneous H_2 + N_2 enrichment on the brake thermal efficiency. Engine speed 2500 rpm, load 2.5 and 5 bar BMEP, SOI 6 CAD BTDC.

6.5 Summary

The effects of H_2 + N_2 rich intake air on the performance, combustion and emissions of an HSDI diesel engine were presented in this chapter and the main findings are summarised below:

- NO_x-smoke trade-off: Simultaneous reductions in NO_x and BSN levels were achieved under low-speed low-load operation. Comparison to the baseline operation revealed a 71.5% reduction in NO_x emissions when a gas mixture consisted of 12% H_2 + N_2 was supplied into the engine. Under both low-speed medium-load and high-speed low-load operations, introduction of H_2 + N_2 into the engine caused a considerable reduction in BSN levels, while NO_x emissions showed only minor changes. Under high-speed medium-load operation, the rate of NO_x change appeared to be very sensitive when the proportion of H_2 + N_2 into the intake air was over 8%. Bearing in mind the NO_x-BSN values, it was revealed that the optimum start of diesel injection was at 3 CAD BTDC when the engine operated under conditions 1-3.
- Combustion analysis: The formation of NO_x emissions was increased with the premixed burn fraction. An increase in the percentage of H_2 + N_2 in the intake air produced either different or similar heat release curves. In the former case, NO_x

emissions increased or decreased, depending on the premixed burn fraction, whereas in the latter case, NO_x emissions remained relatively unaffected due to the similar patterns of the premixed combustion.

- Nitrogen exhaust compounds: When the speed or the load of the engine was increased, the oxidation of NO was reduced because the combustion products contained less amount of oxygen. Although the introduction of $H_2 + N_2$ replaced an equivalent volume of air, under low-speed low-load operation, a higher NO_2 to NO ratio was obtained compared to the baseline operation. It is therefore clear that the type of fuel affects the oxidation of NO. The raw exhaust gases contained marginal N_2O and zero NH_3 emissions. The level of N_2O, although very low, tended to further reduce as the amount of $H_2 + N_2$ increased.
- CO emissions: Under low-load operation (cond. 1 and 3), simultaneous enrichment of the intake air with $H_2 + N_2$ resulted in a considerable CO reduction. Under low-speed medium-load operation, admission of $H_2 + N_2$ into the engine had a minor effect on CO emissions. Concerning the high-speed medium-load operation, introduction of $H_2 + N_2$ over 4% led to an increase in CO emissions compared to the baseline values.
- Brake thermal efficiency: Enrichment of the intake air with a mixture of $H_2 + N_2$ had a detrimental effect on the brake thermal efficiency. The results revealed that the engine was more fuel efficient under low-speed (1500 rpm) compared to high-speed (2500 rpm) operation. A dominant factor that contributed to the increased brake thermal efficiency under low-speed operation was the position of the peak in-cylinder pressure, which was closer to the TDC.

CHAPTER 7

ENRICHMENT OF THE INTAKE AIR WITH A MIXTURE OF SYNGAS AND NITROGEN

7.1 Introduction

Exhaust gas assisted fuel reforming is an attractive on-board hydrogen production method, which can open new frontiers in diesel engines. Apart from hydrogen, and depending on the reactions promoted, the reformate typically contains a significant amount of carbon monoxide, which is produced as a by-product. Moreover, admission of reformed gas into the engine, through the inlet pipe, leads to an increase in the proportion of nitrogen in the intake charge. It is therefore necessary to study how a mixture of syngas and nitrogen affects the performance, combustion and emissions of a diesel engine, in order to gain a better understanding of the effects of supplying fuel reformer products into the engine.

The production of hydrogen is classified into three categories: thermochemical, electrochemical and biological [167]. In the first category (most hydrogen is derived from this method), separation of hydrogen from a feedstock is achieved through endothermic chemical reactions. The electrochemical method involves water decomposition into hydrogen and oxygen by passing an electric current through the water. Concerning the biological method, hydrogen can be produced from renewable sources by microorganisms using carbohydrate-rich and non-toxic raw materials.

The hydrogen produced from the methods described above can be stored in an automobile either as a gas dissolved in a metal, as a cryogenic liquid or as a compressed gas [168]. Nevertheless, on-board hydrogen storage is deemed challenging as practical issues (weight increase, volume occupation, hydrogen infrastructure and safety) need to be overcome.

A widely acceptable alternative that is currently under research and development stage is the on-board hydrogen production. Adoption of this technique requires the integration of a fuel reformer within the exhaust pipe in order to generate hydrogen through a catalytic interaction of the fuel with hot exhaust gases. The basic idea is to liberate the hydrogen

held in the fuel and exhaust steam and direct it into the combustion chamber. The chemical reactions (7.1)-(7.7) may take place in a reformer supplied with exhaust gas and diesel [96, 140, 168]. Details about reforming reactions can also be found in the references [83] and [169]. It should be clarified that the following reactions do not refer to engine combustion.

Diesel fuel steam reforming:

$$C_{12.31}H_{22.17} + 12.31H_2O \rightarrow 12.31CO + 23.4H_2 \quad (7.1)$$

This reaction is largely endothermic and to be efficient it requires temperatures in the range of 600 to 800 ℃ [170]. Typical diesel exhaust gas temperatures vary from approximately 200 to 700 ℃, depending on the operating conditions of the engine.

Water-gas shift:

$$CO + H_2O \rightarrow CO_2 + H_2 \quad (7.2)$$

Diesel fuel partial oxidation:

$$C_{12.31}H_{22.17} + 6.15O_2 \rightarrow 12.31CO + 11.08H_2 \quad (7.3)$$

Diesel fuel complete oxidation:

$$C_{12.31}H_{22.17} + 17.85O_2 \rightarrow 12.31CO_2 + 11.08H_2O \quad (7.4)$$

Being exothermic, the reactions (7.3) and (7.4), although not desirable due to the drop of product gas calorific value, can raise the exhaust temperature if it is not adequate to drive the steam reforming reaction.

'Dry reforming' reaction:

$$C_{12.31}H_{22.17} + 12.31CO_2 \rightarrow 24.62CO + 11.08H_2 \quad (7.5)$$

Reaction (7.5) requires temperatures over 800 ℃.

Autothermal reforming:

$$C_{12.31}H_{22.17} + 5.65O_2 + H_2O \rightarrow 12.31CO_2 + 12.08H_2O \quad (7.6)$$

Hydrocarbon thermal decomposition:

$$C_{12.31}H_{22.17} \rightarrow 12.31C + 11.09H_2 \quad (7.7)$$

In fact, during a fuel reformation process more than one reaction may take place; nevertheless, promotion of the most desirable can be achieved by tuning the reformation process.

Tsolakis et al. [79] experimentally investigated the effect of REGR on a diesel engine. It was concluded that, in the majority of the test conditions, dual fuel operation (diesel and REGR) resulted in improved NO_x, smoke and engine fuel consumption. The concentration of hydrogen and CO in the exhaust gas was found relatively high at low engine load, and as a result BSFC deteriorated due to the incomplete gaseous fuel utilisation.

Singh Bika [171] used a single-cylinder CI engine fuelled by syngas-diesel in order to study the effect of varying syngas proportions on the cycle efficiency, NO_x and CO emissions. It was found that cycle efficiency reduced when the equivalence ratio of the gaseous fuel was increased. Moreover, it was shown that NO_x emissions remained relatively constant at 2 bar IMEP, while at 4 bar IMEP they increased with diesel fuel substitution. Also, it was proven that CO was utilized more efficiently at the high load condition.

A typical diesel exhaust gas fuel reforming produces a gas mixture that is mostly composed of hydrogen and carbon monoxide. Although the effects of providing syngas into a diesel engine have been investigated by many researchers [80, 172-174], no papers were found dealing with the effects of supplying syngas + N_2. The effects of enriching the intake air with separate and simultaneous hydrogen and nitrogen on the combustion and emissions of the engine were presented in Chapters 4-6. The current chapter aims to take this research effort further by introducing syngas and nitrogen (at varying concentrations) into the engine. The syngas composition resembled that of typical diesel fuel reformation, while the introduction of nitrogen simulated the effect of oxygen concentration reduction in the inlet charge; that is, the increased N_2 to O_2 ratio.

7.2 Methodology

The engine was run in four different operating conditions, which included two different speeds (1500 and 2500 rpm) and two different loads (2.5 and 5 bar BMEP). Start of injection was swept from 12 to 3 CAD BTDC in three degree increments, while the bottled

gases were admitted into the engine in 4% steps (2% syngas + 2% N_2), starting from 4% up to 12%.

The baseline data was obtained by delivering ULSD into the engine. The dual fuel operation was realised by substituting an amount of diesel fuel with gaseous H_2 + CO, while the engine speed and load were maintained constant. The composition of the syngas was 60% H_2 - CO balance. Table 7.1 details the concentration of the syngas in the intake charge as well as the mass flow rate and the energy ratio of the individual gases it was composed of.

Table 7.1: Gaseous fuel concentration, mass flow rate and energy ratio.

Syngas concentration [% vol.]	**2**	**4**	**6**
H_2 fraction [% vol.]	1.2	2.4	3.6
CO fraction [% vol.]	0.8	1.6	2.4
H_2 mass flow rate (1500 rpm) [g/sec]	0.0204	0.0408	0.0612
CO mass flow rate (1500 rpm) [g/sec]	0.1717	0.3434	0.5151
H_2 mass flow rate (2500 rpm) [g/sec]	0.0324	0.0648	0.0972
CO mass flow rate (2500 rpm) [g/sec]	0.2760	0.5520	0.8280
H_2/CO energy ratio (1500 rpm)	1.4116	1.4116	1.4116
H_2/CO energy ratio (2500 rpm)	1.3947	1.3947	1.3947

Table 7.2 illustrates the concentration of the individual gases in the intake charge at the different syngas + N_2 percentages used throughout the experiments, while the schematic representation of the composition of the intake charge is illustrated in Figure 7.1.

Table 7.2: Intake charge composition.

Syngas+N_2 [% vol. of intake air]	**Intake charge composition [% vol.]**			
	N_2	**O_2**	**H_2**	**CO**
0	79	21	0	0
2+2	77.84	20.16	1.2	0.8
4+4	76.68	19.32	2.4	1.6
6+6	75.52	18.48	3.6	2.4

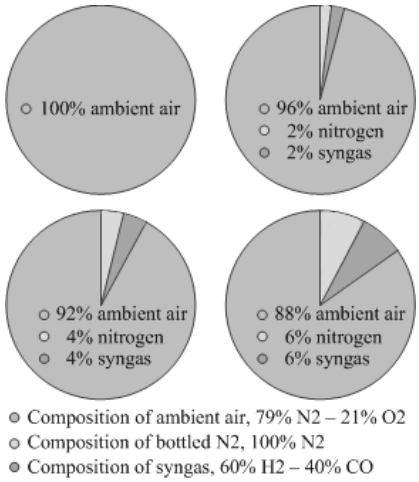

Figure 7.1: Schematic representation of intake charge composition.

The gases were stored in two separate bottles, as shown in Figure 7.2. The first bottle contained the syngas, whereas the second bottle was filled with high-purity nitrogen gas. Both bottles had lines connected to the inlet pipe. Further discussion on the experimental set up can be found in Chapter 3. Also, a detailed description of the components that were fitted along the gas lines, as shown in Figure 7.2, can be found in Sections 4.2, 5.2 and 6.2.

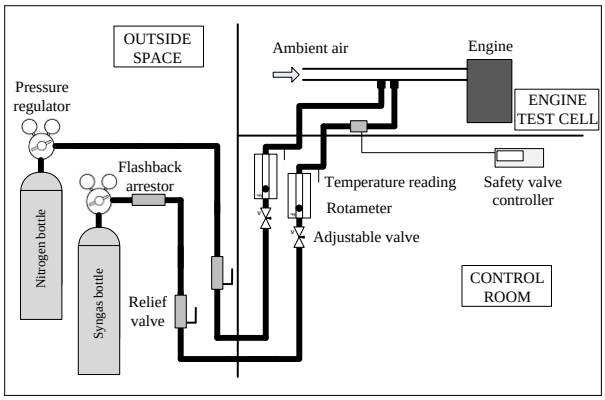

Figure 7.2: Detailed schematic representation of the syngas and nitrogen lines.

7.3 Results and discussion

Apart from presenting the data collected during the experiments, this section provides a discussion on the trends observed when the intake air of the engine was enriched with various amounts of bottled syngas + N_2. The exhaust gas was analysed for NO_x, smoke, CO and CO_2 emissions. Also, the effect of hydrogen-rich and nitrogen-rich combustion on the formation of smoke was isolated in order to investigate whether a CO diluted flame promotes the formation of smoke. Moreover, the utilisation of the bottled CO in the

different operating conditions and CO fractions used was calculated. Based on the in-cylinder pressure data, a combustion analysis was performed to determine the MFB, the maximum pressure and the maximum pressure rise rate. Finally, the effect of syngas + N_2 rich combustion on the brake thermal efficiency is presented and compared to the baseline operation.

7.3.1 Effect of intake air enrichment with a mixture of syngas + N_2 on the NO_x-smoke trade-off

The effect of the enrichment of the intake air with a mixture of syngas + N_2 on NO_x-smoke trade-off is presented in Figures 7.3 and 7.4. The tests were repeated four times and the values reported are mean values. Tables 7.3 and 7.4 show the standard deviation of NO_x and BSN at 8% syngas + N_2. Inclusion of error bars in the figures was proven impractical because standard deviation values were too small compared to the values of the axes.

Table 7.3: Standard deviation of NO_x emissions and BSN. Engine speed 1500 rpm, load 2.5 and 5 bar BMEP, syngas + N_2 concentration 8%.

	Speed 1500 rpm, load 2.5 bar BMEP		**Speed 1500 rpm, load 5 bar BMEP**	
SOI	**STDV of NO_x emissions**	**STDV of BSN values**	**STDV of NO_x emissions**	**STDV of BSN values**
12	9.98	0.00	15.24	0.008
9	7.88	0.00	13.00	0.005
6	5.24	0.00	6.48	0.001
3	6.14	0.00	8.42	0.00

Simultaneous reductions in both NO_x and BSN were achieved over a broad range of the operating window of the engine. In particular, this desirable trend on NO_x-BSN was observed under low-speed low-load, low-speed medium-load and high-speed low-load operations, the values of which are illustrated in Figures 7.3(a), 7.3(b) and 7.4(a), respectively. Figure 7.4(b) shows that under high-speed medium-load operation the added gas had an adverse effect on BSN, although neither the combustion of hydrogen nor the combustion of CO generates smoke. The high dilution level of the intake air was probably the main contributor to the increased BSN as there was less oxygen within the cylinder to react with the diesel fuel.

Table 7.4: Standard deviation of NO_x emissions and BSN. Engine speed 2500 rpm, load 2.5 and 5 bar BMEP, syngas + N_2 concentration 8%.

	Speed 2500 rpm, load 2.5 bar BMEP		**Speed 2500 rpm, load 5 bar BMEP**	
SOI	**STDV of NO_x emissions**	**STDV of BSN values**	**STDV of NO_x emissions**	**STDV of BSN values**
12	7.56	0.008	7.13	0.037
9	6.06	0.00	5.79	0.045
6	8.41	0.001	5.63	0.034
3	6.12	0.008	5.15	0.059

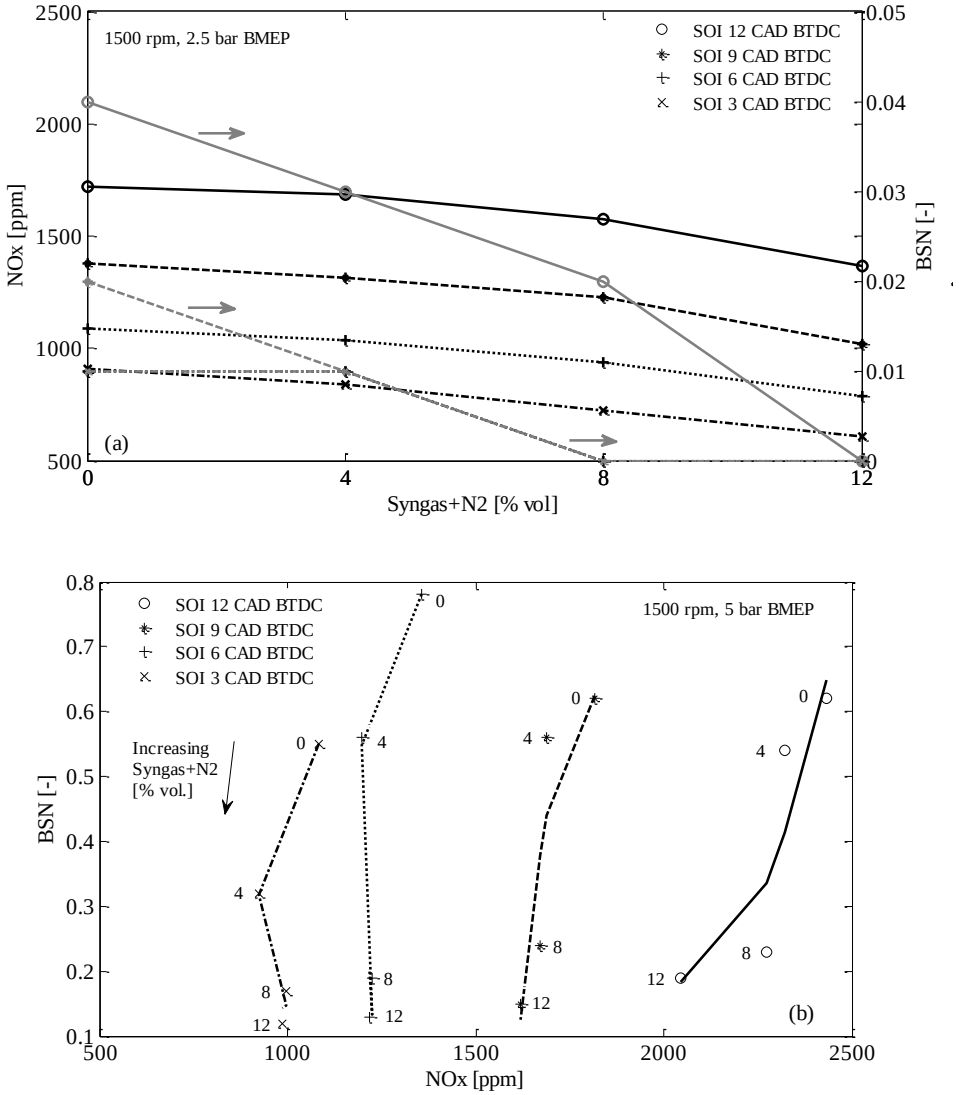

Figure 7.3: Effect of intake air enrichment with a mixture of syngas + N_2 on the NO_x-BSN trade-off. Engine speed: 1500 rpm, load: (a) 2.5 bar BMEP, (b) 5 bar BMEP.

Isolation of the effect of nitrogen and hydrogen can clarify whether the admission of CO (in addition to the dilution effect) contributed to smoke formation. According to Guo et al. [175], the concentration of OH (which contributes to soot oxidation) is lower and the concentration of H (which intensifies the soot surface growth rate) is higher in a CO diluted flame due to the reaction CO + OH = CO_2 + H, whose forward rate is increased when CO is supplied into the engine.

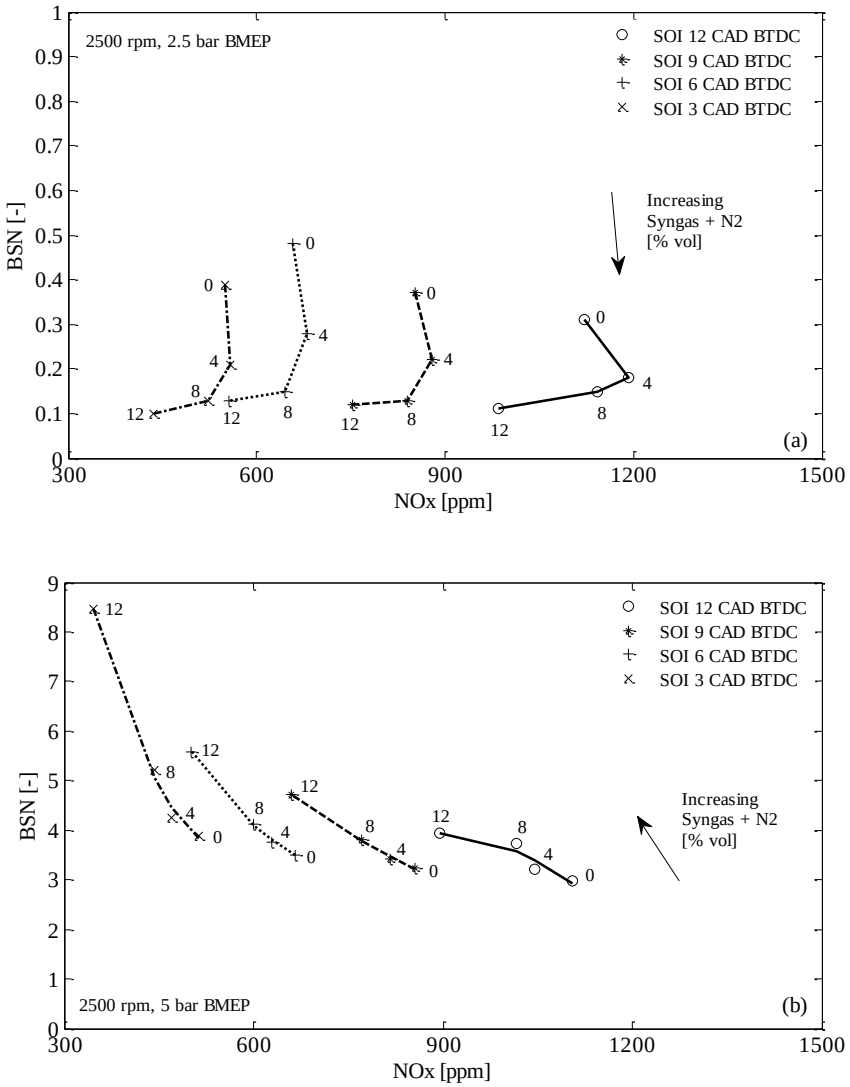

Figure 7.4: Effect of intake air enrichment with a mixture of syngas + N_2 on the NO_x-BSN trade-off. Engine speed: 2500 rpm, load: (a) 2.5 bar BMEP, (b) 5 bar BMEP.

Figure 7.5 shows the results obtained when a mixture of H_2 + CO (w/o N_2) was admitted into the engine. BSN dropped below the values recorded in the baseline operation, and this suggests that under this operating condition smoke formation was very sensitive to the

admission of nitrogen. Isolation of the CO effect (i.e. enrichment of the intake air with hydrogen only) can extent this investigation in order to assess whether CO dilution affects the oxidation of soot, as mentioned by Guo et al. The effect of hydrogen enriched intake air on BSN has already been presented in Chapter 4. Comparison of the data collected in identical operating conditions and gas admission indicated lower BSN levels when the engine was fuelled by a mixture of diesel-H_2. This verifies that a CO diluted flame promotes the formation of smoke.

Because smoke exclusively originates from diesel, the above comparison is valid only if a comparable amount of diesel was delivered into the cylinder when the engine was run on (i) syngas-diesel and (ii) H_2-diesel. The diesel flow rate measurements revealed that in the first case the amount of diesel was slightly lower compared to the second case. This finding can be verified by comparing the energy density (energy per unit volume) of the two gases. The combustion of 1 litre of hydrogen releases 3.4% less energy compared to that released from the combustion of a gas mixture composed of 60% H_2 + 40% CO. From this calculation, it is clear that in the diesel-H_2 mode a slightly higher amount of diesel was required in order to achieve a certain operating condition. This reinforces the conclusion drawn in the previous paragraph as in the higher smoke case (that is, when a mixture of syngas-diesel was used) a smaller quantity of diesel (the smoke producing fuel) was required to achieve a certain speed and load.

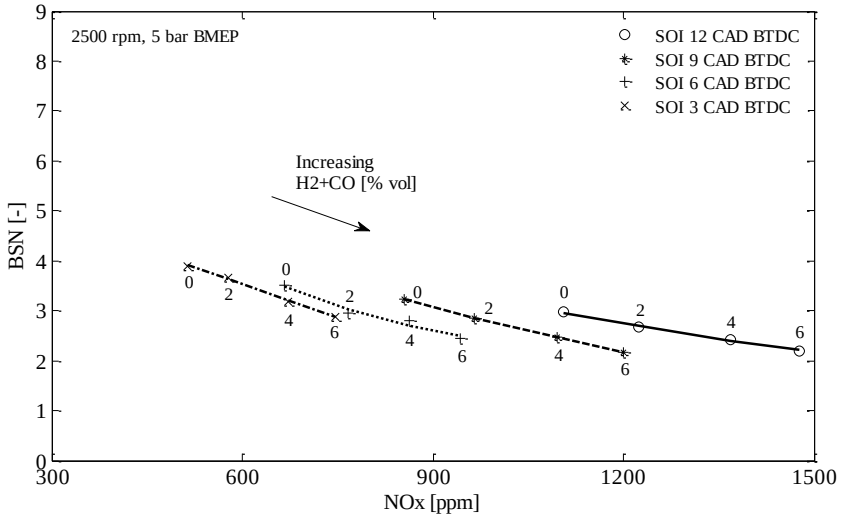

Figure 7.5: Effect of intake air enrichment with a mixture of H_2 + CO on the NO_x-BSN trade-off. Engine speed 2500 rpm, load 5 bar BMEP.

Enrichment of the intake air with a mixture of syngas + N_2 resulted in a reduction in oxygen concentration, which led to a decrease in lambda. From Figures 7.6 and 7.7, it can be concluded that, in the majority of the operating conditions, a decrease in lambda led to simultaneous reductions in NO_x and BSN with a parallel increase in CO emissions.

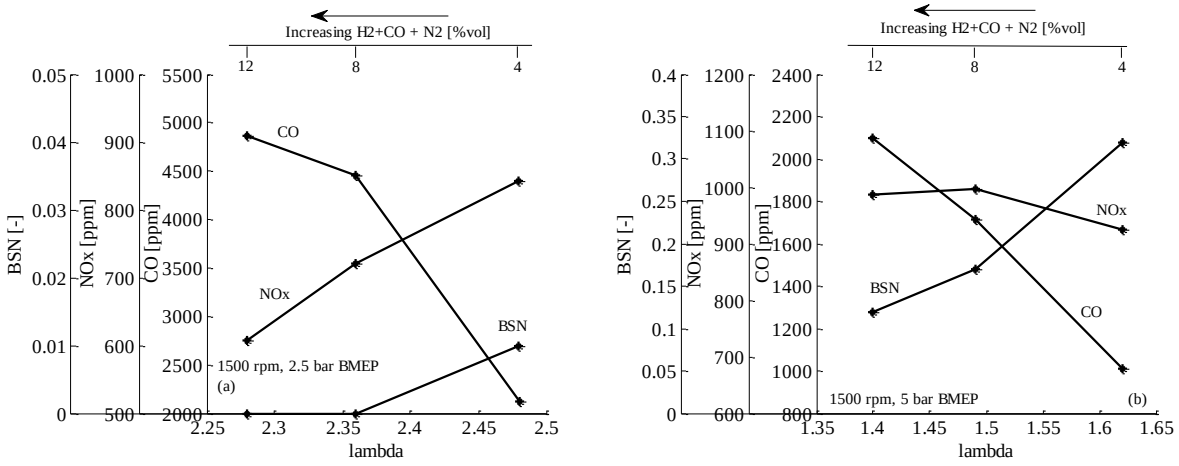

Figure 7.6: Effect of lambda coefficient on the BSN, NO_x and CO. Engine speed: 1500 rpm, SOI: 3 CAD BTDC, load: (a) 2.5 bar BMEP, (b) 5 bar BMEP.

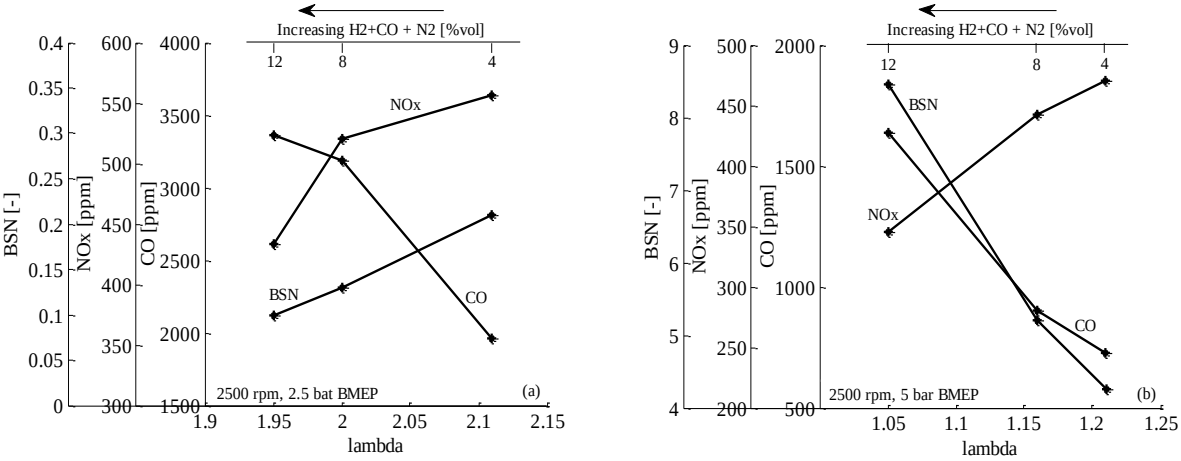

Figure 7.7: Effect of lambda coefficient on the BSN, NO_x and CO. Engine speed: 2500 rpm, SOI: 3 CAD BTDC, load: (a) 2.5 bar BMEP, (b) 5 bar BMEP.

Replacement of part of diesel fuel with syngas was possibly the dominant factor that caused the reduction in BSN levels since dilution of the intake air has typically a detrimental effect on smoke emissions. In Figure 7.7(b), the increase in BSN may have been caused by both the high CO utilisation (as presented in the following section) and the relatively low lambda value. The reduction in NO_x emissions with decreasing the value of

lambda was not unexpected as the concentration of oxygen within the cylinder is a dominant NO_x formation factor. The increase in CO emissions with the reduction in lambda was caused, on the one hand, by the reduction in oxygen concentration, and on the other, by the increase in the amount of bottled CO that was introduced into the engine.

7.3.2 Effect of intake air enrichment with a mixture of syngas + N_2 on the carbon monoxide, carbon monoxide utilisation and carbon dioxide emissions

Enrichment of the intake air with a CO-containing mixture inherently increases the concentration of this pollutant in the exhaust gas. In essence, the increase in CO levels is attributed to the next two factors. The first is the incomplete combustion of the admitted gas, while the second is the slip of the CO-rich intake air during the valve overlap period.

Figures 7.8 and 7.9 depict the CO emissions collected in low- and high-speed operation, respectively. Inset in each of the main figures is an estimation of the CO utilisation in the combustion chamber, the calculation of which is explained later on in this section.

Under low-load operation, the bottled CO was not utilised as efficiently as in medium-load, resulting in significantly high engine-out CO emissions. For instance, comparison of Figure 7.8(a) with Figure 7.8(b) indicates that under low-load operation, the minimum CO utilisation was 72.6% and the maximum 82.8%, whereas under medium-load, it ranged from 88.1% to 92.4%. Concerning the engine speed, it is clear that the high-speed operation was more favourable in terms of CO utilisation.

The above results indicate that the bottled CO was more completely burned at high temperatures. This can be linked, among other factors, with the drop in the lower flammability limit (LFL) of the gas at elevated temperatures [121, 176]. Using Le Chatelier's mixing rule [120], the LFL of the combustible gas mixture (that is, H_2 + CO) was found to be 5.45%, Equation (7.8).

$$\mathrm{LFL_{mix}} = \frac{1}{\sum \frac{x_i}{\mathrm{LFL_i}}} \tag{7.8}$$

where $\mathrm{LFL_{mix}}$ is the lower flammability limit of the mixture, x_i is the concentration of component i in the gas mixture and $\mathrm{LFL_i}$ is the lower flammability limit of component i.

Due to variations in temperature, pressure and oxygen concentration, to name a few factors, the actual LFL was probably different from the calculated value. Nevertheless, the fact that CO utilisation, in the majority of the points tested, improved at 12% bottled gas mixture (6% combustible gas mixture) suggests that the calculated LFL value was not too far from the actual value.

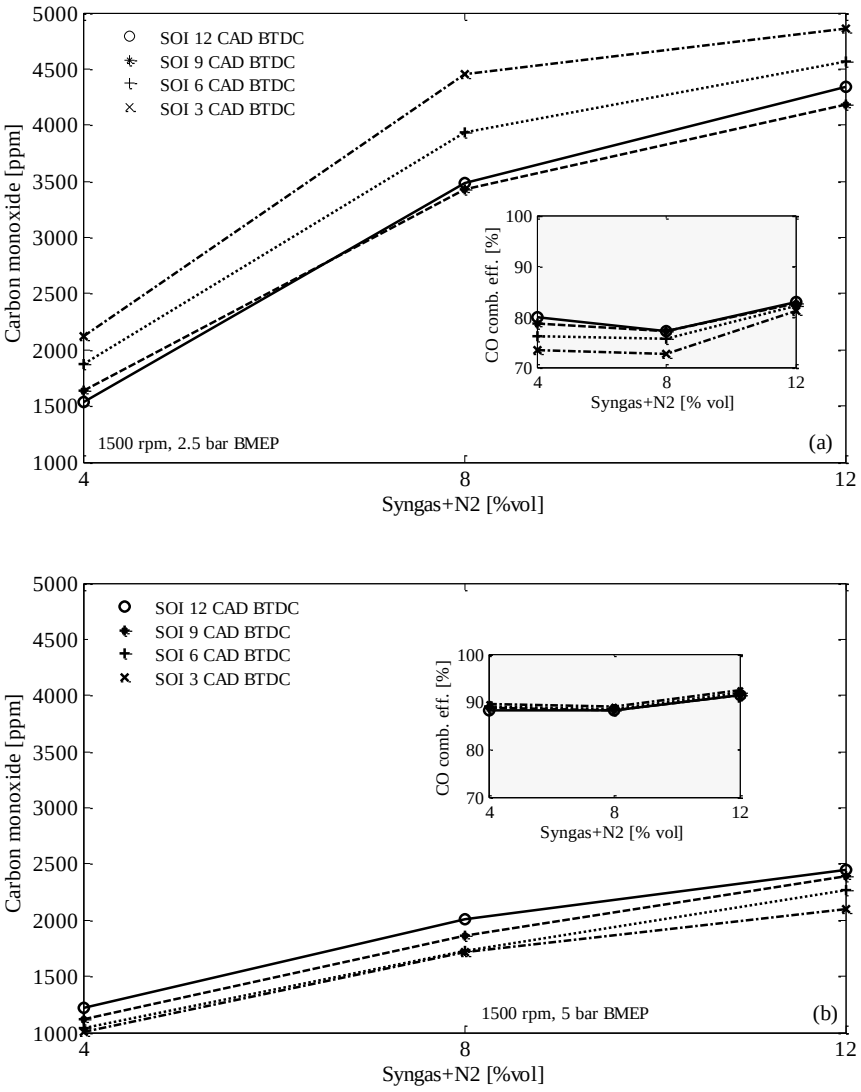

Figure 7.8: Effect of the intake air enrichment with a mixture of syngas + N_2 on the CO emissions. Engine speed: 1500 rpm, load: (a) 2.5 bar BMEP, (b) 5 bar BMEP. Inset is the estimated CO utilisation.

Gatts et al. [128] described a mechanism for the combustion of lean hydrogen, which probably holds true for the combustion of lean H_2 + CO. In particular, it was proposed that when the concentration of hydrogen is below its LFL, it simultaneously burns with diesel

fuel by entraining into diesel vapour since the flame cannot propagate in the lean gas. In addition, it was suggested that a wider diesel spray plume enhances the combustion of the gaseous fuel.

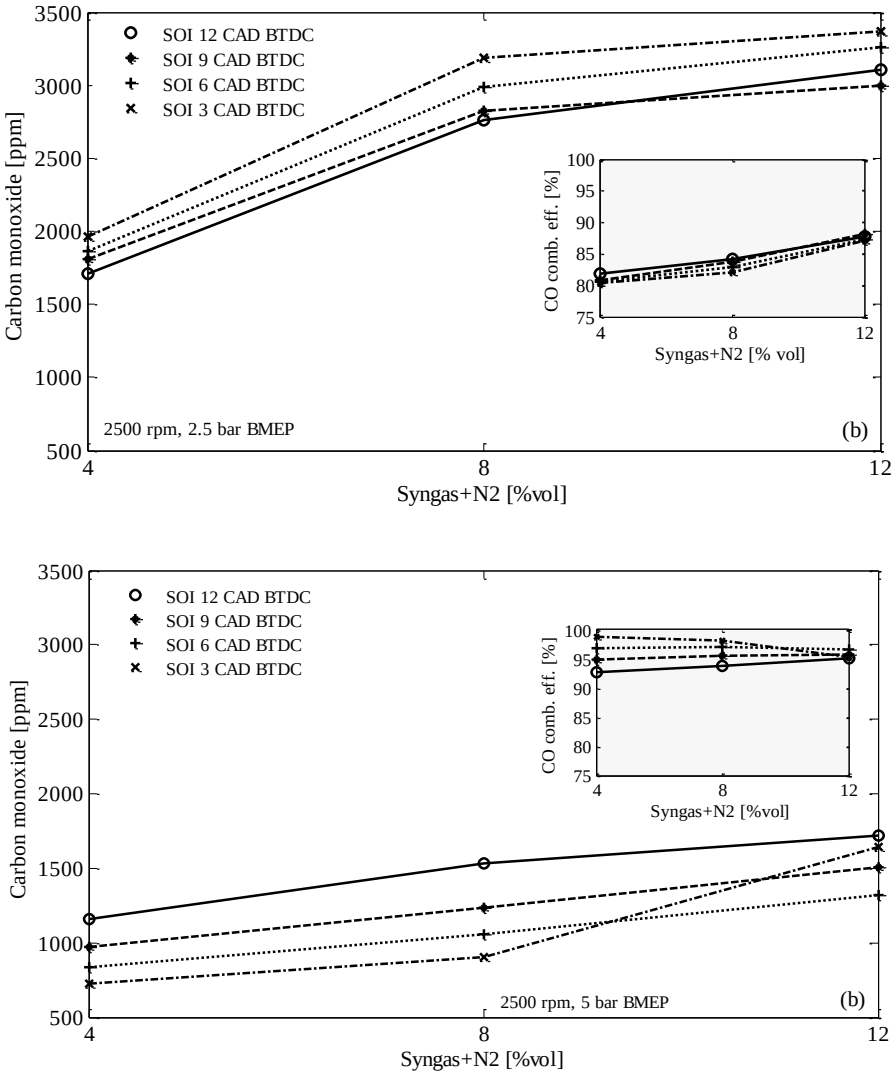

Figure 7.9: Effect of the intake air enrichment with a mixture of syngas + N_2 on the CO emissions. Engine speed: 2500rpm, load: (a) 2.5 bar BMEP, (b) 5 bar BMEP. Inset is the estimated CO utilisation.

The calculation process of the bottled CO utilisation is presented in this paragraph. Equation (7.9) is a simplified one but gives a good indication of the CO utilisation in the combustion chamber.

$$\mathrm{CO_{utilisation}} = 1 - \frac{\mathrm{CO_{meas\ syngas+N_2}} - \mathrm{CO_{est\ H_2+N_2}}}{\mathrm{CO_{sup}}} \times 100 \qquad (7.9)$$

where $CO_{utilisation}$ is the percentage of CO that was utilised [%], $CO_{meas\ syngas+N_2}$ is the CO measured in the exhaust gas when a mixture of syngas + N_2 was admitted into the intake pipe [ppm], $CO_{est\ H_2+N_2}$ is the estimated CO (estimation at equivalent hydrogen fraction) in the exhaust gas when simultaneous H_2 + N_2 was introduced into the intake pipe [ppm], CO_{sup} represents the bottled CO supplied into the engine [ppm].

In order to isolate the contribution from diesel fuel on the CO measured in the exhaust gas, the values obtained when a mixture of H_2 + N_2 was introduced into the engine were subtracted from those obtained when a mixture of syngas + N_2 was used. Since the hydrogen content in the two gas mixtures (4% H_2 + N_2 contained 2% hydrogen, whereas 4% syngas + N_2 contained 1.2% hydrogen taking into account that the composition of the syngas was 60% H_2-CO balance) was not the same, an estimation of CO (through the linear interpolation method) that would be measured in the exhaust gas if the amount of hydrogen was the same is required. The calculation is based on certain assumptions such as possible dissociation reactions that produce CO are still the same when changing H_2 + N_2 with syngas + N_2 in the cylinder, CO generated from diesel fuel is similar when changing H_2 + N_2 with syngas + N_2 and assuming a linear relationship between CO emissions and %H_2 to get the values at 1.2, 2.4 and 3.6 %H_2. As mentioned in Section 7.3.1, the two distinct gaseous fuels (H_2 and H_2 + CO) release similar amounts of energy; hence, this suggests that the amount of diesel required to keep the speed and the load constant when changing H_2 + N_2 with syngas + N_2 in the cylinder is also similar.

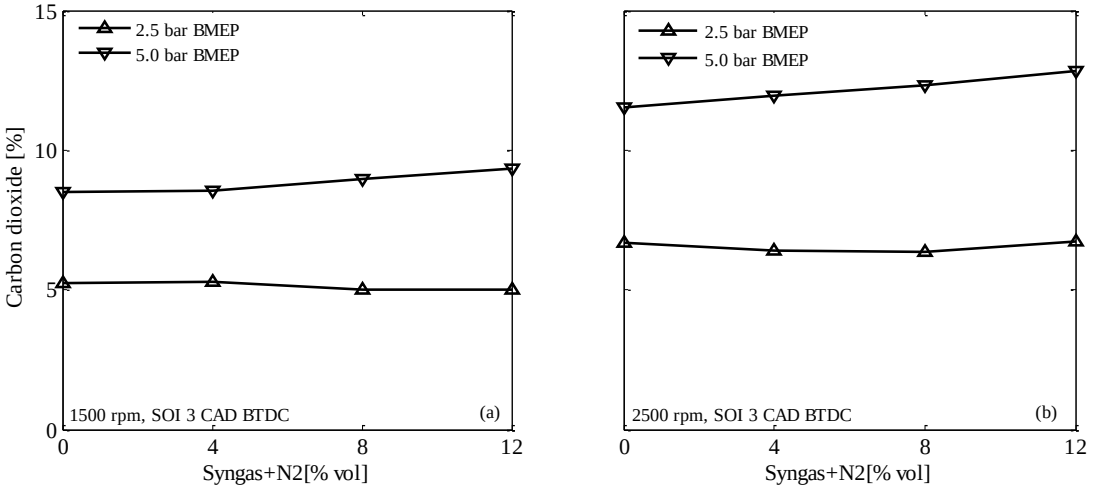

Figure 7.10: Effect of syngas + N_2 on the carbon dioxide emissions. (a) 1500 rpm 2.5 and 5 bar BMEP, (b) 2500 rpm 2.5 and 5 bar BMEP. SOI 3 CAD BTDC.

Figure 7.10 illustrates the CO_2 emissions as a function of the gas mixture delivered into the engine. Taking into account Figures 7.8 and 7.9, it can be deduced that the CO_2 emissions increased when the utilisation of the bottled CO was approximately over 88%. This percentage of CO utilisation was actually observed under medium-load operation. Poorer utilisation of the bottled CO under low-load run resulted in a slight decrease in CO_2 since a considerable amount of the added CO was not burned.

7.3.3 Combustion analysis

A combustion analysis in the two extreme operating conditions (cond. 1 and 4) is illustrated in Figures 7.11 and 7.12. The mass fraction burned, maximum pressure rise rate and maximum in-cylinder pressure obtained at the three different syngas + N_2 fractions used throughout the experiments are presented.

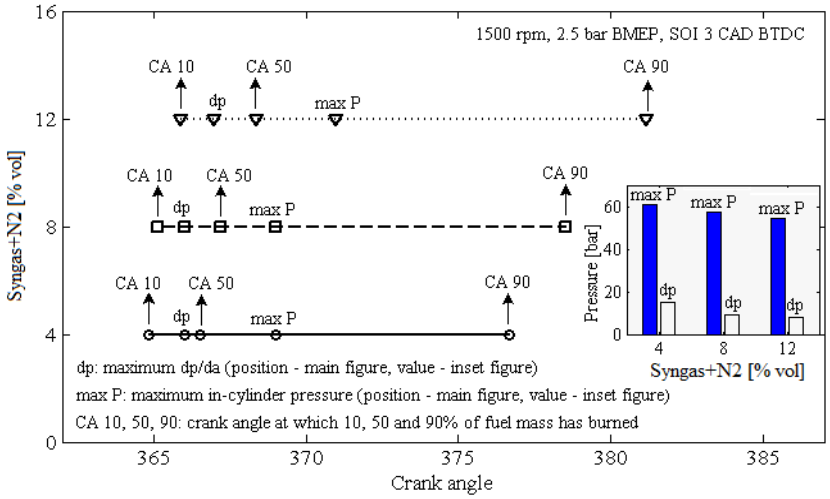

Figure 7.11: Mass fraction burned, maximum pressure rise rate and maximum pressure Engine speed 1500 rpm, load 2.5 bar BMEP, SOI 3 CAD BTDC.

Under low-speed low-load operation, the heat release increased sharply after the onset of combustion, resulting in high pressure rise rate values. As shown in Figure 7.11, the maximum pressure rise rate was always located in between the CA 10 and CA 50 (CA 10 and CA 50 is the crank angle at which 10% and 50% of fuel mass has been burned, respectively). The inset figure reveals that both maximum dp/da and maximum in-cylinder pressure decreased as the concentration of syngas + N_2 in the intake air was increased. The maximum pressure was located after the CA 50 and was always approximately one fifth of the distance, in crank angle degrees, from CA 50 to CA 90. Furthermore, the combustion

duration (CA 10 to CA 90) increased with the percentage of the gas mixture. This result can be linked to the reduction of NO_x emissions when the concentration of the bottled gas mixture was increased, Figure 7.3(a). Under certain conditions, the fuel which is burned faster is the most NO_x emitting one [160, 161, 177]. However, when a mixture of syngas + N_2 was used, this was not the sole contributor to the reduction in NO_x emissions since the reduction in the cylinder pressure with increasing the proportion of syngas + N_2 resulted in a decrease in cylinder temperature, which led to reduced NO_x formation.

Figure 7.12 shows the combustion analysis data that corresponds to high-speed medium-load operation. The maximum pressure rise rate was located straight after the CA 10 and was smaller to that obtained under low-speed low-load run. When the intake air was enriched with a mixture of syngas + N_2, an increase in engine speed resulted in a reduction in maximum dp/da, whereas the effect of load on dp/da varied, depending on engine speed. Under low-speed operation, dp/da increased with increasing the load, whereas under high-speed operation, dp/da dropped with increasing the load.

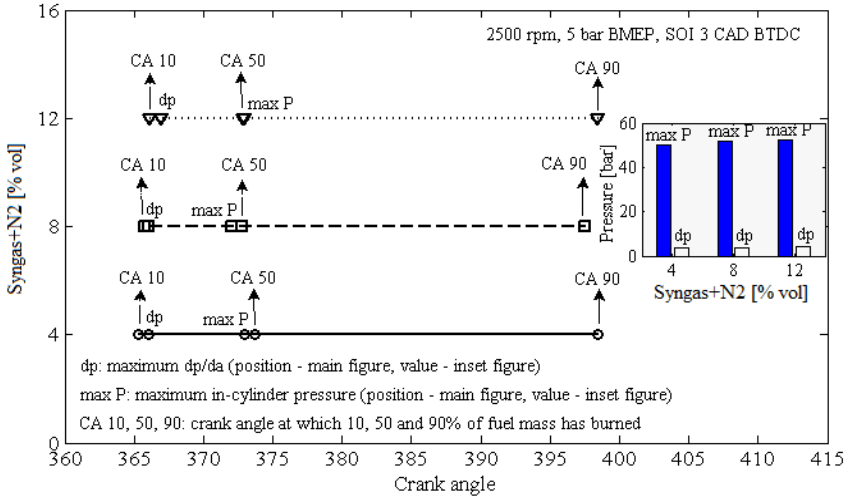

Figure 7.12: Mass fraction burned, maximum pressure rise rate and maximum pressure
Engine speed 2500 rpm, load 5 bar BMEP, SOI 3 CAD BTDC.

Selim [178] performed experiments on a Ricardo E6 engine fuelled by diesel-CNG. It was proven that as the engine speed was increased the pressure rise rate was decreased. Furthermore, it was shown that the pressure rise rate at low speed (1200 rpm) was increased with the load.

Referring again to Figure 7.12, the maximum in-cylinder pressure almost coincided with the CA 50. Comparison with the values obtained under low-speed low-load operation, reveals lower in-cylinder pressure under high-speed medium-load operation. However, in contrast to low-speed low-load operation, an increase in syngas + N_2 proportion resulted in higher in-cylinder pressure. The reduction in NO_x emissions in this operating condition may have been caused by the soot radiative heat loss [179] as the BSN was considerably increased with increasing the amount of syngas + N_2 introduced into the engine, Figure 7.4(b). Finally, comparison with Figure 7.11 reveals that under high-speed operation the combustion took longer to complete (in terms of crank angle degrees).

7.3.4 Effect of intake air enrichment with a mixture of syngas + N_2 on the brake thermal efficiency

Figures 7.13 and 7.14 show the effect of syngas + N_2 rich intake air on brake thermal efficiency under low- and high-speed operation, respectively. In the operating conditions tested, the engine was more efficient when fuelled by neat diesel. Figure 7.13 exhibits a drop in thermal efficiency when a 4% syngas + N_2 mixture was admitted into the engine. An increase in the percentage of syngas + N_2 over 4% had an insignificant effect on brake thermal efficiency.

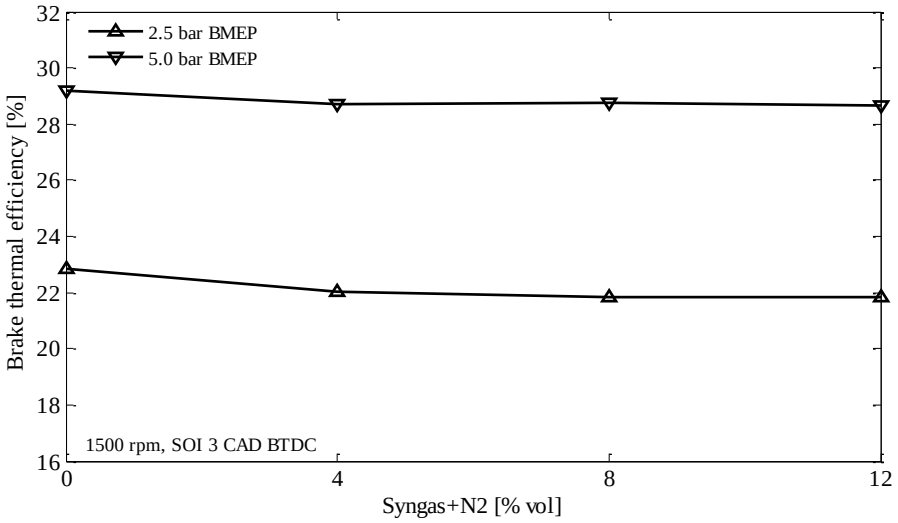

Figure 7.13: Effect of intake air enrichment with syngas + N_2 on brake thermal efficiency. Engine speed: 1500 rpm, load: 2.5 and 5 bar BMEP, SOI: 3 CAD BTDC.

A more intense fuel consumption penalty was observed under high-speed run. The engine became very inefficient under high-speed medium-load operation at 12% syngas + N_2,

although the utilisation of CO was over 95% and hydrogen combustion efficiency was almost 100%, as exhibited in Sections 7.3.2 and 4.3.4, respectively. The flow rate of diesel fuel (not shown separately) was considerably higher under this operating point. The high dilution of the intake air, along with the relatively high equivalence ratio, led to poor diesel utilisation, which was reflected in the unacceptably high BSN values.

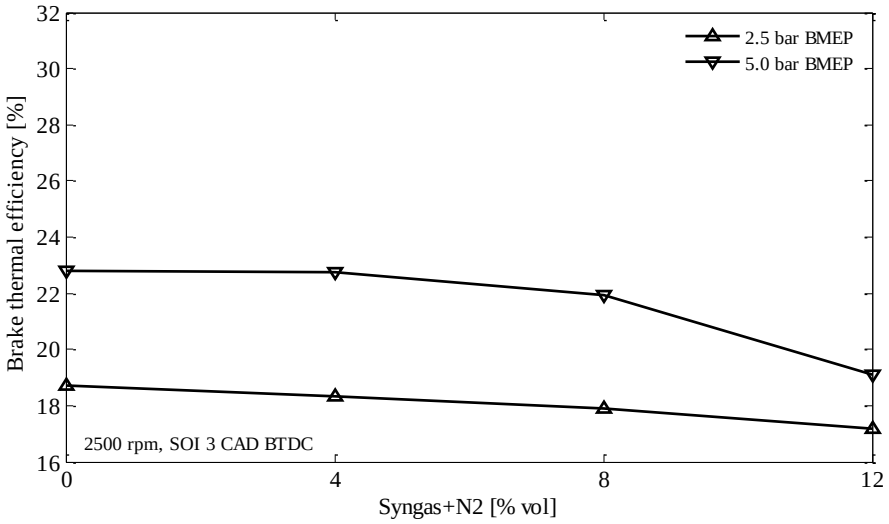

Figure 7.14: Effect of intake air enrichment with syngas + N_2 on the brake thermal efficiency. Engine speed: 2500 rpm, load: 2.5 and 5 bar BMEP, SOI: 3 CAD BTDC.

7.4 Summary

The effect of the intake air enrichment with simulated reformer gas mixture on the performance, combustion and emissions of the engine has been presented in this chapter. The flammable gas was composed of H_2 + CO at a concentration resembling that of a typical fuel reformer. The introduction of bottled nitrogen aimed to simulate the increase in N_2/O_2 proportion in the intake charge. From the results presented, the following conclusions can be drawn.

- Simultaneous reductions in NO_x and BSN were achieved over a broad range of the operating window of the engine. In particular, enrichment of the intake air with a mixture of syngas + N_2, led to simultaneous reductions in NO_x and smoke emissions (compared to the baseline values) when the engine operated under low-

speed low-load, low-speed medium-load and high-speed low-load at syngas + N_2 concentration over 4%.

- Under high-speed medium-load operation, BSN was very sensitive to the admission of nitrogen. In addition, under the same operating condition, isolation of the effect of hydrogen and nitrogen on NO_x and smoke emissions revealed that a CO diluted flame promotes the formation of smoke. Moreover, although higher in-cylinder pressure was recorded when the proportion of syngas + N_2 was increased, NO_x emissions exhibited a decreasing trend. The reduction in NO_x emissions may have been caused by the soot radiative heat loss as BSN was unacceptably high.
- Enrichment of the intake air with a CO-containing mixture caused an increase in the concentration of this pollutant in the exhaust. Estimation of the bottled CO utilisation revealed that by increasing either the load or the speed of the engine, the CO was more efficiently utilised. In essence, this suggests that the combustion of CO was influenced, among other factors, by the in-cylinder temperature.
- An increase in engine speed led to a reduction in maximum dp/da, whereas the effect of load on dp/da varied depending on engine speed. Under low-speed operation, dp/da increased with load, while under high-speed operation, dp/da dropped when the load was increased.
- The engine was more fuel efficient when operating on neat diesel. Under low-speed operation, the brake thermal efficiency dropped when a 4% syngas + N_2 mixture was admitted into the engine. An increase in percentage of syngas + N_2 over 4% had an insignificant effect on brake thermal efficiency. A considerable thermal efficiency reduction was observed under high speed operation.

CHAPTER 8

CONCLUSIONS AND RECOMMENDATIONS FOR FUTURE WORK

8.1 Conclusions

This chapter summarises the major findings of the enrichment of the intake air of an HSDI diesel engine with separate hydrogen and nitrogen, simultaneous hydrogen and nitrogen and a mixture of syngas and nitrogen.

8.1.1 Enrichment of the intake air with hydrogen

The main conclusions from Chapter 4 are summarised below:

1. Replacement of part of diesel fuel with hydrogen has resulted in reduced smoke emissions at the expense of NO_x, apart from the low-speed low-load operation in which NO_x emissions remained relatively unaffected.
2. The residence time was reduced with increasing the engine speed, from 1500 rpm to 2500 rpm, leading to decreased NO_x formation.
3. At a fixed engine speed and load, the production of CO emissions was lower when the engine was fuelled by a mixture of diesel and hydrogen compared to diesel, because the former contained less carbon atoms.
4. When diesel injection was advanced, the fuel was delivered in lower charge density, leading to spray wall impingement and as a result increased THC emissions.
5. The effect of hydrogen enrichment on THC emissions varied, depending on the operating conditions. Although the combustion of hydrogen does not produce THC, the density of the hydrogen-rich intake air was lower compared to air, leading to spray wall impingement when a high quantity of diesel was supplied into the engine; that is, under high-speed medium-load operation.
6. The combustion efficiency of hydrogen increased with increasing the speed, load and percentage of hydrogen.
7. Under low-speed operation, enrichment of the intake air with hydrogen caused a reduction in brake thermal efficiency. Under high-speed operation, a slight

efficiency improvement was achieved but remained within the uncertainty limits of the brake thermal efficiency.

8.1.2 Enrichment of the intake air with nitrogen

The following points summarise the effects of intake air enrichment with nitrogen:

1. The reduction in both oxygen concentration and peak combustion temperature led to decreased NO_x emissions at the expense of smoke and CO emissions.
2. Under high-speed medium-load operation, nitrogen enrichment was very detrimental to smoke emissions. In particular, at 6% bottled nitrogen, BSN more than doubled compared to the baseline operation. The reduction in oxygen concentration led to local fuel-rich zones, a lower peak combustion temperature and poor oxidation of diesel fuel. These factors contributed to the formation of smoke, which was not burned off later on as the in-cylinder temperature remained relatively low due to the dilution of the intake air.
3. At a fixed start of injection, the maximum in-cylinder pressure decreased with the reduction in oxygen concentration.
4. Enrichment of the intake air with nitrogen resulted in longer ignition delay as compared to the baseline operation. Retardation of SOI shortened the ignition delay because the fuel was delivered in a higher in-cylinder temperature.
5. Brake thermal efficiency reduced with the increase in the proportion of nitrogen.

8.1.3 Enrichment of the intake air with simultaneous hydrogen and nitrogen

The purpose of Chapter 6 was to investigate the effect of product gas, mainly consisted of a mixture of H_2 + N_2, on the emissions, combustion and performance of the engine. It should be mentioned that carbon monoxide, at a relatively high concentration, is typically present in diesel reforming product gas; nevertheless, it can be reduced to ppm levels through the water-gas shift reaction, using a good low-temperature catalyst. The major findings of this chapter are listed below:

1. NO_x-smoke trade-off: Simultaneous reductions in NO_x and BSN levels were achieved under low-speed low-load operation. Comparison to the baseline operation revealed a 71.5% reduction in NO_x emissions when a gas mixture consisted of 12% H_2 + N_2 was supplied into the engine. Under both low-speed

medium-load and high-speed low-load operation, introduction of $H_2 + N_2$ into the engine caused a considerable reduction in BSN levels, while NO_x emissions showed only minor changes. Under high-speed medium-load operation, the rate of NO_x change appeared to be very sensitive when the proportion of $H_2 + N_2$ into the intake air was over 8%. Concerning the NO_x-BSN values, it was revealed that the optimum start of diesel injection was at 3 CAD BTDC when the engine operated under the conditions 1-3.

2. Combustion analysis: The formation of NO_x emissions was increased with the premixed burn fraction. An increase in the percentage of $H_2 + N_2$ in the intake air produced either different or similar heat release curves. In the former case, NO_x emissions either increased or decreased, depending on the premixed burn fraction, whereas in the latter case, NO_x emissions remained relatively unaffected due to the similar patterns of the premixed combustion.
3. Nitrogen exhaust compounds: When the speed or the load of the engine was increased, the oxidation of NO was reduced because the combustion products contained less amount of oxygen. Although the introduction of $H_2 + N_2$ replaced an equivalent volume of air, under low-speed low-load operation, a higher NO_2 to NO ratio was obtained compared to the baseline operation. It is therefore clear that the type of fuel affects the oxidation of NO. The raw exhaust gases contained marginal N_2O and zero NH_3 emissions. The level of N_2O, although very low, tended to further reduce as the amount of $H_2 + N_2$ increased.
4. CO emissions: Under low-load operation (cond. 1 and 3), simultaneous enrichment of the intake air with $H_2 + N_2$ resulted in a considerable CO reduction. Under low-speed medium-load operation, admission of $H_2 + N_2$ into the engine had a minor effect on CO emissions. Concerning the high-speed medium-load operation, introduction of $H_2 + N_2$ over 4% led to an increase in CO emissions compared to the baseline values.
5. Brake thermal efficiency: Enrichment of the intake air with a mixture of $H_2 + N_2$ had a detrimental effect on brake thermal efficiency. The results revealed that the engine was more fuel efficient under low-speed (1500 rpm) compared to high-speed (2500 rpm) operation. A dominant factor that contributed to the increased

brake thermal efficiency under low-speed operation was the position of the peak in-cylinder pressure which was closer to the TDC.

8.1.4 Enrichment of the intake air with a mixture of syngas and nitrogen

From Chapter 7, the following conclusions as to the effects of enriching the intake air of the engine with a mixture of syngas and nitrogen can be drawn:

1. Simultaneous reductions in NO_x and BSN were achieved over a broad range of the operating window of the engine. In particular, enrichment of the intake air with a mixture of syngas + N_2, led to simultaneous reductions in NO_x and smoke emissions (compared to the baseline values) when the engine operated under low-speed low-load, low-speed medium-load and high-speed low-load at syngas + N_2 concentration over 4%.
2. Under high-speed medium-load operation, BSN was very sensitive to the admission of nitrogen. In addition, under the same operating condition, isolation of the effect of hydrogen and nitrogen on NO_x and smoke emissions revealed that a CO diluted flame promotes the formation of smoke. Moreover, although higher in-cylinder pressure was recorded when the proportion of syngas + N_2 was increased, NO_x emissions exhibited a decreasing trend. The reduction in NO_x emissions may have been caused by the soot radiative heat loss as BSN was unacceptably high.
3. Enrichment of the intake air with a CO-containing mixture increased the concentration of this pollutant in the exhaust gas. Estimation of the bottled CO utilisation revealed that by increasing either the load or the speed of the engine, the CO was more efficiently utilised. In essence, this suggests that the combustion of CO was influenced, among other factors, by the in-cylinder temperature.
4. An increase in engine speed led to a reduction in maximum dp/da, whereas the effect of load on dp/da varied depending on engine speed. Under low-speed operation, dp/da increased with load, while under high-speed operation, dp/da dropped when the load was increased.
5. The engine was more fuel efficient when operating on neat diesel. Under low-speed operation, the brake thermal efficiency dropped when a 4% syngas + N_2 mixture was admitted into the engine. An increase in percentage of syngas + N_2 over 4%

had an insignificant effect on brake thermal efficiency. A considerable thermal efficiency reduction was observed under high speed operation.

8.2 Significance of this work

The results presented in Chapters 4 and 5 enhance our understanding of how enrichment of the intake air with distinct hydrogen and nitrogen affects the emissions, combustion and performance of a diesel engine. Moreover, the findings from these two chapters, along with the baseline operation, serve as a basis for comparison since the effects of each gas are isolated.

Chapter 6 contributes to the existing knowledge by combining the nitrogen dilution effect with the substitution of an amount of the hydrocarbon fuel with hydrogen. Supply of REGR into the engine causes an increase in nitrogen to oxygen ratio, while at the same time the hydrogen contained in the product gas replaces part of diesel fuel. Apart from providing guidelines for the design of an engine-reformer system, the findings can also benefit the development of an engine equipped with both on-board hydrogen reservoir and air separation membrane.

The results from chapter 7 make several contributions to the current literature. In this chapter, it is considered that the product gas is composed of a mixture of hydrogen, carbon monoxide and nitrogen. The most important outcome of the chapter is that by supplying the engine with a mixture of syngas + N_2, the NO_x and smoke emissions reduce simultaneously over a wide range of the engine operating conditions.

This work has resulted in the publication of three peer-reviewed journal papers, which are listed below:

1. Christodoulou F, Megaritis A. Experimental investigation of the effects of separate hydrogen and nitrogen addition on the emissions and combustion of a diesel engine. Int J Hydrogen Energy 2013;38:10126-40.
2. Christodoulou F, Megaritis A. Experimental investigation of the effects of simultaneous hydrogen and nitrogen addition on the emissions and combustion of a diesel engine. Int J Hydrogen Energy 2014;39:2692-702.

3. Christodoulou F, Megaritis A. The effect of reformer gas mixture on the performance and emissions of an HSDI diesel engine. Int J Hydrogen Energy 2014;39:9798-808.

8.3 Recommendations for future work

Although this work has made considerable contributions to the existing knowledge by examining the effects of the intake air enrichment of a diesel engine with separate hydrogen and nitrogen, simultaneous hydrogen and nitrogen and simultaneous syngas and nitrogen on the emissions, combustions and performance, a number of possible future studies using the same experimental setup could be performed.

It would be interesting to assess whether the increased NO_x emissions, resulting from the admission of hydrogen into the engine, could be reduced by fuelling the engine with emulsified diesel, instead of diesel. The combustion of emulsified diesel has been reported to reduce NO_x and smoke emissions simultaneously by lowering the peak combustion temperature and enhancing the mixing of fuel with air (due to the explosive evaporation of water), respectively. Apart from the expected reduction in NO_x emissions, the micro-explosions in the combustion chamber may enhance the combustion efficiency of hydrogen.

Further experiments could be performed using a pilot injection strategy. Adoption of this technique leads to a reduction in NO_x emissions due to the shorter ignition delay period; therefore, the increased NO_x emissions associated with hydrogen enrichment could be compensated by adopting this injection strategy. In addition, different injection pressures and amount of fuel could be tested at each stage of the injection process.

Another possible future study would be a more detailed combustion analysis when introducing syngas + N_2 into the engine. This would help gain a deeper understanding of the mechanisms behind the simultaneous reductions in NO_x and smoke emissions when using this gas mixture. Also, isolation of the syngas and nitrogen effect in each operating condition could produce interesting findings. Moreover, it is recommended to perform experiments using combined syngas + EGR in boosted and naturally aspirated operation. The percentage of unburned syngas in the exhaust gas could be minimised by employing a control system that would supply syngas into the engine after the exhaust valve closes.

A. EXPERIMENTAL APPARATUS

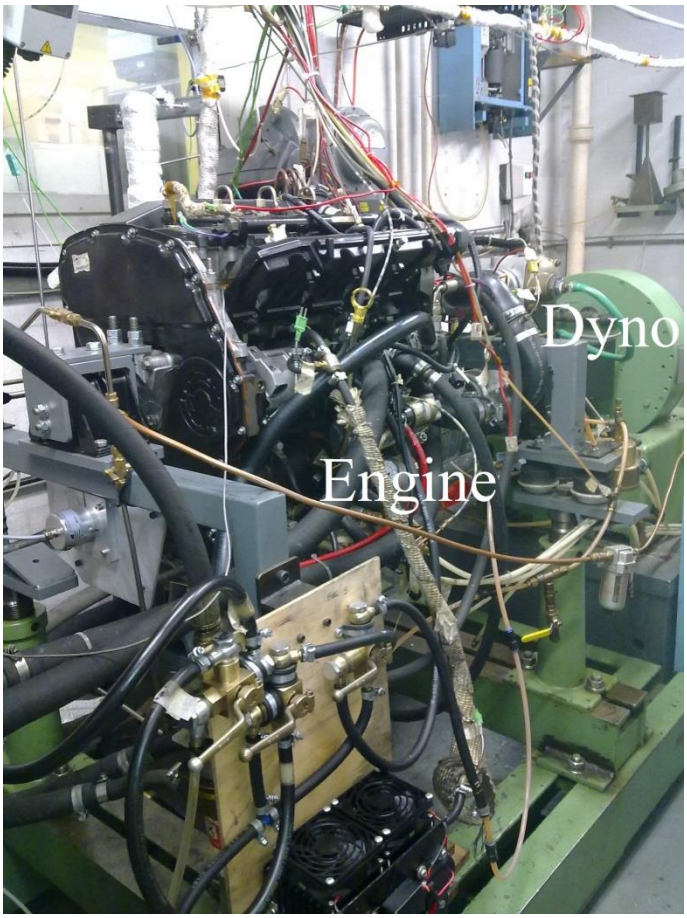

Figure A.1: Ford Puma 2.0 litre HSDI diesel engine.

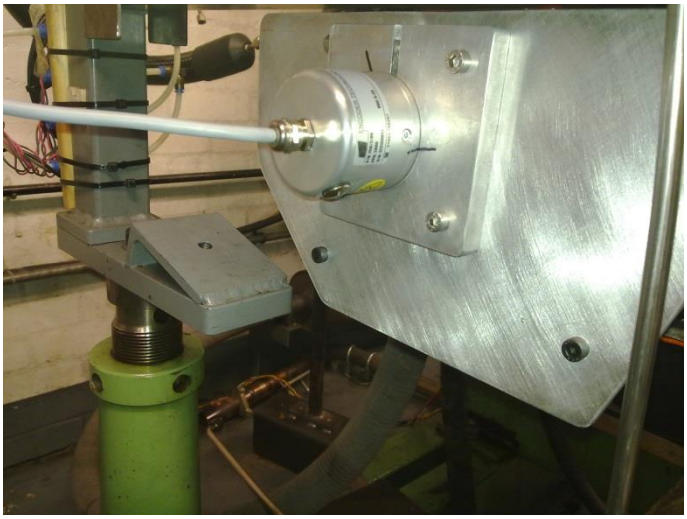

Figure A.2: Encoder Technology ET758 heavy-duty shaft encoder.

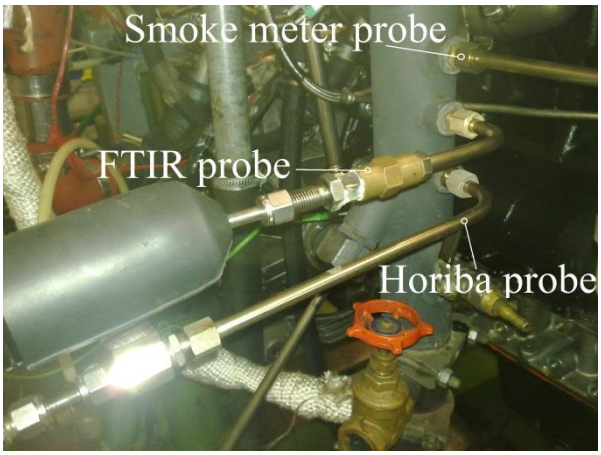

Figure A.3: Sampling point of the smoke meter, FTIR and Horiba.

Figure A.4: E+H Promass 83 Coriolis flow meter.

Figure A.5: Kistler pressure transducer and glow plug adapter

Figure A.6: Hamilton gastight syringe

Figure A.7: Kistler 2629C1 TDC sensor with adapter.

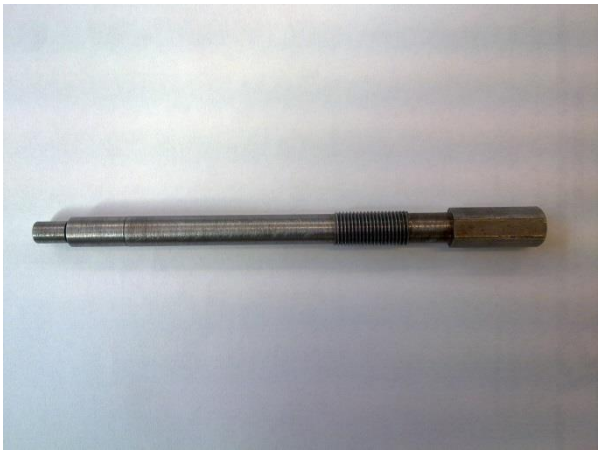

Figure A.8: Dummy glow plug

REFERENCES

[1] Smolinska J. EU economic report 2008 ACEA.

[2] Potter S. In: Hensher DA, Button KJ, editor. 'Transport energy and emissions: Urban public transport', chapter in 'Handbook of transport and the environment' Elsevier; 2003, ISBN 0-08-044103-3

[3] Ehsani M, Gao Y, Gay SE, Emadi A. Modern electric, hybrid electric, and fuel cell vehicles. Texas: CRC Press; 2005.

[4] Chan CC, Chau KT. Modern electric vehicle technology. New York; Oxford University Press; 2001.

[5] Holladay JD, Hu J, King DL, Wang Y. An overview of hydrogen production. Catal Today 2009;139:244–60.

[6] Swain MR, Pappas JM, Adt RR Jr, Escher WJ. Hydrogen-fueled automotive engine experimental testing to provide an initial design-data base. SAE paper; 1981. 810350.

[7] Du X, Wu Y, Fu L, Wang S, Zhang S, Hao J. Intake fraction of PM2.5 and NOx from vehicle emissions in Beijing based on personal exposure data. Atmos Environ 2012;57:233-43.

[8] Payri F, Bermudez VR, Tormos B, Linares WG. Hydrocarbon emissions speciation in diesel and biodiesel exhausts. Atmos Environ 2009;43:1273-79.

[9] Rohr AC, Wyzga RE. Attributing health effects to individual particulate matter constituents. Atmos Environ 2012;62:130-52.

[10] Bertola AG. Technologies for lowest NOx and particulate emissions in DI-diesel engine combustion - influence of injection parameters, EGR and fuel composition. PhD thesis, Swiss federal institute of technology Zurich, Switzerland 2003.

[11] Heywood JB. Internal combustioon engine fundamentals. New York: McGraw-Hill;

1988.

[12] Khair MK, Jaaskelainen H. Emission formation in diesel engines. 2008. Online Source: http://www.dieselnet.com. [Accessed 24 January 2013].

[13] Fluent Inc. Fluent Incorporated. 2003. Online Source: http://jullio.pe.kr/fluent6.1/help/html/ug/node624.htm. [Accessed 27 08 2013].

[14] Habib MA, Elshafei M, Dajani M. Influence of combustion parameters on NOx production in an industrial boiler. Comput Fluid 2008;37:12-23.

[15] Twigg MV, Phillips PR. Cleaning the air we breathe - Controlling diesel particulate emissions from passenger cars. Platinum Met Rev 2009;5327-34.

[16] Majewski A. Diesel particulate matter. 2002. Online Source: http://www.dieselnet.com. [Accessed 30 January 2013].

[17] McEntee JC, Ogneva-Himmelberger Y. Diesel particulate matter, lung cancer, and asthma incidences along major traffic corridors in MA, USA: A GIS analysis. Health Place 2008;14:817–28.

[18] Duggal V, Priede T, Khan I. A study of pollutant formation within the combustion space of a diesel engine. SAE Paper; 1978. 780227.

[19] Chang YJ, Kobayashi H, Kaminoto T. A photographic study of soot formation and combustion in diesel flame with a rapid compression machine. Proceedings of Comodia 1985:149-57.

[20] Du CJ, Kittelson DB. Total cylinder sampling from a diesel engine: Part III - Particle measurements. SAE Paper; 1983. 830243.

[21] Akihama K, Takatori Y, Inagaki K, Sasaki S, Dean AM. Mechanism of the smokeless rich diesel combustion by reducing temperature. SAE paper; 2001. 2001-01-0655.

[22] Raub JA, Mathieu-Nolf M, Hampson NB, Thom SR. Carbon monoxide poisoning - public health perspective. Toxicology 2000;145:1-14.

[23] Leigh-Smith S. Carbon monoxide poisoning in tends - A review. Wilder Environ Med 2004;15:157-63.

[24] Kaur S, Nieuwenhuijsen MJ, Colvile RN. Fine particulate matter and carbon monoxide exposure consentrations in urban street trasport microenvironment. Atmos Environ 2007;41:4781-810.

[25] Mendez S, Kashdan JT, Bruneaux G, Thirouard B, Vangraefschepe F. Formation of unburned hydrocarbons in low temperature diesel combustion. SAE Paper; 2009. 2009-01-2729.

[26] Greeves G, Khan IM, Wang CHT, Fenne I. Origins of hydrocarbon emissions from diesel engines. SAE Paper; 1977. 770259.

[27] Herfatmanesh MR. Investigation of single and split injection strategies in an optical diesel engine. PhD thesis, Brunel University, London 2010.

[28] Environmental Protection Agency, US. EPA. 2012. Online Source: http://www.epa.gov /otaq/consumer/milestones.htm. [Accessed 02 09 2013].

[29] Worldwide emissions standards. Delphi.com 2012.

[30] Majewski WA, Khair MK. Diesel emissions and their control. PA: SAE International; 2006.

[31] Brogan MS, Clark AD, Brisley RJ. Recent progress in NO_x trap technology. SAE paper; 1998. 980933.

[32] Majewski WA. Dieselnet. 2007. Online Source: www.dieselnet.com. [Accessed 08 2013].

[33] Li CG, Mao F, Swartzmiller SB, Wallin SA, Ziebarth RR. Properties and performance of diesel particulate filters of an advanced ceramic material. SAE paper; 2004. 2004-01-0955.

[34] Hemmings S, Megaritis A. Periodically regenerating diesel particulate filter with a

hydrogen/carbon monoxide mixture addition. Int J Hydrogen Energy 2012;37:3573-84.

[35] Musculus MP, Miles PC, Pickett LM. Conceptual models for partially premixed low-temperature diesel combustion. Prog Energ Combust 2013;39:246-83.

[36] Dec JE. A Conceptual Model of DI Diesel Combustion Based on Laser-Sheet Imaging. SAE paper; 1997. 970873.

[37] Flynn PF, Durrett RP, Hunter GL, Zur Loye AO, Akinyemi OC, Dec JE, Westbrook CK. Diesel combustion: An integrated view combining laser diagnostics, chemical kinetics, and empirical validation. SAE paper; 1999. 1999-01-0509.

[38] Li Z, Song C, Song J, Lv G, Dong S, Zhao A. Evolution of the nanostructure, fractal dimension and size of in-cylinder soot during diesel combustion process. Combus Flame 2011;158:1624-30.

[39] Arregle J, Lopez JJ, Garcıa JM, Fenollosa C. Development of a zero-dimensional Diesel combustion model. Part 1: Analysis of the quasi-steady diffusion combustion phase. Appl Therm Eng 2003;23:1301-17.

[40] Tsolakis A. Exhaust gas fuel reforming for compression ignition engines fuelled by diesel and biodiesel. PhD thesis, University of Birmingham, United Kingdom 2004.

[41] Zhang Q, Yao M, Zheng Z, Liu H, Xu J. Experimental study of n-butanol addition on performance and emissions with diesel low temperature combustion. Energy 2011;47:515-21.

[42] Ghorbanpour M, Rasekhi R. A parametric investigation of HCCI combustion to reduce emissions and improve efficiency using a CFD model approach. Fuel 2013;106:157-65.

[43] Parks JE, Prikhodko V, Storey JME, Barone TL, Lewis SA, Kass MD, Huff SP. Emissions from premixed charge compression ignition (PCCI) combustion and affect on emission control devices, Catal Today 2010;151:278-84.

[44] Benajes J, Molina S, García A, Belarte E, Vanvolsem M. An investigation on RCCI combustion in a heavy duty diesel engine using in-cylinder blending of diesel and

gasoline fuels. Appl Therm Eng 2014;63:66-76.

[45] Feng H, Zheng Z, Yao M, Cheng G, Wang M, Wang X. Effects of exhaust gas recirculation on low temperature combustion using wide distillation range diesel. Energy 2013;51:291-6.

[46] Han X, Zheng M, Wang J. Fuel suitability for low temperature combustion in compression ignition engines. Fuel 2013;109:336-49.

[47] Stanglmaier RH, Roberts CE. Homogeneous charge compression ignition (HCCI); Benefits, compromises and future engine applications. SAE paper; 1999. 1999-01-3682.

[48] Neely GD, Sasaki S, Huang Y, Leet YA, Stewart DW. New diesel emission control strategy to meet US tier 2 emissions regulations. SAE paper; 2005. 2005-01-1091.

[49] Guo H, Hosseini V, Neill WS, Chippior WL, Dumitrescu CE. An experimental study on the effect of hydrogen enrichment on diesel fueled HCCI combustion. Int J Hydrogen Energy 2011;36:13820-30.

[50] Boot MD, Luijten CCM, Somers LMT, Eguz U, van Erp DDTM, Albrecht A, Baert RSG. Uncooled EGR as a means of limiting wall-wetting under early direct injection conditions. SAE paper; 2009. 2009-01-0665.

[51] Beatrice C, Del Giacomo N, Guido C. Benefits and drawbacks of compression ratio reduction in PCCI combustion application in an advanced LD diesel engine. SAE paper; 2009. 2009-01-1447.

[52] Leermakers CAJ, Luijten CCM, Somers LMT, Kalghatgi GT, Albrecht BA. Experimental study of fuel composition impact on PCCI combustion in a heavy-duty diesel engine. SAE paper; 2011. 2011-01-1351.

[53] Splitter D, Wissink M, DelVescovo D, Reitz R. RCCI engine operation towards 60% thermal efficiency. SAE paper; 2013. 2013-01-0279.

[54] Hanson R, Kokjohn S, Splitter D, Reitz R. Fuel effects on reactivity controlled compression ignition (RCCI) combustion at low load. SAE paper; 2011. 2011-01-0361.

[55] Curran S, Hanson R, Wagner R, Reitz R. Efficiency and emissions mapping of RCCI in a light-duty diesel engine. SAE paper; 2013. 2013-01-0289.

[56] Denso, DieselNet ECOpoint Inc. 2013. Online Source: http://www.dieselnet.com/news/2013/06denso.php. [Accessed 27 01 2014].

[57] Agarwal AK, Chaudhary V, Agarwal A, Shukla PC. Comparative study of macroscopic spray parameters and fuel atomization behaviour of SVO (Jatropha), its biodiesel and blends. Therm Sci 2013;17:217-32.

[58] Chen PC, Wang WC, Roberts WL, Fang T. Spray and atomization of diesel fuel and its alternatives from a single-hole injector using a common rail fuel injection system. Fuel 2013;103:850-61.

[59] Kuti OA, Zhu J, Nishida K, Wang X, Huang Z. Characterization of spray and combustion processes of biodiesel fuel injected by diesel engine common rail system. Fuel 2013;104:838-46.

[60] Mendez S, Thirouard B. Using multiple injection strategies in diesel combustion: potential to improve emissions, noise and fuel economy trade-off in low CR engines. SAE paper; 2008. 2008-01-1329.

[61] Badami M, Mallamo F, Millo F, Rossi EE. Influence of multiple injection strategies on emissions, combustion noise and BSFC of a DI common rail diesel engine. SAE paper; 2002. 2002-01-0503.

[62] Boggavarapu P, Singh S. Computational study of injection rate-shaping for emissions control in diesel engines. SAE paper; 2011. 2011-26-0081.

[63] Mahr B. Future and Potential of Diesel Injection Systems. Conferenc on Thermo- and Fluid-Dynamic Processes in Diesel Engines, 2002.

[64] Wakasaka Y, Azensu A. Effect of fuel injection rate shaping and injection pressure on intermittent spray combustion. SAE paper; 2000. 2000-01-2793.

[65] Wakasaka Y, Azensu A, Oikawa C. Effect of fuel injection rate shaping on spray combustion. Proceedings of the 15th Internal Combustion Engines Symposium, 1999.

[66] Ghaffarpour M, Baranescu R. NOx reduction using injection rate shaping and intercooling in diesel engines. SAE paper; 1996. 960845.

[67] Wakisaka Y, Azetsu A. Effects of fuel injection rate shaping on combustion and emission formation in intermittent spray. SAE paper; 2002. 2002-01-1159.

[68] Antunes JMG. The use of hydrogen as a fuel for compression ignition engines. PhD thesis, Newcastle University, United Kingdom 2010.

[69] Saravanan N, Nagarajan G, Dhanasekaran C, Kalaiselvan KM. Experimental investigation of hydrogen port fuel injection in DI diesel engine. Int J Hydrogen Energy 2007;32:4071-80.

[70] Shirk MG, McGuire TP, Neal GL, Haworth DC. Investigation of a hydrogen-assisted combustion system for a light-duty diesel vehicle. Int J Hydrogen Energy 2008;33: 7237-44.

[71] McWilliam L, Megaritis T, Zhao H. Experimental investigation of the effects of combined hydrogen and diesel combustion on the emissions of a HSDI diesel engine. SAE paper; 2008. 2008-01-1787.

[72] Bose PK, Maji D. An experimental investigation on engine performance and emissions of a single cylinder diesel engine using hydrogen as inducted fuel and diesel as injected fuel with exhaust gas recirculation. Int J Hydrogen Energy 2009;34:4847-54.

[73] Christodoulou F, Megaritis A. Experimental investigation of the effects of separate hydrogen and nitrogen addition on the emissions and combustion of a diesel engine. Int J Hydrogen Energy 2013;38:10126-40.

[74] Köse H, Ciniviz M. An experimental investigation of effect on diesel engine performance and exhaust emissions of addition at dual fuel mode of hydrogen. Fuel Process Technol 2013;114:26-34.

[75] Lata DB, Misra A, Medhekar S. Effect of hydrogen and LPG addition on the efficiency and emissions of a dual fuel diesel engine. Int J Hydrogen Energy 2012;37:6084-96.

[76] Pullagura G, Kumar KR, Verma PC, Jaiswal A, Prakash R, Murugan S. Experimental investigation of hydrogen enrichment on performance and emission behaviour of compression ignition engine. Int J Hydrogen Energy 2012;37:1223-32.

[77] Wichterlová B, Sazama P, Breen JP, Burch R, Hill CJ, Capek L, Sobalíka Z. An in situ UV–vis and FTIR spectroscopy study of the effect of H2 and CO during the selective catalytic reduction of nitrogen oxides over a silver alumina catalyst. J Catal 2005;235:195-200.

[78] Bromberg L, Cohn DR, Wong V. Regeneration of diesel particulate filters with hydrogen rich gas. MIT Plasma Science and Fusion Centre 2005, PSFC/RR-05-2.

[79] Tsolakis A, Megaritis A, Yap D, Abu-Jrai A. Combustion characteristics and exhaust gas emissions of a diesel engine supplied with reformed EGR. SAE paper; 2005. 2005-01-2087.

[80] Sahoo BB, Sahoo N, Saha UK. Effect of H2:CO ratio in syngas on the performance of a dual fuel diesel engine operation. Appl Therm Eng 2012;49:139-46.

[81] Bika AS, Franklin L, Kittelson D. Cycle efficiency and gaseous emissions from a diesel engine assisted with varying proportions of hydrogen and carbon monoxide (synthesis gas). SAE paper; 2011. 2011-01-1194.

[82] Dong C, Zhou Q, Zhao Q, Zhang Y, Xu T, Hui S. Experimental study on the laminar flame speed of hydrogen/carbon monoxide/air mixtures. Fuel 2009;88:1858-63.

[83] Zhao H. Advanced direct injection combustion engine technologies and development: Diesel engines (Volume 2). Cambridge: Woodhead Publishing Ltd and CRC Press;

2009.

[84] Wikipedia. 2013. Online Source: http://en.wikipedia.org/wiki/Autogas. [Accessed 07 11 2013].

[85] Sita Rama Raju AV, Musa SE, Ramesh A, Nagalingam B. Development and testing of a learn burn spark ignition engine operation on LPG. Proceedings of the XV national conference on I.C. engines and combustion, Chennai, 1997.

[86] Fontaras G, Manfredi U, Martini G, Dilara P, Deregibus G. Experimental assessment of a diesel-LPG dual fuel supply system for retrofit application in city busses. SAE paper; 2012. 2012-01-1944.

[87] Lata DB, Misra A, Medhekar S. Investigations on the combustion parameters of a dual fuel diesel engine with hydrogen and LPG as secondary fuels. Int J Hydrogen Energy 2011;36:13808-19.

[88] Saleh HE. Effect of variation in LPG composition on emissions and performance in a dual fuel diesel engine. Fuel 2008;87:3031-39.

[89] Fontaras G, Martini G, Manfredi U, Marotta A, Krasenbrink A, Maffioletti F, Terenghi R, Colombo M. Assessment of on-road emissions of four Euro V diesel and CNG waste collection trucks for supporting air-quality improvement initiatives in the city of Milan. Sci Total Environ 2012;426:65-72.

[90] Abdelaal MM, Hegab AH. Combustion and emission characteristics of a natural gas-fueled diesel engine with EGR. Energ Convers Manage 2012;64:301-12.

[91] Namasivayam AM, Korakianitis T, Crookes RJ, Bob-Manuel KD, Olsen J. Biodiesel, emulsified biodiesel and dimethyl ether as pilot fuels for natural gas fuelled engines. Appl Energ 2010;87:769-78.

[92] Board NB. Biodiesel org, National biodiesel board. 2013. Online Source: http://www.biodiesel.org/what-is-biodiesel/biodiesel-basics. [Accessed 31 20 2013].

[93] Labecki L. Combustion and emission characteristics of biofuels in diesel engines. PhD thesis, Brunel University, United Kingdom 2010.

[94] Lapuerta M, Armas O, Rodriguez-Fernandez and J. Effect of biodiesel fuels on diesel engine emissions. Prog Energ Combust 2008;34:198-223.

[95] Atadashi IM, Aroua MK, Abdul Aziz A. High quality biodiesel and its diesel engine application: A review. Renew Sust Energ Rev 2010;14:1999–2008.

[96] Tsolakis A, Megaritis A, Wyszynski ML, Low temperature exhaust gas fuel reforming of diesel engine. Fuel 2004;83:1837-45.

[97] Tsolakis A, Megaritis A. Exhaust gas fuel reforming for diesel engines - A way to reduce smoke and NOx emissions simultaneously. SAE Paper; 2004. 2004-01-1844.

[98] Abu-Jrai A, Tsolakis A, Megaritis A. The influence of H2 and CO on diesel engine combustion characteristics, exhaust gas emissions, and after treatment selective catalytic NOx reduction. Int J Hydrogen Energy 2007;32:3565-71.

[99] Ajhar M, Follmann M, Matthias C, Melin T. Membranes producing nitrogen-enriched combustion air in diesel engines: Assessment via dimensionless numbers. J Membrane Sci 2008;323:105-12.

[100] Poola RB, Longman DE, Anderson JL, Stork KC, Sekar R, Callaghan K,Nemser S. Membrane-Based Nitrogen-Enriched Air for NOx Reduction in Light-Duty Diesel Engines. SAE paper; 2000. 2000-01-0228.

[101] Li T, Izumi H, Shudo T, Ogawa H, Okabe Y. Characterization of Low Temperature Diesel Combustion with Various Dilution Gases. SAE paper 2007. 2007-01-0126.

[102] Ladommatos N, Balian R, Horrocks R, Cooper L. The effect of exhaust gas recirculation on combustion and NOx emissions in high-speed-direct-injection diesel engine. SAE paper; 1996. 960840.

[103] Ajhar M, Follmann M, Matthias C, Melin T. Membranes producing nitrogen-enriched combustion air in diesel engines: Assessment via dimensionless numbers. J Membrane

Sci 2008;323:105–12.

[104] Poola RB, Longman DE, Anderson JL, Callaghan K, Nemser S, Bell R. Membrane-based nitrogen-enriched air for NOx reduction in light-duty diesel engines. SAE paper; 2000. 2000-01-0228.

[105] Li T, Izumi H, Shudo T, Ogawa H, Okabe Y. Characterization of low temperature diesel combustion with various dilution gases. SAE paper; 2007. 2007-01-0126.

[106] Hsu BD. Practical diesel-engine combustion analysis. Warrendale: SAE International; 2002.

[107] Khair MK, Jaaskelainen H. Exhaust gas recirculation. DieselNet; 2012.

[108] Ladommatos N, Balian R, Horrocks R, Cooper L. The effect of exhaust gas recirculation on soot formation in a high-speed direct-injection diesel engine. SAE paper; 1996. 960841.

[109] Feng H, Zheng Z, Yao M, Cheng G, Wang M, Wang X. Effects of exhaust gas recirculation on low temperature combustion using wide distillation range diesel. Energy 2013;51:291-96.

[110] Singh SK, Agarwal AK, Srivastava DK, Sharma M. Experimental investigation of the effect of exhaust gas recirculation on lubricating oil degradation and wear of a compression ignition engine. J Eng Gas Turb Power 2006;128:921-7.

[111] George S, Balla S, Gautam M. Effect of diesel soot contaminated oil on engine wear. Wear 2007;262:1113-22.

[112] Rajput RK. Electrical and Electronic Measurements and Instrumentation. New Delhi: S. Chand Group; 2013.

[113] K2BW Environmental Equipment Services Co. 2013. Online Source: http://www.k2bw.com/5_c_18.htm. [Accessed 09 12 2013].

[114] DieselNet, Ecopoint Inc. 2007. Online Source: http://www.dieselnet.com/tech/measure

_gas.php. [Accessed 09 12 2013].

[115] Thet K, Woo N. UC Davis ChemWiki. Online Source: http://chemwiki.ucdavis.edu/Analytical_Chemistry/Instrumental_Analysis/Chromatography/Gas_Chromatography. [Accessed 12 12 2013].

[116] MKS Instruments, MKS type multigas analyser hardware instruction manual. MKS instruments; 2006.

[117] AVL List GmbH, AVL 415 variable sampling smoke meter operating manual. AVL; 1991.

[118] White CM, Steeper RR, Lutz AE. The hydrogen-fueled internal combustion engine: a technical review. Int J Hydrogen Energy 2006;31:1292-305.

[119] Zink Hamworthy J. The John Zink Hamworthy combustion handbook. Florida: Taylor&Francis; 2012.

[120] Mashuga CV, Crowl DA. Derivation of Le Chatelier's mixing rule for flammable limits. Process Saf Prog 2000;19:112-7.

[121] Wierzba I, Kilchyk V. Flammability limits of hydrogen–carbon monoxide mixtures at moderately elevated temperatures. Int J Hydrogen Energy 2001;26:639-43.

[122] Choudhuri AR, Gollahalli SR. Characteristics of hydrogene-hydrocarbon composite fuel turbulent jet flames. Int J Hydrogen Energy 2002;28:445-54.

[123] Verhelst S, Verstraeten S, Sierens R. A comprehensive overview of hydrogen engine design features. J Auto Eng 2007;8:911-20.

[124] Cecrle E, Depcik C, Guo J, Peltier E. Analysis of the effects of reformate (hydrogen/carbon monoxide) as an assistive fuel on the performance and emissions of used canola-oil biodiesel. Int J Hydrogen Energy 2012;37:3510-27.

[125] Homsy SC, Atreya A. An experimental heat release rate analysis of a diesel engine operating under steady state conditions. SAE paper; 1997. 970889.

[126] Egnell R. Combustion diagnostics by means of multizone heat release analysis and NO calculation. SAE paper; 1998. 981424.

[127] Korakianitis T, Namasivayam A, Crookes R. Diesel and rapeseed methyl ester (RME) pilot fuels for hydrogen and natural gas dual-fuel combustion in compression ignition engines. Fuel 2011;90:2384-95.

[128] Gatts T, Liu S, Liew C, Ralston B, Bell C, Li H. An experimental investigation of incomplete combustion of gaseous fuels of a heavy-duty diesel engine supplemented with hydrogen and natural gas. Int J Hydrogen Energy 2012;37:7848-59.

[129] Christodoulou F, Giannakakis P, Kalfas A. Performance benefits of a portable hybrid micro-gas-turbine power system for automotive applications. J Eng Gas Turb Power 2011;133:022301-8.

[130] Lata DB, Misra A. Theoretical and experimental investigations on the performance of dual fuel diesel engine with hydrogen and LPG as secondary fuels. Int J Hydrogen Energy 2010;35:11918-31.

[131] Singh R, Maji S. Dual fuelling of a twin-cylinder compression ignition engine with diesel and CNG. J Eng Appl Sci 2012;7:90-9.

[132] Chokri B, Ridha E, Rachid S, Jamel B. Experimental study of a diesel engine performance running on waste vegetable oil biodiesel blend. J Energ Resour Technol 2012;134:032202-7.

[133] Bromberg L, Cohn DR, Rabinovich A, Heywood J. Emissions reductions using hydrogen from plasmatron fuel converters. Int J Hydrogen Energy 2001;26:1115-21.

[134] Bari S, Mohammad Esmaeil M. Effect of H2/O2 addition in increasing the thermal efficiency of a diesel engine. Fuel 2010;89:378-83.

[135] Banerjee R, Kumar Bose P. An experimental investigation on the potential of hydrogen in the reduction of the emission characteristics of an existing four-stroke single-cylinder diesel engine operating under EGR. Int J Green Energy 2012;9:84-110.

[136] Das LM. Hydrogen-oxygen reaction mechanism and its implication to hydrogen engine combustion. Int J Hydrogen Energy 1996;21:703-15.

[137] Tsolakis A, Hernandez JJ, Megaritis A, Crampton M. Dual fuel diesel operation using H_2. Effect on particulate emissions. Energ Fuel 2005;19:418-25.

[138] DieselNet, Ecopoint Inc. 2010. Online Source: https://www.dieselnet.com/tech/emi_gas.php#hc. [Accessed 27 02 2014].

[139] Derwent R, Simmonds P, O'Doherty S, Manning A, Collins W, Stevenson D. Global environmental impacts of the hydrogen. Int J Nucl Hydrog Prod Appl 2006;1:57-67.

[140] Hemmings S, Megaritis A. The effect of a H2/CO mixture at varying ratios on the diesel particulate filter regeneration process: towards an optimised fuel reformer design - diesel engine aftertreatment system. Int J Hydrogen Energy 2012;37:12332-41.

[141] Abu-Jrai A, Tsolakis A, Theinnoi K, Megaritis A, Golunski S. Diesel exhaust-gas reforming for H2 addition to an aftertreatment unit. Chem Eng J 2008;141:290-7.

[142] Bond SW, Alvarez R, Vollmer MK, Steinbacher M, Weilenmann M, Reimann S. "Molecular hydrogen (H2) emissions from gasoline and diesel vehicles. Sci Total Environ 2010;408:3596-606.

[143] Karim GA, Wierzba I, Boon S. Some considerations of the lean flammability limits of mixtures involving hydrogen. Int J Hydrogen Energy 1984;10:117-23.

[144] Kennedy IM. Models of soot formation and oxidation. Prog Energy Combust 1997;23:95-132.

[145] Sjöberg M, Dec JE. An investigation into lowest acceptable combustion temperature for hydrocarbon fuels in HCCI engines. P Combust Inst 2005;30:2719-26.

[146] Minagawa T, Kosaka H, Kamimoto T. A study on Ignition Delay of Diesel Fuel Spray via Numerical Simulation. SAE paper; 2000. 2000-01-1892.

[147] Herzog PL, Burgler L, Winklhofer E, Zelenka P, Cartellieri W. NO_x reduction

strategies for DI diesel engines. SAE paper; 1992. 920470.

[148] Schaefer M, Hofmann L, Girot P, Rohe R. Investigation of NOx- and PM-reduction by a combination of SCR-catalyst and Diesel Particulate filter for heavy-duty diesel engine. SAE paper; 2009. 2009-01-0912.

[149] Buyukkaya E, Cerit M. Experimental study of NOx emissions and injection timing of a low heat rejection diesel engine. Int J Therm Sci 2007;47:1096-106.

[150] Schubiger R, Bertola A, Boulouchos K. Influence of EGR on combustion and exhaust emissions of heavy duty DI-diesel engines equipped with common-rail injection systems. SAE paper; 2001. 2001-01-3497.

[151] Ladommatos N, Abdelhalim SM, Zhao H, Hu Z. The dilution, chemical and thermal effects of exhaust gas recirculation on diesel engine emissions - part 1 : Effect of reducing inlet charge oxygen. SAE paper; 1996. 1996-05-01.

[152] Mkilaha ISN, Inoue M, Kawai D, Naruse I, Ohtake K. Simultaneous reduction of particulate matter and NOx in a diesel engine by compressed gas injection: macroscopic study at residual load. IMechE 1997;211:227-36.

[153] Papagiannakis RG, Hountalas DT. Experimental investigation concerning the effect of natural gas percentage on performance and emissions of a DI dual fuel diesel engine. Appl Therm Eng 2003;23:353-65.

[154] Cho Y, Song S, Chun KM. H2 effects on diesel combustion and emissions with an LPL-EGR system. Int J Hydrogen Energy 2013;38:9897-906.

[155] Mohon Roy M, Najmul Hoque SM, Ariful Islam M, Rahman Mustafizur M. Use of exhaust gas recirculation (EGR) and cyclonic separator for simultaneous NO_x and PM reduction in DI diesel engines. J Pertol Gas Eng 2011;2:54-63.

[156] Nakatani K, Hirota S, Takeshima S, Itoh K, Tanaka T, Dohmae K. Simultaneous PM and NO_x reduction system for diesel engines. SAE paper; 2002. 2002-01-0957.

[157] Johnson TV. Review of diesel emissions and control. SAE Int J Fuels Lubr 2010;3:16-29.

[158] Yoshinobu Y, Tsuda Y, Ueda H, Nakanishi Y, Gong J. Simultaneous reduction of NO_x and PM in diesel exhaust based on electrochemical reaction. SAE Int J Fuels Lubr 2010;3:50-60.

[159] Ragland KW, Bryden KM. Combustion engineering. Florida: Taylor & Francis; 2011.

[160] Peirce DM, Alozie NS, Hatherill DW, Ganippa LC. Premixed burn fraction: Its relation to the variation in NO_x emissions between petro- and biodiesel. Energ Fuels 2013;27:3838-52.

[161] Shin B, Cho Y, Han D, Song S, Min Chun K. Investigation of the effects of hydrogen on cylinder pressure in a split-injection diesel engine at heavy EGR. Int J Hydrogen Energy 2011;36:13158-70.

[162] Hori M, Matsunaga N, Marinov N, Pitz W, Westbrook C. An experimental and kinetic calculation of the promotion effect of hydrocarbons on the NO-NO2 conversion in a flow reactor. Combust Inst 1998;27:389-96.

[163] Ambs J, McClure B. The influence of oxidation catalyst on NO2 in diesel exhaust. SAE paper; 1993. 932494.

[164] Jobson E, Smedler G, Malmberg P, Bernler H, Hjortsberg O, Gottberg I, et al. Nitrous oxide formation over three-way catalyst. SAE paper; 1994. 940926.

[165] Koike N, Odaka M. Methane and nitrous oxide emission characteristics from automobiles. SAE paper; 1996. 960061.

[166] Lipman T, Delucchi M. Emissions of nitrous oxide and methane from conventional and alternative fuel motor vehicles. Clim Change 2002;53:477-516.

[167] Chaubey R, Sahu S, James O, Sudip M. A review on development of industrial processes and emerging techniques for production of hydrogen from renewable and

sustainable sources. Renew Sust Energy Rev 2013;23:443-62.

[168] Jamal Y, Wyszynski M. On-board generation of hydrogen-rich gaseous fuels - a review. Int J Hydrogen Energy 1994;19:557-72.

[169] Tsolakis A, Megaritis A, Golunski SE. Reaction profiles during exhaust assisted reforming of diesel engine fuels. Energ Fuels 2005;19:744-52.

[170] Kopasz J, Wilkenhoener R, Ahmed S, Carter J, Krumpelt M. In: Gregoire Padro CE, Lau F, editors. 'Fuel flexible reforming of hydrocarbons for automotive applications', chapter in 'Advances in hydrogen energy' Springer; 2002, ISBN 0-306-46429-2.

[171] Singh Bika A. Synthesis gas use in internal combustion engines. PhD thesis, University of Minnesota, United States 2010.

[172] Sahoo BB, Saha UK, Sahoo N. Theoretical performance limits of a syngas-diesel fueled compression ignition engine from second law analysis. Energy 2011;36:760-9.

[173] Azimov U, Okuno M, Tsuboi K, Kawahara N, Tomita E. Multidimensional CFD simulation of syngas combustion in a micro-pilot-ignited dual-fuel engine using a constructed chemical kinetics mechanism. Int J Hydrogen Energy 2011;36:13793-807.

[174] Garnier C, Bilcan A, Le Corre O, Rahmouni C. Characterisation of a syngas-diesel fuelled CI engine. SAE paper; 2005. 2005-01-1731.

[175] Guo H, Thomson KA, Smallwood GJ. On the effect of carbon monoxide addition on soot formation in a laminar ethylene/air coflow diffusion flame. Combust Flame 2009;156:1135-42.

[176] Kondo S, Takizawa K, Takahashi A, Tokuhashi K. On the temperature dependence of flammability limits of gases. J Hazard Mater 2011;187:585-90.

[177] Christodoulou F, Megaritis A. Experimental investigation of the effects of simultaneous hydrogen and nitrogen addition on the emissions and combustion of a diesel engine. Int J Hydrogen Energy 2014;39:2692-702.

[178] Selim M. Pressure-time characteristics in diesel engine fuelled with natural gas. Renew Energy 2001;22:473-89.

[179] Musculus MP. Measurements of the influence of soot radiation on in-cylinder temperatures and exhaust NOx in a heavy-duty DI diesel engine. SAE paper; 2005. 2005-01-0925.